



Western Washington University
Western CEDAR

WWU Graduate School Collection

WWU Graduate and Undergraduate Scholarship

Winter 2016

Exploring the Biofuel Potential of Isochrysis sp.

John R. Williams II

Western Washington University, willi310@students.wvu.edu

Follow this and additional works at: <https://cedar.wvu.edu/wwuet>

 Part of the [Chemistry Commons](#)

Recommended Citation

Williams, John R. II, "Exploring the Biofuel Potential of Isochrysis sp." (2016). *WWU Graduate School Collection*. 503.

<https://cedar.wvu.edu/wwuet/503>

This Masters Thesis is brought to you for free and open access by the WWU Graduate and Undergraduate Scholarship at Western CEDAR. It has been accepted for inclusion in WWU Graduate School Collection by an authorized administrator of Western CEDAR. For more information, please contact westerncedar@wvu.edu.

Exploring the Biofuel Potential of Isochrysis sp.

By

John R. Williams II

Accepted in Partial Completion of the
Requirements of the Degree

Master of Science

Kathleen L. Kitto, Dean of the Graduate School

ADVISORY COMMITTEE

Chair, Dr. Gregory W. O'Neil

Dr. James Vyvyan

Dr. Mark Bussell

MASTER'S THESIS

In presenting this thesis in partial fulfillment of the requirements for a master's degree at Western Washington University, I grant to Western Washington University the non-exclusive royalty-free right to archive, reproduce, distribute, and display the thesis in any and all forms, including electronic format, via any digital library mechanisms maintained by WWU.

I represent and warrant this is my original work, and does not infringe or violate any rights of others. I warrant that I have obtained written permissions from the owner of any third party copyrighted material included in these files.

I acknowledge that I retain ownership rights to the copyright of this work, including but not limited to the right to use all or part of this work in future works, such as articles or books.

Library users are granted permission for individual, research and non-commercial reproduction of this work for educational purposes only. Any further digital posting of this document requires specific permission from the author.

Any copying or publication of this thesis for commercial purposes, or for financial gain, is not allowed without my written permission.

John Williams II

May 2nd, 2016

Exploring the Biofuel Potential of Isochrysis sp.

A Thesis Presented to The
Faculty of Western Washington
University

In Partial Fulfillment of the
Requirements for the Degree
Master of Science

By

John R. Williams II

May 2016

Abstract

A select few strains of marine microalgae, such as *Isochrysis* sp., produce high-melting (~70 °C) lipids known as long-chain alkenones that detrimentally affect biodiesel fuel quality. A method has been developed for the production of an alkenone-free *Isochrysis* biodiesel. This material was prepared on sufficient scale to allow for extensive analysis according to ASTM standards. Results revealed that while cold flow improved by removal of these high-melting components, a cloud point was still unattainable due to the fuels dark pigment. Further effort in relating the presence of alkenones and the resulting cloud point of the biodiesel, led to decolorization of algal biodiesel in order to obtain a cloud point value. The decolorization of the biodiesel resulted in improved fuel properties and allowed for measurement of the cloud point of the fuel. In parallel to the biodiesel production from *Isochrysis* sp. value added products biosynthesized by the algae have been isolated and investigated for their ability to offset fuel prices.

Acknowledgements

Research Advisor: Dr. Gregory W. O'Neil

Thesis Committee Members: Dr. James Vyvyan
Dr. Mark Bussell

Project Contributors: Noah Burlow, Garrett Gilbert, Aarron Culler, Josh Corless, Samuel Schneider, Sophia Schiefelbein, and Julia Wilson-Peltier

Research Group Members: Sara Schaefer, Steven Swick, Jamie Welch, Iris Phan, Trevor Stockdale, and Emily Schneider;

Instrument Technicians: Charles Wandler
Dr. Hla Win-Piazza
Dan Carnevale
Sam Danforth

Financial Support National Institutes of Health, Research Corporation for Science Advancement, MJ Murdock Charitable Trust

Western Washington University Department of Chemistry

Table of Contents

I.	Abstract.....	iv
II.	Acknowledgments	v
III.	List of Schemes	ix
IV.	List of Figures and Tables	x
1.	Background of Biofuels	
1-1	Government mandates to increase biofuel incorporation	1
1-2	Distinctions between generations of biofuels.....	3
1-3	First Generation	3
1-4	Second Generation	5
1-5	Third Generation.....	7
2.	Algal Biofuels	
2-1	DOE Involvement	9
2-2	Fuel Products from Algae.....	10
2-3	Fuel Properties and Standards	10
2-4	<i>Isochrysis sp.</i>	12
2-5	Long chain Alkenones	15
2-6	Alkenones as Biogeochemical.....	16
2-7	Calculating UK'37	20
3.	Isochrysis Biofuels	
3-1	Reed.....	24
3-2	Necton.....	24
3-3	One Step Processing of Commercial <i>Isochrysis sp.</i>	24
3-4	Extraction of <i>Isochrysis sp.</i>	25
3-5	Acid-Catalyzed Esterification of the Algal Oil to Produce a Crude Biodiesel.....	26
3-6	Analysis of <i>Isochrysis</i> Crude Methyl Esters.....	27
3-7	Production of an Alkenone-Free Biodiesel.. ..	27
3-8	Fuel Properties.....	30
3-9	Cetane number.	31
3-10	Kinematic Viscosity.	34

3-11	Oxidative Stability.	35
3-12	Density and Lubricity.	35
3-14	Glycerol and Heteroatom Content.	36
3-15	Cold Flow Properties of the Alkenone-Free Isochrysis Biodiesel.....	37
3-16	Decolorization of algal Biodiesel from Isochrysis sp.....	38
3-17	Decolorization of the biodiesel using montmorillonite K 10.	38
3-18	FAME analysis of decolorized Isochrysis biodiesel.	38
3-19	Pigment removal and cloud point analysis of an Isochrysis biodiesel.....	40
3-20	Cetane number.	41
3-21	Kinematic viscosity.....	42
3-22	Oxidative stability.	42
3-23	Lubricity and density.....	44
3-24	Glycerol and FFA and moisture content.	45
3-25	Comparison of Biodiesel Production.	46
4.	Isolation of value added products from Isochrysis sp.	
4-1	Production of Jet Fuel Range Hydrocarbons as a Coproduct of Algal Biodiesel by Butenolysis of Long-Chain Alkenones.....	50
4-2	Cross-Metathesis of Alkenones with 2-Butene.	51
4-3	Synthesis of an alkenone-derived polyester monomer via cross metathesis.	62
4-4	Fucoxanthin Isolation from Waste Algal Biomass as an Added Coproduct to Isochrysis Biofuels.....	69
4-5	Investigation of Heterogeneous Catalysis for Isochrysis biofuel production.	79
4-6	Catalysis Systems.	80
4-7	Catalyst Preparation and Characterization.....	80
4-7	Product Analysis.....	82
V.	Experimental	85
VI.	Conclusion	91
VII.	References	93

Table of Schemes

Scheme 1.	Second generation biofuel reactions	7
Scheme 2.	Rate of carbon entering and leaving the cell.....	17
Scheme 3.	One step esterification of algal Biodiesel	24
Scheme 4.	Synthesis of Alkenone Free Biodiesel (two step)	28
Scheme 5.	Introduction of functionality to alkenone subunit via cross metathesis.....	49
Scheme 6.	Mechanism of Ethenolysis and Butenolysis	52
Scheme 7.	Alkenone Butenolysis Reaction.....	53
Scheme 8.	Comparison of Methyl Oleate and Alkenone Butenolysis Reactions	58
Scheme 9.	Diacid and diol formation of polyester	63
Scheme 10.	Methyl acrylate cross-metathesis from the major alkenone components in our sample	65
Scheme 11.	Schematic with yields of fucoxanthin isolation as a coproduct of parallel biodiesel and jet fuel production from the marine microalgae Isochrysis.	71
Scheme 12.	Proposed cracking products of squalene and alkenone (37:2)	84

Figures and Tables

Figure 1.	Atmospheric CO ₂ increase overtime	2
Figure 2.	Congressional Volume for renewable fuels projection	3
Table 1.	Specifications in Biodiesel Standards That are directly influenced by Fatty Acid Profile of the Biodiesel Fuel	10
Figure 3.	Lipid content screening of multiple algal species	12
Figure 4.	CP temperature versus Alkenone content in B20	14
Table 2.	Composition of <i>Isochrysis sp.</i> Crude FAME	13
Figure 5.	Compilation of long term ϵ_p values from Alkenones	18
Figure 6.	UK'37 equation for estimating past sea surface temperatures based of 37 carbon Alkenone unsaturation.	20
Table 3	Dry <i>Isochrysis</i> Biomass content	25
Figure 7	UV absorbance spectra of algal oil and crude biodiesel	26
Figure 8.	GC-FID chromatograms of alkenone-free biodiesel and purified alkenones.	29
Table 4.	Fuel Properties of the Alkenone-Free <i>Isochrysis</i> Biodiesel.	31
Table 5.	Comparison of fuel properties for alkenone-free <i>Isochrysis</i> FAME (Iso-ME) and values for methyl esters from soybean (SME) and canola (CME).	31
Table 6.	FAME Composition of Alkenone-Free <i>Isochrysis</i> Biodiesel Samples.	33
Table 7.	Elemental Analysis.	37
Table 8.	Fuel Properties of Non-decolorized (Non-D) and Decolorized <i>Isochrysis</i> (D-Iso) Biodiesel Fuels.	39
Table 9.	FAME Composition of Non-Decolorized (Non-D),23 and Decolorized <i>Isochrysis</i> Biodiesel (D-Iso) Samples.	43
Figure 9.	Comparison of algal biomass from commercial sources	46
Table 10.	FAME composition of biodiesel produced from commercial Iso-Paste and Iso-Powder <i>Isochrysis sp.</i>	48
Figure 10.	Comparison of non-decolorized (left) and decolorized (right) <i>Isochrysis</i> biodiesel fuels.....	48
Figure 11.	<i>Isochrysis</i> extraction and fractionation scheme with yields given in parentheses for the different products obtained from each step.	51
Table 11.	Results from Butenolysis Reactions of Alkenone Mixtures Isolated from <i>Isochrysis</i>	54
Figure 12.	GC-FID chromatograms for starting alkenones and butenolysis products obtained by reaction with cis-butene and catalyst Ru-HG	55

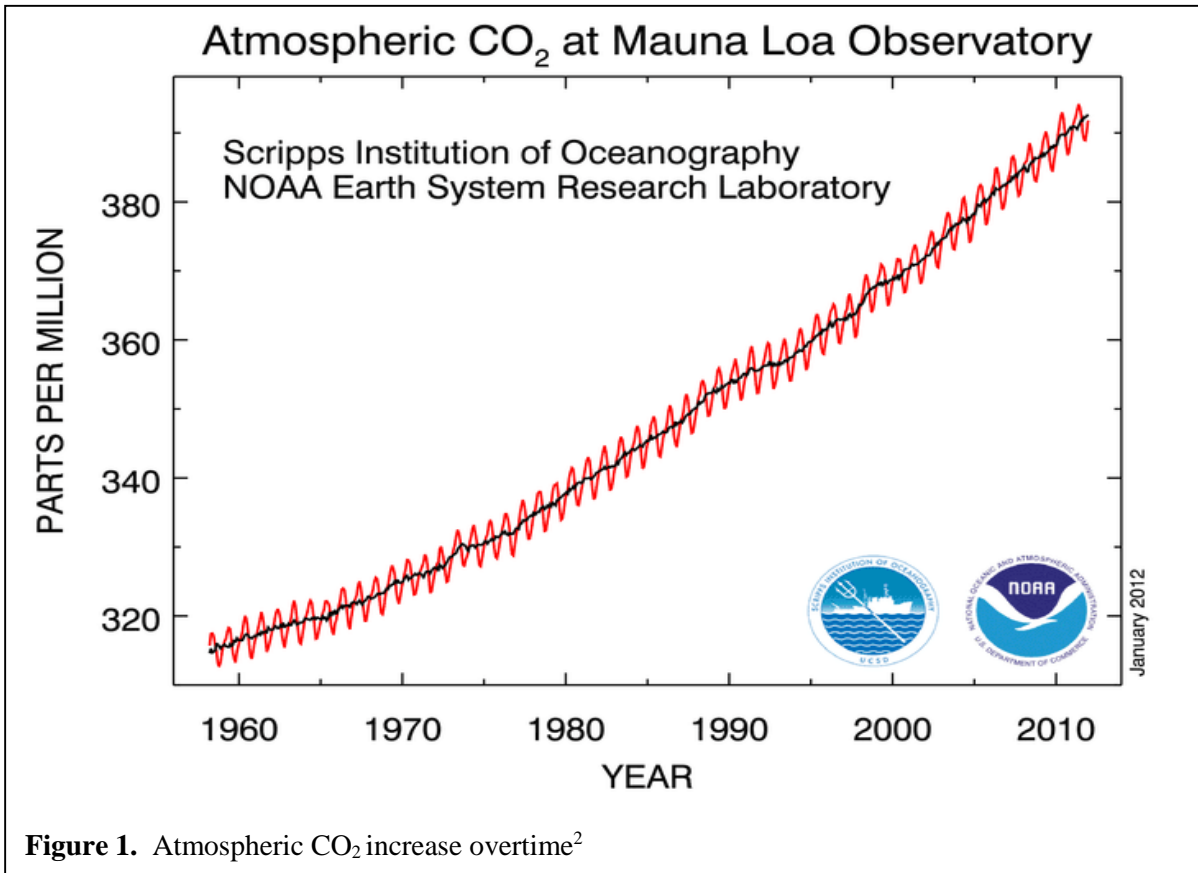
Figure 13.	Results from butenolysis kinetic experiments by analyzing aliquots from a single reaction.....	56
Table 12.	Alkenone Composition and Expected Butenolysis Products	59
Figure 14.	GC × GC–FID chromatogram of the alkenone butenolysis product mixture obtained after 30 min using cis-2-butene and catalyst Ru-HG.....	60
Figure 15.	GC × GC–TOF chromatogram “plan view” of the alkenone butenolysis products	62
Figure 16.	GC×GC-TOF chromatogram of product mixture obtained by cross-metathesis of alkenones with methyl acrylate catalyzed by the Hoveyda-Grubbs catalyst.	63
Figure 17.	Comparison of predicted vs. actual amounts of methyl acrylate alkenone cross-metathesis products.....	64
Figure 18.	Ruthenium hydride species formed from decomposition of Ruthinium metathesis catalyst.....	66
Table 13-15.	Comparison of monomer products from influences of metathesis additives	67
Figure 19.	GC×GC-TOF chromatogram of the alkenone/methyl acrylate cross-metathesis reaction using Grubbs’ second-generation catalyst conducted in the presence of benzoquinone	68
Figure 20.	GC×GC-TOF chromatogram of the alkenone/methyl acrylate cross-metathesis reaction using Grubbs’ second-generation catalyst conducted in the presence of benzoquinone showing identification of incomplete metathesis products and n-alkenes.....	69
Figure 21.	UV absorbance spectra of red fractions obtained by chromatography of the neutral lipids and a fucoxanthin standard solution.....	72
Table 16.	Yields and corresponding fucoxanthin content for algal oils obtained by sequential hexanes/ethanol extraction of dry Isochrysis biomass	73
Figure 22.	HPLC chromatogram of e-AO and fucoxanthin	73
Figure 23.	UV absorbance spectra of Isochrysis hexane extract and subsequent ethanol extract in acetone	74
Figure 24.	¹ H NMR spectrum (500 MHz, CDCl ₃) of e-AO (a, top), enriched-AO (b, middle), and fucoxanthin standard (c, bottom).....	75
Table 17.	Comparison of fucoxanthin recoveries from Reed and Necton Isochrysis.....	78
Figure 25.	Structural comparison of alkenone and squalene	80
Figure 26.	XRD pattern of prepared catalyst, Platinum reference, and Rhenium reference	81
Figure 27.	Overlay of GC-MS spectrum for alkenone with 1Pt-3Re-ASA (black) and squalene with 1Pt-3Re-ASA (blue)	83

Chapter 1: Background of Biofuels

Government mandates to increase biofuel incorporation

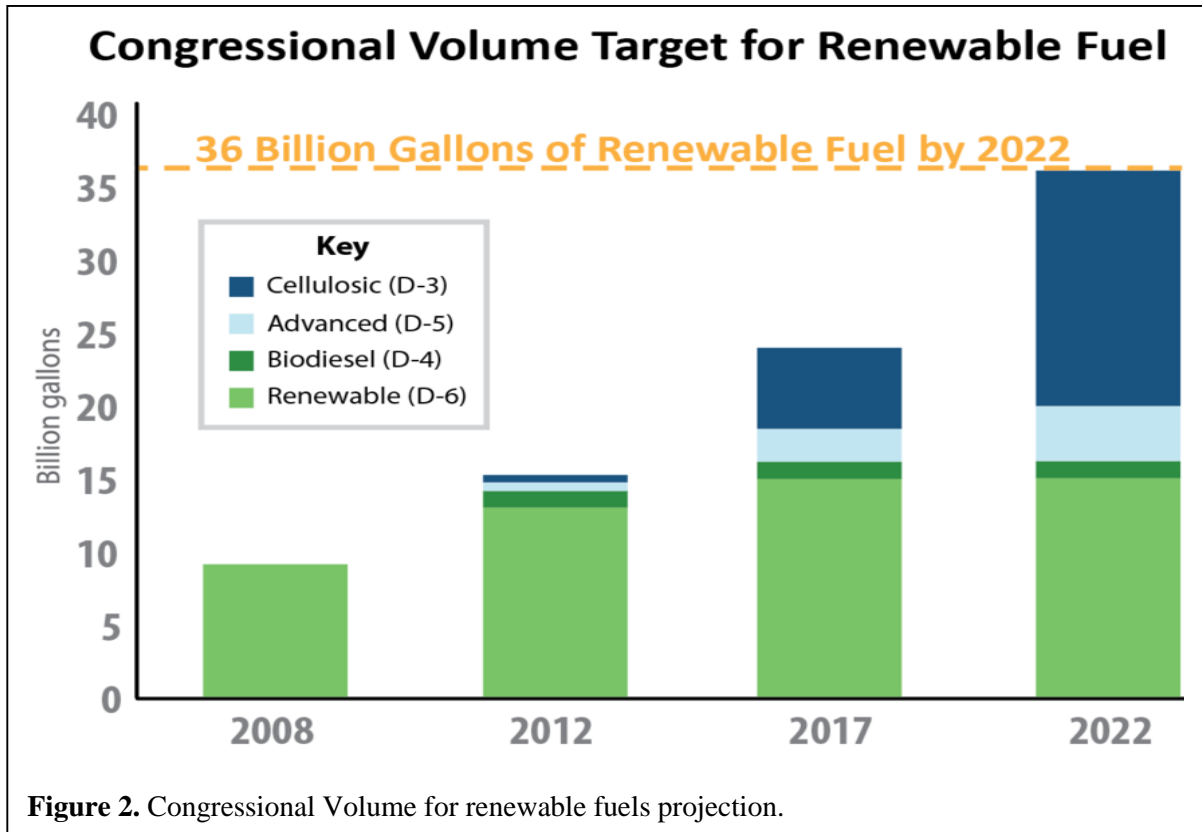
An abundance of research has shown that human activities including fossil fuel use, agriculture and land use have been the dominant causes of increased concentrations of greenhouse gases in the atmosphere over the past 250 years, thus making it extremely likely that human activities have had a net warming effect of the Earth since 1750¹. The changing climate has been noticed across disciplines and can be seen in nearly every corner of the globe's regions its ecosystems. Ocean and polar scientists have recorded dramatically higher arctic temperatures, ocean levels, and higher ocean acidity, which alter the characteristics of the most fundamental organisms of the ocean food chain.¹ Atmospheric research has shown that CO₂ concentrations have increased by more than 40% since pre-industrial times, from approximately 280 parts per million by volume (ppmv) in the 18th century to 396 ppmv in 2013. In April of 2014, the monthly average CO₂ concentration at Mauna Loa exceeded 400 ppm for the first time in human history (Figure 1). Current CO₂ levels are higher than they have been in at least 800,000 years.² The scientific community has responded by calling for renewable alternative energy sources that reduce the amount of carbon dioxide we put into the atmosphere. In an attempt to halt and reverse damage done to Earth's atmosphere and environment by anthropogenic emissions of greenhouse gases, government mandates have been put in place by many nations. The United States Environmental Protection Agency (EPA) is a federal agency of the U.S.

government which was created for the purpose of protecting human health and the environment from the impact that human activity can have by writing and enforcing regulations based on laws passed by Congress.³



The Renewable Fuel Standard (RFS) program was created under the Energy Policy Act of 2005 (EPAAct) by Congress, which amended the Clean Air Act (CAA). The Energy Independence and Security Act of 2007 (EISA) further amended the CAA by expanding the RFS program. EPA implements the program in consultation with U.S. Department of Agriculture and the Department of Energy. The RFS is a national policy that requires a certain volume of renewable fuel to replace or reduce the quantity of petroleum-based transportation fuel, heating oil or jet fuel. The four renewable fuel categories under the RFS are biomass-based diesel, cellulosic biofuel, advanced biofuel, total renewable fuel. After implementation, the 2007 enactment of EISA significantly expanded the size of the program to include

boosting the long-term goal to 36 billion gallons of renewable fuel and extending yearly volume requirements out to 2022 (Figure 2.)



Distinctions between generations of biofuels

First Generation

First Generation biofuels are fuels produced directly from edible arable crops. The two predominant first generation fuels are biodiesel and bioethanol, where the oils or Free Fatty Acids (FFA) are extracted from the biomass for use in biodiesel or the sugars are extracted from the biomass and fermented to make bioethanol. Common feedstocks for biodiesel production are soybean in the

United States and rapeseed in Europe. Bioethanol in the United States is industrially produced from corn and from sugarcane in Brazil. Both fuels are attractive replacements for petroleum fuels because they can be used in existing engines with little or no modification, and can take advantage of much of the existing petroleum fuel infrastructure. For instance, biodiesel can be used directly in a conventional diesel engine with no engine modification and makes use of our existing fuel distribution network. Biodiesel compared to petroleum diesel reduces particulates from 30-90% and since it contains no sulfur, it also allows for the use of better particulate traps in the exhaust systems of vehicles⁴, which can reduce the particulates even further. Biodiesel can be used in many blends but, the most common are: B100 (pure biodiesel), B20 (20% biodiesel, 80% petroleum diesel), B5 (5% biodiesel, 95% petroleum diesel) and B2 (2% biodiesel, 98% petroleum diesel).⁵ Bioethanol is most often used as a biofuel additive for gasoline in conventional engines as E10 (10% ethanol and 90% gasoline) and gives a similar octane improvement to the additive methyl tert butyl ether (MTBE), but is preferred due to evidence of groundwater contamination by MTBE. While ethanol is in some respects a better substitute for MTBE, blends greater than E15 require modification to conventional gasoline engines due to issues of corrosion which must also be addressed for our current fuel distribution and storage infrastructure. First generation biofuels also present a food versus fuel dilemma, and controversies associated with diverting farmland or edible crops to biofuels production which strains the food supply can create other adverse effects on local and global economies (*vide infra*).

There has been approximately a 100 million tonne per year increase in the use of corn to produce ethanol in the U.S. over the past 10 years, and projections of greater future use have raised concerns that reduced exports of corn and other agricultural products would lead to land-use changes and cause negative environmental impacts, such as limited CO₂ sequestration. The concerns have been bolstered by agricultural and trade models, indicating that large-scale corn ethanol production leads

to substantial decreases in food exports, increases in food prices, and greater deforestation globally.⁶ Work by the World Bank Policy Research Group from 2008 found that biofuels produced from grains have raised food prices by between 70 to 75 percent on the poor in developing countries who, on average, spend half of their household incomes on food.⁷ First generation biofuels also have a vulnerability to crop shortfall from extreme weather conditions such as drought. In 2012, the U.S. experienced the hottest July and most severe drought in 50 years and this resulted in a 12% decrease in corn production. This underscores the vulnerability of food-based feedstocks to extreme environmental conditions that could become more frequent and of higher intensity as a result of long-term climate change.⁸

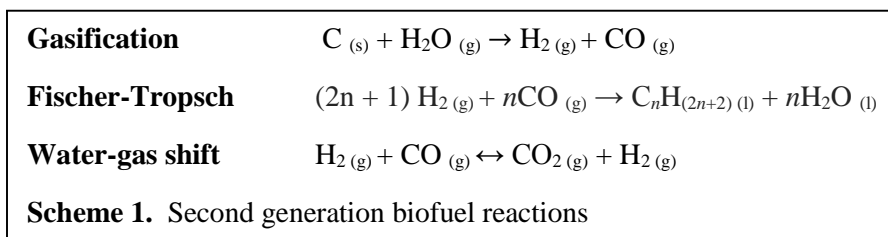
Second Generation

Second generation biofuels, like first-generation biofuels, are considered renewable fuels that can be manufactured from various sources of organic carbon using biomass feedstocks that are renewed rapidly as part of the carbon cycle. In contrast to first-generation biofuels, second generation biofuels are produced from non-edible crops such as wood, organic waste, food crop waste and dedicated fuel crops (e.g. switchgrass). In some cases, these can be waste material from first generation biomass feedstocks. One example would be corn stover, or the stalks, cobs, and other plant material that are generally left in the field after harvesting corn. This waste corn material is rich in lignin, cellulose and hemicellulose. The distinction between cellulose and hemicellulose is that where cellulose is a homopolymer of glucose, hemicellulose is a heteropolymer of primarily pentoses (xylose and arabinose) and hexoses (glucose, galactose, and mannose). The heteropolymer nature of hemicellulose makes it easier to degrade into fermentable sugars, which is currently the major challenge associated with cellulosic fuels.⁹ Depending on the treatment of the biomass, other

products beside bioethanol can be obtained from second-generation biofuel feedstocks. Some of the most common methods to convert waste plant material into fuel are processes such as gasification, pyrolysis, and Fischer–Tropsch reactions. Pyrolysis describes the thermochemical conversion of organic material at elevated temperatures in the absence of oxygen. It involves the simultaneous irreversible change of chemical composition of the organic material and its physical phase. Products from pyrolysis reactions generally include both gas and liquid phase hydrocarbons as well as solid residues that are rich in carbon content. Flash pyrolysis which operates at a faster rate than traditional pyrolysis has been shown to produce high yields (75%) of lower weight liquid fuels from high weight bio oil.¹⁰ Gasification is a process that aims to convert biomass materials into carbon monoxide, hydrogen and carbon dioxide. Like pyrolysis, this is achieved by reacting the material at high temperatures (>700 °C), without combustion, within a controlled atmosphere of oxygen and/or steam. The resulting gas mixture containing CO and H₂ is referred to as syngas and can be further transformed into fuel via the Fischer-Tropsch process. The Fischer–Tropsch method is a process where a mixture of carbon monoxide and hydrogen is converted into liquid hydrocarbons by a series of complex chemical reactions under heterogeneous catalysis.

While second generation biofuels address some of the issues associated with first generation biofuels such as increasing the cost competitiveness with petroleum by using waste material to produce additional fuels and the possible avoidance of the food versus fuel dilemma by only using waste biomass, most still require a large amounts of potable water and cultivatable land. The interdependence between energy production and water resources has recently been emphasized in several studies.¹¹ When reporting water usage, both evapotranspiration (ET) and withdrawal estimates are relevant for metrics of consumption. ET affects the water supply, because more ET translates into less runoff and less local recharge, while withdrawals of water relate to the demand (consumption) of water. A combination of larger ET (temporal reduction of supply) and larger

irrigation (more demand) can result in a less sustainable growth environment for second generation fuels.⁹ Much like first-generation biofuels, second-generation biofuels are also criticized by limited ability to reduce CO₂ emissions. Work recently published by Liska and coworkers in 2014 showed that removal of corn residue from biofuels can decrease soil organic carbon (SOC) and increase CO₂ emissions because residue C in biofuels is oxidized to CO₂ at a faster rate than when added to soil and the net CO₂ emissions from residue removal are not adequately characterized in biofuel life cycle assessment.¹²



Third Generation

The term third generation biofuels has only recently entered the mainstream, and refers to specially engineered energy crops such as algae as its feedstock source. The algae are proposed to act as a source for low-cost, energy dense fuel, from an entirely renewable source. Third generation biofuels are able to overcome many of the issues that decrease the viability of first- and second-generation biofuels. These include avoidance of food versus fuel controversies along with concerns about using drinkable water related land use issues that both first and second generation fuels suffer from since they are based on edible arable crops as a feedstock. Algae has been predicted to be able to sequester more CO₂ than agricultural crops and is able to avoid the CO₂ emitted from SOC as it is not grown in soil. A further benefit of algae based biofuels is that production of fuel per unit biomass are far greater than first- second-generation feed stocks. The large diversity of algal species also offers a wide range

of fuels that can be manufactured, plus various species of algae capable of being grown in varying climates. In fact, algae have been demonstrated to produce up to 9,000 gallons of biofuel per acre, which is 10-fold what the best traditional feedstock have been able to generate. According to the US Department of Energy (DOE), yields that are 10 times higher than second generation biofuels mean that only 0.42% of the U.S. land area would be needed to generate enough biofuel to meet all of the U.S. needs. As with all biofuel feedstocks, algal biofuels have their challenges. Algae, even when grown in waste water, require large amounts of water, nitrogen and phosphorus to grow and has been criticized for not being entirely carbon neutral (i.e. like all biofuels, combustion produces CO₂). With regards to the fuel, through our own work it is becoming clear that biodiesel produced from algae tends to be less oxidatively stable than biodiesel produced from soybean. This is largely because the oil found in algae tends to be highly unsaturated and thus more prone to degradation¹³ (algal biodiesel fuel properties are discussed at length in Chapter 3). Nonetheless, there remains significant interest in algae as a sustainable and domestic source of renewable fuels.

Chapter 2: Algal Biofuels

DOE Involvement

The idea of producing fuel from algae is not new. Sparked by the oil shock which affected the U.S in 1978, the United States Department of Energy (DOE) sponsored a program for nearly 30 years known as the Aquatic Species Program (ASP) initially aimed specifically at the development of transportation fuel from algae. One conclusion from the study, as detailed in a report by Sheehan et al., was that the cultivation of algae solely for the purpose of biofuel production was not cost competitive¹⁴ at that time, and the program was defunded in 1996. Since that time, the cost of crude petroleum has dramatically increased from \$18.46 per barrel (42 gallons = 159 L) in 1996 to nearly \$47 per barrel in 2016.¹⁵ This has led to a renaissance in algal biofuel research, spurred in part by legislative action. For example in January 2010, U.S. Energy Secretary Steven Chu announced \$80 million in government funding for biofuel research with much of the funding going to algae biofuel research and development. Combined with ongoing issues of national security and the increasing number of environmental concerns from industrial petroleum extracting and processing, there has been a great resurgence of interest in algae as a potential source of biofuels. The DOE has established a new National Algal Biofuels Technology Roadmap, and one can now find a large number of reviews and commentaries dedicated to the topic.¹⁶

Fuel Products from Algae

Algae is a broad term encompassing many different species, from micro algae to macroscopic kelp. This diversity of species presents the opportunity to produce many different biofuels in varying global regions. Unique benefits of algae when compared to traditional agricultural biodiesel feedstocks include very high reported productivities for some species of algae, simultaneous wastewater treatment with algae cultivation, its ability to remove CO₂ from industrial flue gases by algae bio-fixation and the avoidance of certain food versus fuel controversies.¹⁷ The unique environmental requirements of algae lets it be grown in water unsuitable for human consumption (e.g. brackish or wastewater) and flue gas containing CO₂ in fluctuating amounts and purity can be feed directly into the algae. Where some combustion products in flue gas (e.g. NO_x or SO_x) can be effectively directed and used as nutrients for microalgae during growth. To date, the majority of algal biofuel research has focused on the production of biodiesel, defined as monoalkyl esters of fatty acids (most commonly fatty acid methyl esters, or FAME) prepared by transesterification of acylglycerols.¹⁸ Industrially produced biodiesel is used to formulate a wide range of blends with petrodiesel that can be used as is without any engine modifications or changes to our transportation fuel network.

Table 1. Specifications in Biodiesel Standards Directly Influenced by the Fatty Acid Profile¹⁹

specification	ASTM D6751	EN 14214
cetane number	47 minimum	51 minimum
kinematic viscosity at 40 °C (mm ² /s)	1.9–6.0	3.5–5.0
cloud point	report	
cold-filter plugging point		not specified; depends upon the location and time of year
oxidative stability at 110 °C (h); Rancimat test	3 minimum	6 minimum

Fuel Properties and Standards

Regardless of the source, biodiesel must conform to the standards described in the documents ASTM D6751 or EN 14214 (Table 1) to be approved for commercialization in the U.S or Europe, respectively.

These standards include specifications related to physical properties of the fuel such as lubricity and kinematic viscosity, combustion characteristics defined by the cetane number (CN), and chemical stability in the form of oxidative stability. Additional recommendations for cold flow properties such as the cloud point (CP) or cold filter plugging point (CFPP) are also included. Cloud point is simply reported as this property can be allowed to vary depending upon the time of year and geographic location of production.¹⁹ Kinematic viscosity is a measure of the liquid fuel's resistance to gradual deformation by shear stress or tensile stress. For liquids, it corresponds to the informal notion of "thickness". Cetane number (CN), is a measure of a fuel's ignition delay, the time period between the start of injection and the first identifiable pressure increase during combustion of the fuel. Fuels with a desirable high cetane value will have shorter ignition delay periods than lower cetane fuels in a modern diesel engine. Oxidative stability is a measure of how long it takes for the biodiesel to succumb to decomposition when it is exposed to a stream of oxygen at an elevated temperature and is measured by the volatiles that come off and are detected. Cloud point is the temperature at which solids begin to form in biodiesel and create a cloudy appearance. Fuels with a low cloud point value are desirable.

Recently the O'Neil group reported on biodiesel produced from the marine microalgae *Isochrysis* sp.²¹ *Isochrysis* was selected in part because it is one of only a few species of algae that is farmed industrially, harvested for purposes of mariculture, and therefore representative of the scale necessary for biofuel production. Otherwise *Isochrysis* species have been cited in reviews related to algal biofuels, noted for its high lipid content, desirable FFA (Free Fatty Acid) profile, fast growth rate, and nontoxicity, which made it an attractive candidate for biodiesel synthesis.²⁰

Isochrysis sp.

Like many potential algal biofuel feedstocks, *Isochrysis* has been the subject of extensive lipid content screening studies¹⁸. Reported “lipid contents” in these studies generally refer to fatty acids (FAs), although the term lipid encompasses numerous types of hydrophobic natural products. This is because the target product for algal biofuels has primarily been FAMES or biodiesel, produced from the FAs. The individual fatty acids (or FAMES) make up the FA profile, reported as C#:# referring to the carbon chain length and number of double bonds, respectively. The fuel properties of a given biodiesel are dependent on the FA profile that comprises the biodiesel fuel. From the amount of each individual FAs in the profile, predictions can be made about the overall fuel properties of a biodiesel.

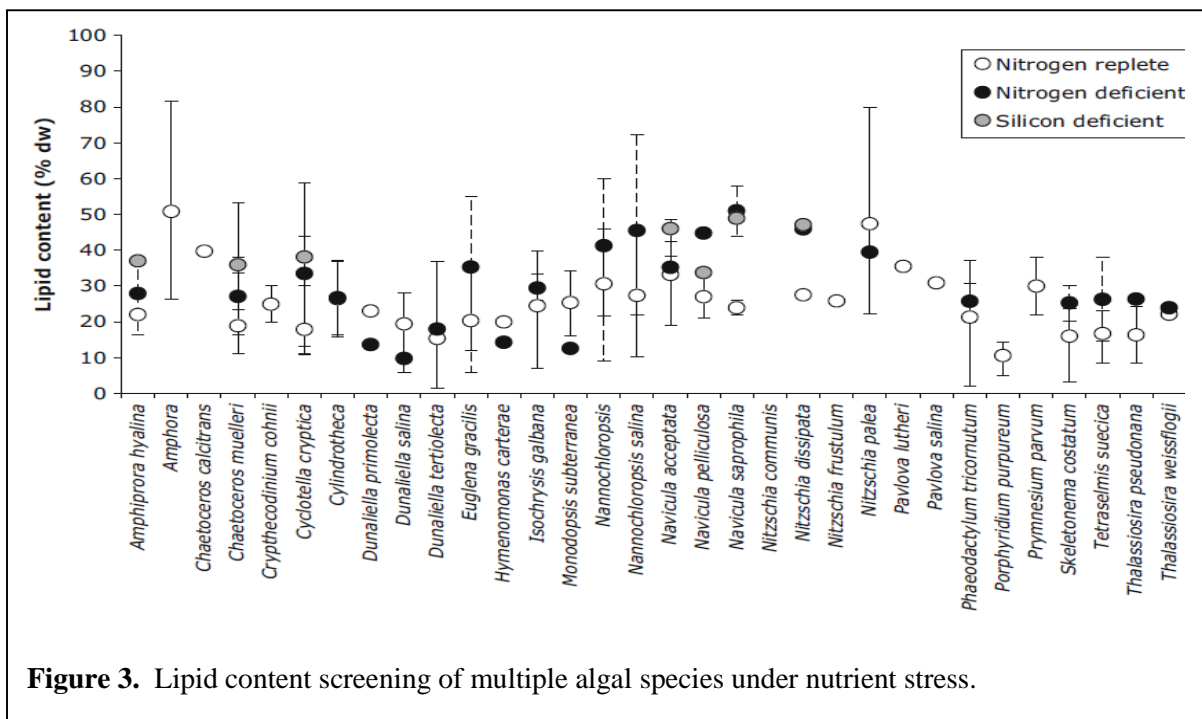


Figure 3. Lipid content screening of multiple algal species under nutrient stress.

For example, if we look at industrial biofuel feed stocks such as oil palm tree and rapeseed, we can make predictions about, for instance, the cloud point of their corresponding biodiesel based on the major FAs present in their profile. Palm tree oil, which produces a majority (40-50%) of palmitic acid

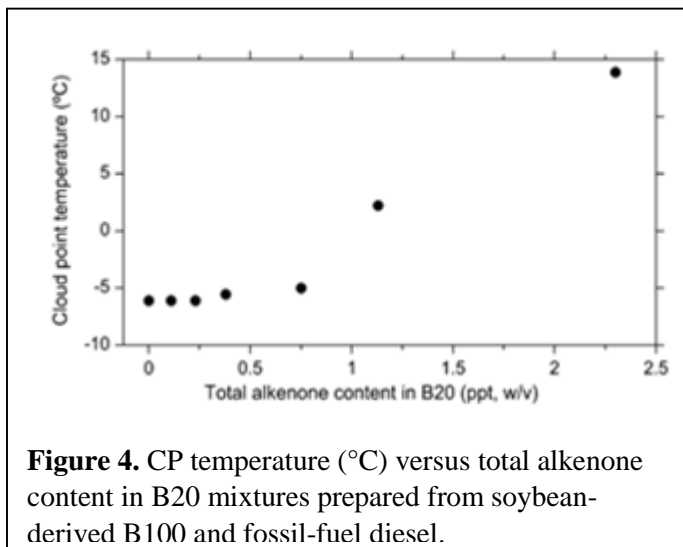
(C:16:0) would lead us to predict that biodiesel produced from this feedstock would have poor cold flow properties. This is because the neat FA palmitic acid, with its long saturated carbon chain has a cloud point of 8 °C. Similar predictions can be made for rapeseed, where the major FA is C18:1 (52-65%), and has a cloud point of -3 °C. The difference between these two FAs and their cloud point values comes from the presence of the cis double bond that is present in C:18:1 and is absent in C:16:0. However, there is an inverse relationship between CP and oxidative stability. This is because the double bond of the carbon chain in C:18:1, that was useful for favorable CP, is now an unfavorable reactive site for oxidation. The sterics of the double bond in rapeseed oil makes it difficult for the carbon chains of the FA to stack on one another and makes it problematic for the FA to become solid at low temperature. If we look to the oxidative stability value for these feed stocks, we will see an inverse relationship between CP and oxidative stability. Similar to CP, kinematic viscosity also decreases with an increasing number of cis double bonds in the fatty acid chain.

Table 2. Composition of *Isochrysis* sp. Crude FAME

FAMES	mg/g of crude FAME ^a	mg/g of <i>Isochrysis</i> sp. algal oil ^b	mg/g of dry weight of <i>Isochrysis</i> sp.
C14:0	85.0	75.9	15.9
C16:0	63.4	56.7	11.9
C16:1n-7	35.6	31.8	6.7
C18:0	ND ^c	ND	ND
C18:1n-9	60.0	53.6	11.3
C18:2n-6	26.1	23.3	4.9
C18:3n-6	4.75	4.24	0.9
C18:3n-3	34.2	30.5	6.4
C18:4n-3	115	102	21.5
C18:5	26	23	4.8
C20:5n-3	9.7	8.7	1.8
C22:6n-3	74.2	12.7	13.9
total FAMES	533	423	76.0
total alkenones	141	126	24.2
total FAMES + alkenones	675	549	100

^aCrude FAME is based on the operationally defined method of Johnson and Wen.¹⁷ ^bAlgal oil is the hexane extract of the *Isochrysis* sp. biomass. ^cND = not detected.

This is often the case for biodiesel fuel properties, where a structural characteristic such as unsaturation, gives a favorable value for one test (CP) but, then an unfavorable value (oxidative stability) for another. The FAME profile of *Isochrysis sp.* biodiesel can be seen in Table 2. From this profile we can see that the majority of the FAMES are unsaturated (72%) in profile, and we would predict that the fuel would have favorable cold flow properties, a low kinematic viscosity and poor oxidative stability. However, biodiesel produced directly from *Isochrysis* (so-called crude FAME), suffers from severe cold flow issues (described as a dark-green solid at room temperature).²¹ The poor cloud point of this biodiesel was unexpected based solely on the FAMES, and was attributed to contamination of the fuel by polyunsaturated long-chain alkenones (PULCAs). As further evidence, alkenones were added incrementally to a B20 biodiesel blend. The cloud point of the resulting fuel showed a clear correlation between higher cloud points for fuels with a higher alkenone concentration.



The initial B20 mixture had a cloud point of -6.1 °C, which increased markedly with the alkenone content (Figure 4). In particular for B20 with 0.75–1.13 ppt (w/v) alkenones, the CP temperature jumped from -5 to 2.2 °C. The samples that were tested for CP in Figure 4. were also analyzed by GC,

to show that a B20 sample with the added amount of 2.25 ppt (w/v) of alkenones, that resulted in a CP value change of roughly 20 C (-5 to 15 C) was barely detectable in the chromatogram (Figure 8.).

Long chain Alkenones

Long-chain unsaturated methyl and ethyl ketones are part of a group of unusual compounds, including related alkenes and alkenoates, collectively referred to as polyunsaturated long chain alkenones (PULCAs)^{22, 23} that are biosynthesized by a phylum of algae called the haptophytes. Members of the haptophytes are primarily unicellular, photosynthetic, and are often important sources of food for aquatic communities. Prymnesiophyte algae are predominantly marine and are mostly tropical species of micro algae. The group occurs worldwide, and several species have global distributions. Other species include the widely distributed coccolithophorid *Emiliana huxleyi* and the closely related species *Gephyrocapsa oceanica*.^{24, 25}

Alkenone structures consist of an ethyl or methyl ketone connected to a long linear carbon chain backbone (typically between 35 and 41 carbons) containing between one and three *trans* double bonds separated by five methylene units. This is in stark contrast to fatty acids containing a carboxylic acid connected to a much shorter 14 to 22 linear carbon chain with zero to six *cis* methylene interrupted double bonds. Melting points (mp) of individual components are a good indicator of the cloud point of a biodiesel fuel, with higher mp corresponding to a higher (unfavorable) cloud point. For FAMEs, the melting point increases with increasing carbon chain length and decreases with increasing unsaturation or number of double bonds (assuming *cis*-alkene geometry). For this reason, certain classes of FAMEs with high melting points, such as those with *trans* double bonds, are undesirable in biodiesel. Imahara and co-workers demonstrated that even minor amounts of higher melting components can have a dramatic impact on biodiesel cold flow properties.²⁶ Specifically, the

addition of small amounts of methyl palmitate (C16:0) or methyl stearate (C18:0) to representative biodiesel mixtures greatly increased CP values. Importantly, irrespective of the biodiesel composition, mixtures with fixed C16 or C18 saturated ester content had nearly identical CPs. *Trans*-Methyl oleate (C18:1) has a melting point of 45 °C, and would be unsuitable as a component of biodiesel even in small quantities.²⁶ Alkenones, with their even longer chain length and *trans* double bonds results in higher high melting points (pure C36:2 alkenone has a melting point of 58 °C.²⁷ It therefore seems clear that the cold flow problems associated with *Isochrysis* biodiesel are due to alkenones, yet prior to our own work there had been no reports connecting or relating alkenones to biodiesel fuel properties. This was surprising given other reports on *Isochrysis* biodiesel and the long history of alkenone-related research (*vide infra*).²⁷

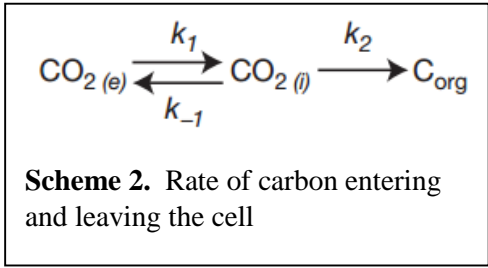
Alkenones as Biogeochemical Indicators

Alkenones are arguably the most studied class of lipids found in the marine environment. This is because of their ability to be used as proxies for various measurements of environmental conditions, such as sea surface temperatures and CO₂ concentrations. More recently alkenones have appeared as indicators for hydrologic, salinity, and depositional changes. The application of alkenones as a proxy requires a full account of the uncertainties, such as the range of other physical and chemical parameters that impact the proxy.²⁸ The structural elements mentioned previously that distinguish alkenones from fatty acids (e.g. *trans* non-methylene interrupted double bonds) make these compounds resistant to degradation, and therefore accurate proxies for many measurements. Early efforts in understanding the stable carbon isotopes in marine plankton resulted in an appreciation for alkenones in regards to determining dissolved CO₂ concentrations, their rate of growth, and the metabolic pathways effecting the magnitude of carbon isotope fractionation. The total isotope

fractionation between the substrate carbon ($\delta^{13}\text{C}_{\text{DIC}}$) and the organic carbon ($\delta^{13}\text{C}_{\text{org}}$) is approximated by the term $\Delta_{\text{DIC-org}}$. (where $\Delta_{\text{DIC-org}}$ is defined as the variable ϵ_p in relation to aqueous carbon dioxide (Equation 1)).²⁹ $\delta^{13}\text{C}_{\text{org}}$ is able to be directly measured in geologic archives, but $\delta^{13}\text{C}_{\text{CO}_2(\text{aq})}$ cannot, and requires a proxy such as the $\delta^{13}\text{C}$ value of approximate age of carbonate minerals, assuming that conversion of DIC of aqueous CO_2 to solid carbonate. Interpretation of algal ϵ_p values (Equation 1) is based on a model that describes the isotope fractionation, in terms of flow of carbon, including movement of carbon into the cell and out of the cell back into the environment (leakage).³⁰

$$\epsilon_p = \epsilon_t + f (\epsilon_f + \epsilon_t) \dots\dots\dots [1]$$

The flow of inorganic carbon is ultimately fixed as organic carbon in the system. In the carbon fluxes $\text{CO}_{2(\text{e})}$ represents the ambient $\text{CO}_{2\text{aq}}$ concentration, $\text{CO}_{2(\text{i})}$ is the concentration of $\text{CO}_{2\text{aq}}$ inside the cell, k_1 , k_{-1} are the rate constants for the flux of carbon into and out of the cell and k_2 is the rate constant for the fixation of carbon fixed as organic carbon (Scheme 2).



ϵ_p is then expressed as the isotope fraction of the carbon in the cell reservoir fixed as organic matter or that is lost from leakage occurring during the carbon transport and fixation.³⁰ The terms ϵ_f and ϵ_t represent the carbon isotope fractionations for carbon fixation and diffusive transport. Where f is the fraction of inorganic carbon that diffuses back into the environment.³¹ By substitution of flux

(Equation 2) into Equation 3, we can now described Equation 3 in terms of CO₂ concentrations diffusion fractionation Equation 3:

$$f = \frac{k_{-1}C_i}{k_1C_e} \dots\dots\dots [2]$$

$$\epsilon_p = \epsilon_t + (\epsilon_f + \epsilon_t) \frac{C_i}{C_e} \dots\dots\dots [3]$$

Taking the carbon demand into account in terms of carboxylation growth rate by redefining the term C_i/C_e to its algebraic equivalent leads to Eq. 4.³¹

$$\epsilon_p = \epsilon_t + (\epsilon_f + \epsilon_t) \left(1 - \frac{C_e - C_i}{C_e}\right) \dots\dots\dots [4]$$

This model for carbon flux was then used as a framework for correlating ε_p to ambient CO₂ concentration in work by Hollander and McKenzie (Figure 5.):³²

$$\epsilon_p = A[\log(\text{CO}_{2\text{aq}})] + B \dots\dots\dots [5]$$

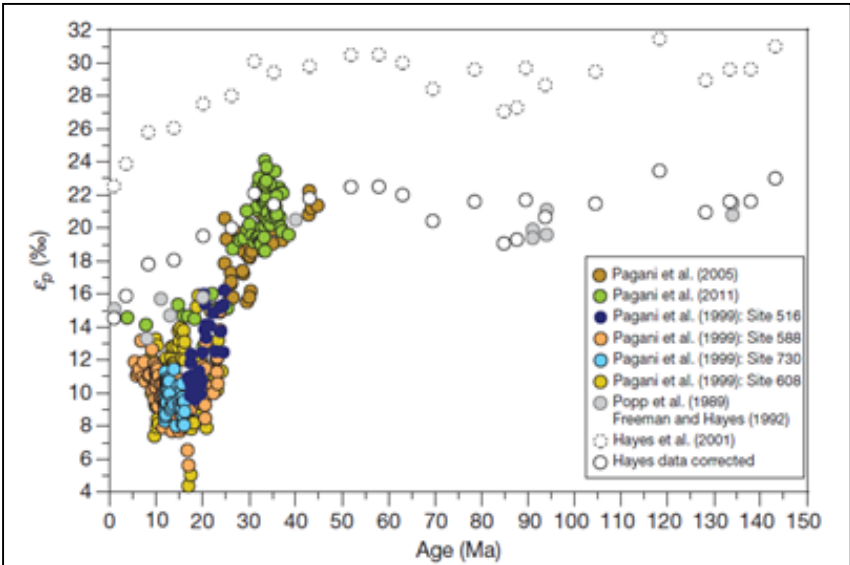


Figure 5. Compilation of long term ε_p values from alkenones, geographies, and bulk organic carbon.

The work by Hollander et. al used marine setting values and from the literature to approximate A and B showing that ancient CO₂ levels can be approximated from both bulk and biomarker-derived (alkenone) ϵ_p records.³² The data that was calculated from alkenones as a biomarker proxy showed a general logarithmic form (Figure 5). The application of alkenones in CO₂ reconstruction was recognized as a significant step forward given early recognition that alkenone production is limited to few algae, thus reducing diverse algal influences on the expression of ϵ_p and that the alkenones are found in measurable abundances in marine sediments. While the alkenones have been used to elucidate past CO₂ concentration through carbon flux and isotope ratios models, the biological function still remains unclear. It is likely that alkenones share a similar role to other neutral lipids and are used as energy storage reserves for the organism. Work by Pond and Harris showed that in the species *Emiliania huxleyi* alkenones are present in all growth phases of the organism, but the cellular pools increase during the stationary phase or the phase where growth stops. This is typical for energy storage lipids.^{33, 34} Work by Epstein, Prahel and coworkers found that there is a trend of an increased PULCA production under nitrogen or phosphorus depleted environments, across strains of alkenone-producing algae. While the magnitude of this increased alkenone production varied widely across strains of algae, the change resulted in 10-20% increase in the cell in the stationary phase on average.^{35, 36} Research by Prahel et al. showed that under energy depleted growth conditions or a dark environment, the PULCA pools in the cell decrease as the PULCAs go through a series of metabolic pathways that breaks down the alkenones into smaller units that are either oxidized to release energy, or used in other anabolic reactions. Work by Epstein and coworkers proposed that the unsaturation profile of the alkenones affects its melting point and this is used to regulate membrane fluidity. However, alkenones were unable to be detected in haptophyte membranes, it was therefore proposed that the change in unsaturation and associated melting point affects the ease

by which the alkenones are catabolized³⁵ (where more double bonds = higher melting = more easily consumed).

Calculating $U_{37}^{k'}$

Another important role for alkenones is their ability to serve essentially as a paleothermometer. Alkenone producing species are known to respond to changes in their environment, such as changes in water temperature which they are grown in. The temperature of water results in the algae altering the relative ratio of the different alkenones that are biosynthesized. At higher growing temperatures the algae produce alkenones that have fewer numbers of double bonds than when the algae is grown in colder water. This means that the relative degree of unsaturation of alkenones can be used to estimate the temperature of the water in which the alkenone-producing organisms grew. The relative degree of unsaturation is typically described as an Unsaturation Index of di- versus tri- unsaturated C37 alkenones. This gives us the $U_{37}^{k'}$ value which can be calibrated to the growth temperature (Figure 6.).³⁷ From these values, past ocean temperatures are estimated by calculating the $U_{37}^{k'}$ at different depths within a sediment core representing different time periods. An enormous number of studies over the last 30 years have made use of alkenone $U_{37}^{k'}$ calculations to track for instance changes in global temperatures.³⁸

$$U_{37}^{k'} = \frac{[C_{37:2}]}{[C_{37:2}] + [C_{37:3}]}$$

Figure 6. $U_{37}^{k'}$ equation for estimating past sea surface temperatures based of 37 carbon alkenone unsaturation.

Care must be taken when calculating the UK'37 because in addition to temperature, the unsaturation profile of the alkenones (and FAs), can be altered by certain environmental strains on the organism. Specifically, lower CO₂ concentrations have been shown to increase the FA 22:6 content in *Isochrysis*, whereas 14:0 FA was found to be dominant when CO₂ concentrations return to normal conditions. Increased CO₂ concentration was also observed to increase the overall amount of fatty acid accumulation in work by Salina and coworkers.³⁹

Nitrogen starvation can have dramatic effects on the biosynthesis of alkenones and other lipids. In fact the effects of nitrogen deficiency in algal culture samples have shown improvements to biosynthesis and accumulation of lipids⁴⁰⁻⁴³ and triglycerides.^{44, 45} Nitrogen is an essential part of the organism with regard to structural and functional proteins in the cells and accounts for 7%–20% of cell dry weight.⁴⁶ The stress caused by this starvation effects the proteins of the algae in an inversely, resulting in a reduction of protein content in the organism.⁴⁷⁻⁵² This skews the lipid/protein ratio towards lipids at the expense of growth rate⁴⁸. Attempts to increase lipid content with limited nitrogen should be evaluated with caution because algae also tend to divert their photosynthetically fixed carbon to carbohydrate synthesis while, decreasing oxygen evolution, carbon dioxide fixation, and chlorophyll content⁵⁰. Nitrogen starvation is also able to change the enzyme balance of cells, and increase the synthesis of lipids and decrease in chlorophyll synthesis leading to excess carotenoids in the cells *Dunaliella* sp.⁵³ Certain strains of algae, such as *Haemaantococcus pluvialis* have also been observed to accumulate high amounts of carotenoids, astaxanthin and its acylesters (up to 13% w/w), when grown under nitrogen-depleting conditions.⁵⁶⁻⁵⁸

Similar to nitrogen starvation, phosphorus starvation can also favorably effect lipid production in the algae. It has demonstrated that phosphorus is the primary limiting nutrient for microalgae in many natural environments, not nitrogen.⁵⁷ Phosphorus is a crucial component required for growth and development of cells in the algae.⁵⁸ Phosphorus is approximately 1% of dry weight of algae⁵⁹, but it is

likely required in massive excess, compared to nitrogen, since not all phosphate is bioavailable because of the formation of complexes ions with metals.⁵⁹ Immediate effects of phosphorus limitation include a consequential reduction in the rate of light utilization required for carbon and leads to accumulation of lipids. In the species *Scenedesmus sp.* The total lipid content was observed to increase from 23% to 53% when phosphorus concentration was reduced by half (2.0 mg/L to 1.0mg/L).

Chapter 3: *Isochrysis* Biofuels

Isochrysis is one of only a few species of algae that is currently grown industrially, harvested as a primary component of shellfish and shrimp feed. The availability of *Isochrysis* in multi-kilogram quantities has enabled our group to synthesize larger quantities (hundreds of mL) of algal biodiesel. This has allowed our group to obtain actual experimental fuel property data for our biodiesel. Many biodiesel fuel property tests require large volumes of fuel, for instance cetane requires approximately 70 mL of the fuel.¹⁹ Ideally this is run in duplicate or triplicate, meaning that substantial amounts of biodiesel are required. As a result, much of current algal biodiesel research relies on predictions of fuel from the FAME profiles of microscale biodiesel synthesis. Others have utilized simulated algal biodiesel for their studies (e.g. blends of vegetable and fish oils) because in general algal biodiesel is scarce. Knothe recently predicted the fuel properties of algal biodiesel by studying the properties of individual polyunsaturated FAMES (PuFAMES) that are common to many algal biodiesel fuels. His study, however, only included neat C20:4 and C22:6 FAMES, because other PuFAMES were not available.⁶⁰ The Industrial production of *Isochrysis* therefore provides a unique opportunity to perform a fundamental study of the fuel properties of algal biodiesel tested against a battery of ASTM standards. For our work, *Isochrysis* has been purchased from the following suppliers:

Reed

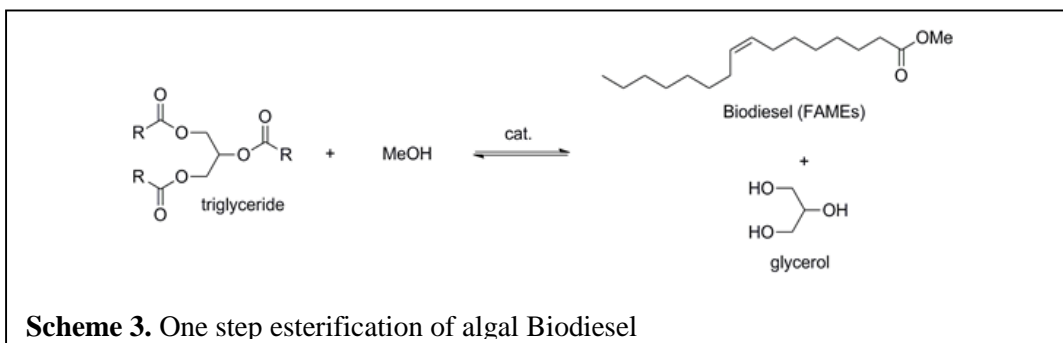
Reed Mariculture Inc. is based from San Jose, California, USA. They produce *isochrysis* sp. As a wet paste which is 80% water by mass.

Necton

Necton produces *Isochrysis* sp. In Belamandil Natural Park of Ria Formosa, in Olhão, Portugal. The *Isochrysis* biomass is processed by drying and milling the biomass into a fine powder.

One Step Processing of Commercial *Isochrysis* sp.

To investigate the extent of the impact of alkenones on biodiesel cold-flow properties, Reed algal biomass was dried and the triacylglycerides were extracted from the biomass with boiling hexanes in a Soxhlet apparatus. The resulting hexane extract (“hexane algal oil”) was esterified in the presence of an acid to produce the corresponding crude FAME (i.e. biodiesel, Scheme 3).



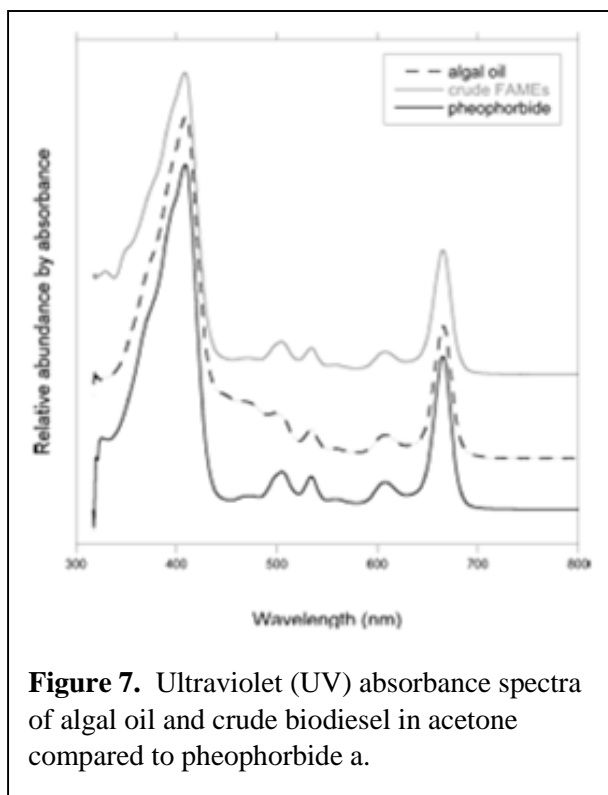
Extraction of *Isochrysis sp.*

The elemental composition of the dry biomass was tested before n-hexanes extraction, after n-hexanes extraction and the resulting hexane algal oil. The carbon, hydrogen, and nitrogen content for the dry *Isochrysis sp.* biomass were 47.7, 6.95, and 6.26% (Table 3).

Table 3. Isochrysis Dry Biomass Content

sample	carbon (%)	hydrogen (%)	nitrogen (%)	ash (%)
freeze-dried <i>Isochrysis sp.</i> biomass	47.7	6.95	6.26	14.9
dry biomass after n-hexane extraction	39.6	6.19	8.41	12.1
algal oil of <i>Isochrysis sp.</i>	74.3	10.4	0.82	
crude biodiesel of algal oil	78.2	11.2	1.13	

The post hexane extraction biomass had an elemental composition of the carbon, hydrogen, and nitrogen contents of the remaining were 39.6, 6.19, and 8.41%, respectively. Concentration of the hexane algal oil was performed by rotary evaporation of n-hexanes and yielded a dark-green/near-black “grease-like” material that could be handled as a liquid and poured from flask to flask when heated to 40 °C. The elemental composition of the hexane algal oil had carbon, hydrogen, and nitrogen contents of 74.3, 10.4, and 0.82%. The algal biomass was 19.1% w/w of the dry algal biomass compared to the advertised 17% by Reed mariculture for their *Isochrysis sp.* The proton NMR spectrum of the algal oil showed the presence of lipid material. The ultraviolet absorbance spectrum showed maxima at 410 nm, 505, 534, 609, and 665 nm, which are key indicators of chlorophyll degradation products pheophytin and pheophorbide (Figure 7). An additional red shoulder at 410 showed the presence of additional carotenoid pigments.



Acid-Catalyzed Esterification of the Algal Oil to Produce a Crude Biodiesel.

The esterification of the algal oil yielded a dark forest green substance which was solid at room temperature. The reaction converted 90% of the algal oil to crude FAME, which is in the same range as many recent studies. The crude FAME had an elemental composition of carbon, hydrogen, and nitrogen were 78.2, 11.2, and 1.13%, respectively. The proton NMR spectrum of the product showed a strong singlet peak at 3.7 ppm, a signal for methyl ester protons of the product FAMEs during the acid catalyzed esterification. The absorbance spectrum of the algal biodiesel was indistinguishable from that of pure pheophorbide and pheophytine (Figure 7).

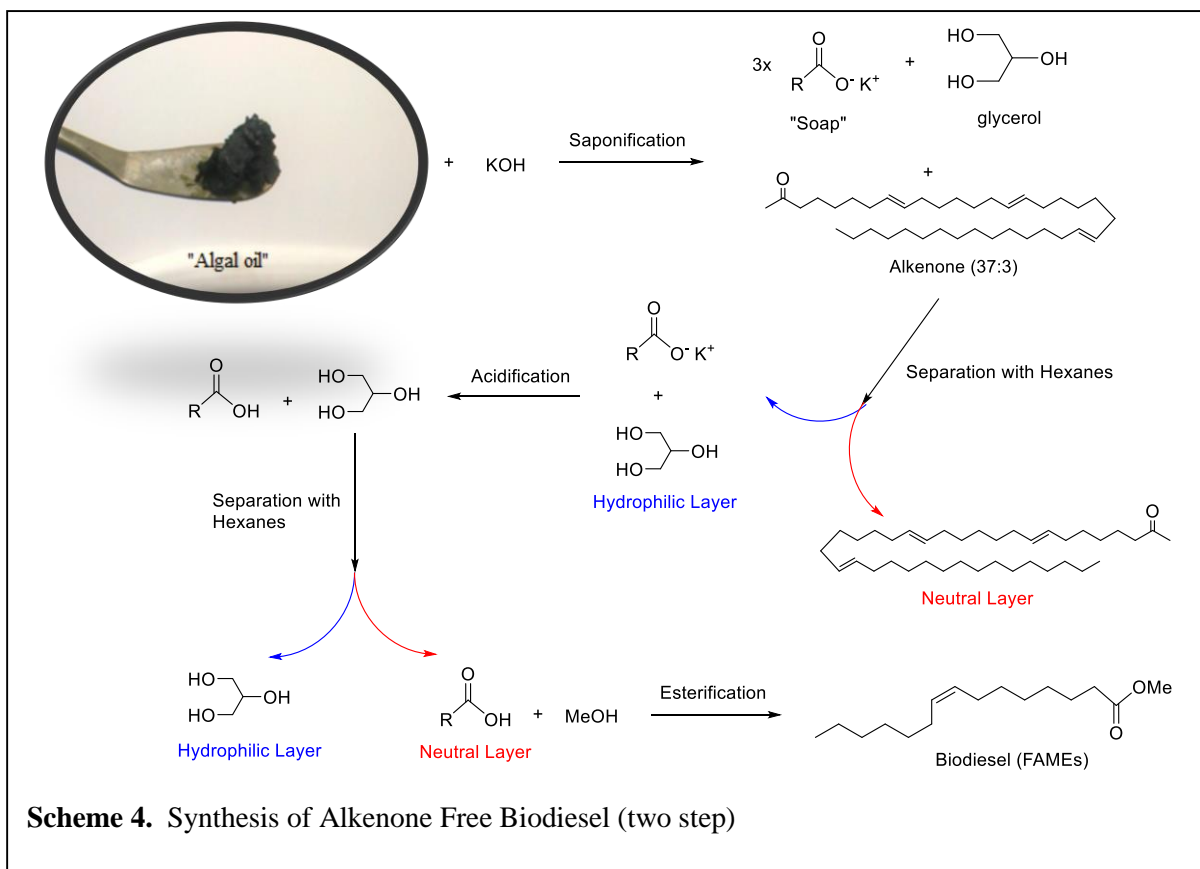
Analysis of *Isochrysis* Crude Methyl Esters.

The profile for the composition of the lipids in the *Isochrysis sp.* crude biodiesel indicated major FAME's present were 18:4n3, with a concentration of 104 mg/g and the fatty acid 22:6n-3, or docosahexaenoic acid (DHA) with a concentration of 74.6 mg/g of crude biodiesel. Other FAME's in the profile can be seen in (Table 4). The GC-FID of the crude biodiesel showed the presence of FAME's accompanied by late running peaks corresponding to the PULCA's. The presence of the alkenones in the biodiesel indicates that they are released from the lipid bodies in the cell during solvent extraction. This is not a complete surprise as it is well known that *Isochrysis sp.* and other members of prymnesiophyte taxa biosynthesize PULCA's. Our crude FAME sample had an alkenone concentration of 141 mg/g of crude FAME, made up of mostly 37:2 and 37:3 alkenones. The total lipid content of the sample was 67.5% of the crude product and was similar to literature values. There was no presence of free sterols or alcohols detected, and the 1.13% nitrogen in the crude biodiesel likely indicates the presence of chlorophyll-based pigments (Table 2).

Production of an Alkenone-Free Biodiesel.

Alkenones represent a significant proportion of the *Isochrysis* total lipid extract (TLE), are unaffected by transesterification, and remain a component of the resulting biodiesel. Their presence detrimentally affects the biodiesel cold flow fuel properties due to the high-melting points of these compounds. Otherwise, *Isochrysis sp.* is attractive as a biodiesel feedstock under the aspects of favorable growth properties and history of commercial mariculture. We therefore set out to devise a method for producing an alkenone-free *Isochrysis* biodiesel. It was thought that in addition to creating an improved biodiesel fuel, the method would also allow for the isolation of alkenones as a secondary

product stream. A traditional method for removing high-melting components and improving cold flow properties of biodiesel is winterization. In this method, the sample is cooled and the high melting point compounds are removed through filtration. We decided to investigate an alternative method for cold flow improvement by the removal of the alkenones from our crude FAME taking advantage of the different functionality of the acyl glycerols and that of the alkenones. Triglycerides esters are prone to saponification under aqueous basic conditions, which produces water-soluble FA salts (i.e. soaps). Alkenones remain unchanged during saponification which would allow for the alkenones (and other neutral lipids) to be selectively removed from the soaps by serial extraction in a separatory funnel with a nonpolar organic solvent such as hexanes. In the event, saponification of the algal oil was performed by first dissolving in a solution of MeOH (50 mL), CHCl₃ (25 mL), and H₂O (20 mL).



To this, KOH (4.0 g) is added to the solution and the mixture is then heated under reflux for 3 h at 60 °C (Scheme 4). Once separated, the isolated soaps can then be re-acidified with 6 M HCl and extracted from the aqueous phase to give the free fatty acids (FFAs). The FFAs are subsequently converted to a now alkenone-free FAME via acid catalyzed Fischer-esterification. Specifically, the free fatty acids (2 g) are dissolved in equal volumes of MeOH and CH₃Cl (8 mL ea.) and transferred to a high pressure flask. Sulfuric acid (1ml) is then added, the flask is sealed and heated for 1 h at 90 °C under pressure. The reaction mixture is then washed with deionized water, the layers are separated, and CH₃Cl is removed from the organic layer by rotary evaporation. In this way, an alkenone-free biodiesel is able to be collected in a 92% yield from the FFAs. This method for removal of alkenones from crude FAME proved to be remarkably efficient with consistent quantitative mass recoveries (60% FFAs and 40% neutral lipids) and a biodiesel free of alkenone contamination (Figure 8).

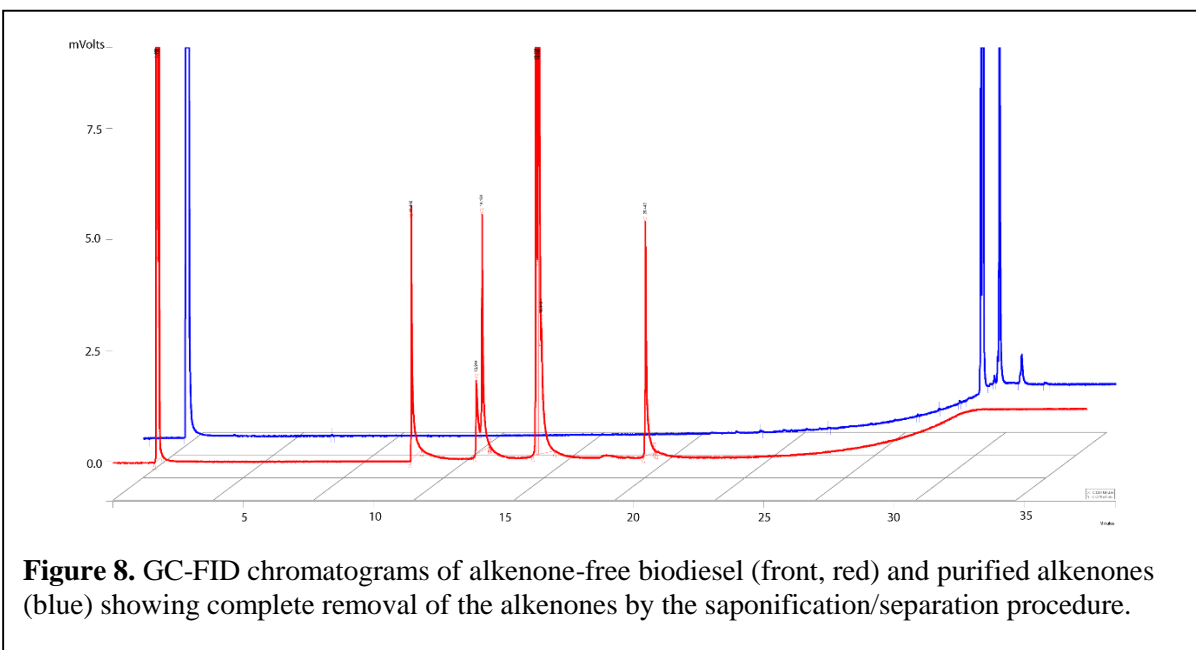


Figure 8. GC-FID chromatograms of alkenone-free biodiesel (front, red) and purified alkenones (blue) showing complete removal of the alkenones by the saponification/separation procedure.

Fuel Properties

The FAME profile of our alkenone-free biodiesel is given in Table 6. From this we can predict certain fuel properties. For instance due to the high amount of unsaturated FAMES, we would predict a low kinematic viscosity, favorable cloud point, and a poor oxidative stability. Unfortunately, these types of predictions are considered state of the art for most experimental algal biofuel research. This is due to the challenges associated with making sufficiently large amounts of material required for performing the various tests. As a result, many of these studies rely on calculations or simulations. As an example Fisher et al. recently published a report entitled “Measurement of Gaseous and Particulate Emissions from Algae-Based Fatty Acid Methyl Esters”, wherein exhaust emissions of an algal biodiesel were simulated by mixing vegetable oil and fish oil FAMES. The authors go on to state that this was done because of the scarcity of authentic algal biodiesel in a volume required to perform testing with.⁶¹ Recently Knothe investigated the fuel properties of neat FAME derived from two (C20:4 and C22:6) highly polyunsaturated fatty acids (HiPUFA) in connection with algal biodiesel.⁶² Other unsaturated algal FAMES were excluded for testing due to problems associated with cost and availability of pure standards. The commercial availability of multi-kilogram quantities of *Isochrysis* and efficiency of our processing allowed us to prepare sufficient quantities of our alkenone-free biodiesel with which to perform the various fuel tests contained in the document ASTM D6751. The results presented in Table 4 were published in the ACS journal *Energy & Fuels*, and represents to date one of the most complete reports on the fuel properties of a biodiesel made from algal oils.⁶³ As mentioned, many of the values listed in Table 4 are dependent on the fatty acid profile (e.g., cetane, kinematic viscosity, viscosity, and oxidative stability) and can be predicted as shown in Table 5. Since we were able to obtain actual data for these properties, by comparison we could therefore assess the accuracy of those predictions. The results for each of the fuel properties are discussed in detail in the following sections.

Table 4. Fuel Properties of the Alkenone-Free *Isochrysis* Biodiesel.

Property	Result	ASTM D6751	EN 14214
Cetane number	36.53	47 min	51 min
Kinematic viscosity (40°C, mm ² /s) ^{a)}	2.46	1.9-6.0	3.5-5.0
Oxidative stability (h)	0.06	3 min	6 min
Density (15°C, kg/m ³)	934.92	---	860-900
Lubricity (µm; HFRR)	260	520 max (ASTM D975)	460 max (EN 590)
Free glycerol (mass %)	0	0.020 max	0.02 max
Total glycerol (mass %)	0.029	0.240 max	0.250 max
Monoglycerides (mass %)	0.034	0.40 max	0.70 max
Na (ASTM D6751: ppm (µg/g) / EN 14214: mg/.kg)	3.5	5 max combined	5.0 max combined
K (ASTM D6751: ppm (µg/g) / EN 14214: mg/.kg)	0.2		
Mg (ASTM D6751: ppm (µg/g) / EN 14214: mg/.kg)	0	5 max	5.0 max combined
Ca (ASTM D6751: ppm (µg/g) / EN 14214: mg/.kg)	1.1		
P (ASTM D6751: % mass / EN 14214: mg/.kg)	0	0.001 max ^{b)}	4.0 max ^{b)}
S (ASTM D6751: % mass (ppm) / EN 14214: mg/kg)	170	0.0015 (15) max ^{b)} mass (for blending with 15 ppm sulfur diesel fuel	10 max ^{b)}

^{a)} Determined on an individual batch (~10 g) prior to blending. ^{b)} Limits listed as given in the standards.

Table 5. Comparison of fuel properties for alkenone-free *Isochrysis* FAME (*Iso*-ME) and values for methyl esters from soybean (SME) and canola (CME).

	<i>Iso</i> -ME	SME	CME
Cetane number	36.5 (40.3) ^A	52.1 ^B (49-50) ^C	50.4 ^D (54) ^E
Kinematic viscosity (40°C, mm ² /s)	2.46 (3.2) ^A	4.12 ^F	4.42 ^F
Oxidative stability (h)	0.06	5.0 ^F	6.4 ^F
Lubricity (µm; HFRR)	260	136 ^F	169 ^F

^ACalculated value according to reference 31. ^BExperimental value for commercial SoyGold (AEP; Omaha, NE). ^CCalculated value from reference 52, the range is due to slightly differing fatty acid profiles given in numerous references not cited. ^DReported value for optimized CME from reference 53. ^ECalculated according to reference 31 from the fatty acid profile given in reference 54. ^FReported values from reference 54.

Cetane number

CN is an indicator of the combustion characteristics of diesel, where a higher value is desirable. Higher CN equates to a shorter delay between the injection event and combustion, resulting in reduced engine knock which also improves exhaust emissions. CN values for biodiesel can be estimated by the sum of the CNs for each individual neat or pure methyl ester in the FAME profile (Table 6) by application of the CN equation. Where CN_{mix} is the CN for the biodiesel sample, A_c is the concentration or the % volume of the individual FAME in the biodiesel sample, and CN_c is the CN of the individual neat methyl ester.

$$CN_{mix} = \sum A_c \times CN_c \dots \dots \dots [6]$$

The predicted CN value by application of the CN equation to the data in Table 6 would be approximately 40.08 (eq. 6). This value is slightly higher than the measured value of 36.5 (Table 4). One must keep in mind when comparing CN values, that these values are not absolute and the result can often vary. Regardless, from our measured CN and our predicted CN value, it can be concluded that the CN value for the alkenone-free Isochrysis biodiesel is below the required minimum specification in the ASTM D6751 (47 min) and even more so for the stricter EN 14214 (51 minimum). Alkenones themselves would most likely have a high CN value because of the of their long carbon chain and by their removal this may decrease the overall CN of the fuel. However if one were to try to use alkenones to increase the CN value for our algal biodiesel, it would likely require large quantities to meet the minimum ASTM, and of course this would be at the expense of cold-flow. Nonetheless, the effect of alkenone content in fuel and the corresponding CN effect is of interest and may be investigated in future research.

Table 6. FAME Composition of Alkenone-Free *Isochrysis* Biodiesel Samples.

FAMES	Sample-1 (%)	Sample -2 (%)^C	Sample -3 (%)^H
14:0	16.7	13.7	11.3
15:0	0.3	0.2	0.2
16:0	12.9	10.8	9.4
16:1 Δ 9	6.9	5.3	5.5
16:2	0.8	0.7	0.4 ^E
16:3	2.1	ND	ND
17:1 Δ 9	ND	ND	0.1
18:0	0.1	ND	ND
18:1	11.8 ^A	11.8 ^A	10.5 ^A
18:2	8.0 ^B	6.4	7.9
18:3	5.2	7.2 ^C	8.0 ^F
18:4	18.2	22.2	21.8
18:5	ND	2.6	2.2 ^G
20:5	2.9	0.8	1.1
22:5	ND	1.7	1.5
22:6	7.9	11.65	12.1
Σ	93.8	95.0	92

^ACombined 18:1 Δ 9 + 18:1 Δ 11. ^BIncluding a likely 18:2 with double bond positions not determined (1.4%). ^CNote that a fatty acid profile of the hexanes extract (“algal oil”) used to produce this FAME was also determined and the values were very similar. ^DLikely a mixture of two double bond positional isomers. ^ECombined % of two double bond positional isomers (Δ 6,9 and Δ 9,12). ^FCombined Δ 6,9,12 and Δ 9,12,15 isomers. ^GSlight ambiguity with assignment. ^HLarger volume blended sample (## mL) prepared by combining individual batches and used for fuel testing.

Kinematic Viscosity

The kinematic viscosity (KV) of biodiesel has a general trend where the KV decreases with an increasing number of cis double bonds present in the FAME. Algal biodiesel is characterized by high polyunsaturated fatty acid methyl ester content and we would therefore expect the biodiesel to have low KV. Similarly to the way that a CN value can be estimated from individual component FAMES that make up the total sample, KV can also be predicted from the individual KVs of individual neat FAMES. With the ratio of the FAMES that is present in the sample and their KV, a KV for the total sample can be predicted. From the values listed in Table 6, the KV of our alkenone-free biodiesel is calculated to be approximately 3.2 mm²/s. A KV of 2.46 mm²/s at 40°C was measured, which was lower than this calculated value. Two additional samples of algal *Isochrysis* FAME were prepared (~10 mL) to check the accuracy of the KV value, but regrettably no reliable data could be collected as these later samples tended to plug various viscometer tubes that were tried during analysis. After further inspection, it was found that some insoluble material in the samples were to blame for the failed runs. This is possibly accredited to the fact that the FFA profile in Table 6 only tallies up to a value slightly higher than 90%. The remaining approximate 10% material is composed of numerous unidentifiable components that are each present in small amounts. This unidentified material may also contribute to the difference between the calculated and measured values for KV. Inhomogeneity has been recently reported in the literature for blended biodiesel sample produced from *Isochrysis galbana*, where the collected sediment had a similar FFA profile.⁶³ The measured KV for this sample was reported to be 4.10 mm²/s and was tested with the same ASTM Standard D445 method. Interestingly this value is higher than both our measured and calculated value for our *Isochrysis sp.* FAME. No FAME profile was reported in this work by Kumar and coworkers making comparison of predicted fuel properties not possible. If our measured KV of our algal biodiesel is in fact accurate, this would

potentially be advantageous and falls into the prescribed range that is mandated by the ASTM D6751. While it is below the range specified by the EN 14214 where the minimum of viscosity specification is $3.5 \text{ mm}^2/\text{s}$, there is no technical reason for this value as conventional petrodiesel fuels tend to exhibit KV values below $3.5 \text{ mm}^2/\text{s}$.

Oxidative Stability

Fatty acids with high amounts of unsaturation, cis double bonds that are interrupted by methylene units, yield fuels with a poor oxidative stability. Algal biodiesel produced from *Isochrysis* sp. has significant amounts of HiPUFAMES and would therefore be expected to have poor oxidative stability.). This prediction was found to be true as the measured oxidative stability was found to be only 0.06 h, whereas the minimum prescribed in the standards is 3 h. For perspective, the oxidative stabilities by Rancimat induction times of neat FAMES C20:4 and C22:6 were recently found to be 0.09 and 0.07 h, respectively.⁶² From this comparison, it is not surprising algal biodiesel produced from *Isochrysis* would have poor oxidative stability.

Density and Lubricity

Lubricity and density of any liquid fuel are important because of the effect they can have on engine performance. Lubricity values for biodiesel are often not problematic. This is likely credited to the ester carbonyl functional group and biodiesel has even been shown to restore lubricity to low value blends of low sulfur (1– 2%) petrodiesel. The measured lubricity for our alkenone-free biodiesel was similar to biodiesel fuels from other feedstocks, being well below the maximum wear scars of 460 and 520 μm prescribed in the petrodiesel standards EN 590 and ASTM D975, respectively.⁶⁴ In regards to density of biodiesel, this value is dependent on the raw material used in the production of resulting

fuel profile. Work by Pratas and coworkers demonstrated that density could be accurately predicted for 10 biodiesel samples using linear mixing rules provided that the composition of the fuel and the densities of the neat FAMES are known. Knothe has measured the densities of neat FAMES C20:2, C20:3, C20:4, and C22:6. Each of these individual FAMES exceeded the maximum specification of European standards, EN 14214, but it was concluded that other FAMES present in an algal biodiesel with lower density would likely offset the higher density of the HiPUFAMES producing a mixture within the specified range. The measured density of alkenone-free *Isochrysis* biodiesel at 15 °C was found to be 934.92 kg/m³, which is higher than the maximum prescribed value in EN 14214 (900 kg/m³). If the high density is accredited to the HiPUFAMES in our biodiesel sample (42% ≥ 4 double bonds, Table 6) then our *Isochrysis* biodiesel might be used as a gauge to compare with other algal biodiesel mixtures. For example, from a recent publication, 12 algal classes were reported to have a range of 26 to 59%⁶⁵, where half of these samples had a HiPUFA content greater than 42%. These may then be expected to exhibit densities greater than that of the EN 14214 maximum.

Glycerol and Heteroatom Content

The amount of glycerol (total and free) in the biodiesel was much lower than the allowed maximum levels of the ASTM. The low glycerol content is not surprising as our method extracts and separates the FFAs from the glycerol in the aqueous layer, with a nonpolar solvent. Sulfur was the only heteroatom that exceeded specification of the ASTM. It is thought that the high sulfur content in the *Isochrysis* biodiesel is due to the high amount of inorganic sulfates present in the F/2 algal culture medium that in which the algae is grown.⁶⁶ The elemental analysis results appear to support this source of sulfur as the highest content was found in the starting algal biomass (Table 7). Analysis of the algal oil and FFAs only showed trace amounts (<0.1% w/w) with most of the sulfur remaining in

the biomass after extraction with hexanes. However, maximum allowable sulfur levels are exceedingly low (15 ppm/ 10 ppm, ASTM D6751/EN 14214) making the alkenone free biodiesel fail (170 ppm) the strict sulfur specifications.

Table 7. Elemental Analysis.

Sample	%Carbon	%Hydrogen	%Nitrogen	%Sulfur	%Ash
Freeze-dried <i>Isochrysis</i> sp. biomass	50.49	6.83	7.24	1.15	5.8
Hexane-extracted <i>Isochrysis</i> . biomass	43.94	6.18	8.67	1.02	9.2
Algal oil of <i>Isochrysis</i>	70.69	10.18	-	trace*	-
<i>Isochrysis</i> FFAs	76.02	11.05	-	trace*	-
<i>Isochrysis</i> Alkenone-Free Biodiesel	78.55	10.96	0.77	trace*	-
<i>Isochrysis</i> Neutral Lipids	70.55	10.37	0.55	-	6.5

* < 0.1% Note: The biodiesel would still exceed the sulfur specification in biodiesel standards according to our analysis as the specification for sulfur is well below 0.1%.

Cold Flow Properties of the Alkenone-Free *Isochrysis* Biodiesel

Previous work by the O’Neil group demonstrated the dramatic and detrimental effect of high melting alkenones on the cold flow property of biodiesel.⁶³ As predicted, removal of alkenones from the biodiesel markedly improved the cold flow properties compared to the alkenone-containing FAME mixture (liquid vs. solid at room temperature). A significant amount of solids (40% w/w) that were originally present in the algal oil were removed by the saponification and extraction procedure (Table 2.). Unfortunately, the dark color of the alkenone-free biodiesel prevented us from obtaining CP or PP values due to limitations in seeing when the fuel starts to solidify.

Decolorization of algal Biodiesel from *Isochrysis* sp.

While the CP of our alkenone-free biodiesel clearly improved, our inability to measure a CP prevented us from confirming and quantifying our original hypothesis connecting alkenones to the obvious poor cold-flow properties of our crude biodiesel. In an effort to measure the CP of our alkenone-free *Isochrysis* biodiesel, we investigated a method to remove pigments using MK10 clay. This procedure had been previously reported by Kulkarni and coworkers.⁷¹ Additionally, a comparison of fuel properties for our decolorized vs. non-decolorized biodiesel revealed insights into the impact of pigments like chlorophylls on fuel properties.

Decolorization of the biodiesel using montmorillonite K 10

Decolorization of our green alkenone-free biodiesel was performed by stirring over 20% (w/w) MK10 for 1 h at 60 °C, which proved to be an efficient method in removal of pigments. This could be seen qualitatively by the color change of biodiesel from dark green to a bright orange. During this process the MK10 changes from a white powder to black. Upon storage of the decolorized fuel a small amount of grainy material precipitated out of the fuel (<10% w/w) and this material could be easily removed by decanting or if necessary through centrifugation. The mass recovery for the particulate-free biodiesel were typically 85–95% (w/w).

FAME analysis of decolorized *Isochrysis* biodiesel

The FAME profile of the decolorized and non-decolorized biodiesel were nearly identical showing viability in the application of the decolorization process (Table 1). For each biodiesel sample tested (one non-decolorized and three decolorized) the major fatty acid in the profile was 18:4, at

approximately 21 mg/g of crude FAME. The non-decolorized biodiesel samples had the highest amount of polyunsaturated fatty acid content (Non-D, 42.4%) but, the decolorized all four samples were in a similar range (e.g. 39.7% = 10.3 (18:3) + 21.0 (18:4) + 8.4 (22:6) for D-Iso-1). Other individual FAMES for each of the individual batches are listed in Table 8.

Table 8. Fuel Properties of Non-decolorized (Non-D) and Decolorized *Isochrysis* (D-Iso) Biodiesel Fuels.

Property	Non-D	D-Iso-1	D-Iso-2 ^d	ASTM D6751	EN 14214
Cetane number	36.53	42.3	48.4	47 min	51 min
Kinematic viscosity (40°C, mm ² /s) ^a	2.46	3.38	3.76	1.9-6.0	3.5-5.0
Oxidative stability (110°C; h)	0.06	0.35	0.05	3 min	6 min
Cloud Point (°C)	ND	-6.0, -6.0 ^c	-5.8, -5.6 ^c	Report	
Pour Point (°C)	ND	-8.6, -8.4 ^c	-6.0, -6.0 ^c	Report	
Density (15°C, kg/m ³)	934.92	895.52	898.54	---	860-900
Lubricity (µm; 60°C; HFRR)	260	131, 125 ^c	136, 133 ^c	520 max (ASTM D975)	460 max (EN 590)
Free glycerol (mass %)	0	0.004	0.0045	0.020 max	0.02 max
Total glycerol (mass %)	0.029	0.025	0.033	0.240 max	0.25 max
Monoglycerides (mass %)	0.034	0.029	0.020	0.40 max	0.70 max
Acid Value (mg KOH·g ⁻¹)	ND	3.029	5.139	0.50 max	0.50 max
Moisture	ND	345 ppm	ND	0.05% max (v/v)	500 max mg/kg

^aDetermined on an individual batch (~10 g) prior to blending. ^bLimits listed as given in the standards. ^cDuplicate measurements. ^dPrepared from an older algal oil, stored at ~20 °C for two years (ref. Table 1). ^eND = Not determined.

The D-iso-2 sample had been produced from an algal oil that was stored for two years at 20 °C and was found to have a slightly higher proportion of saturated algal FAMES (30.6% vs. 26.5% for D-Iso-3)

and a lower unsaturated FAME content, which is consistent with stability trends for these compounds. For all samples that were tested, 95% of the sample was identified as FAME. It is worth noting that none of the FAME would meet the EN 14214 requiring <1% FAMEs with more than three double bonds. The ASTM D6751 does not have this stringent limitation as the addition of antioxidants are used to overcome this issue in American markets.¹⁹

Pigment removal and cloud point analysis of an *Isochrysis* biodiesel

With regard to cold flow properties, the most stringent is the cloud point, which can be correlated to other tests such as cold filter plugging point. Experimental data on CP values for algal biodiesel are quite rare with the exceptions being work by Suganya T., Rao YR and coworkers.^{67, 68} For example, the fairly extensive testing of a biodiesel from the microalgae *Schizochytrium limacinum* lacked a CP value.⁶⁹ It could be that the overall unavailability of CP data for algal biodiesel is due to similar difficulties we have encountered with our initial *Isochrysis* biodiesel being too dark to measure a CP. Like all photosynthetic organisms, *Isochrysis* also contains the chlorophylls and pheophytins pigments that have potential to degrade into compounds like pheophorbides. It has been reported⁷⁰ that chlorophyll and its derivatives have a detrimental effect on the stability of the vegetable oils.⁷¹ Methods utilizing solid materials such as clays and activated carbon have been used to selectively chlorophylls and pheophytins from these mixtures. The work by Issariyakul and Dalai is an example who showed the effectiveness of montmorillonite K 10 (MK10) clay for selectively removing pigments from greenseed canola oil for use in biodiesel production.⁷²

Application of Issariyakul and Dalai method using MK10 at a 20% (w/w) ratio to our green non-decolorized biodiesel resulted a notable reduction in pigment content by visual inspection of color change (Figure 8). Further UV-vis analysis of decolorized algal biodiesel showed an absence of

chlorophylls and pheophytins peaks in the absorbance spectrum of the now orange/red biodiesel. Likely the selective (90% mass recovery) interaction between the acidic MK10 and the pigments involves the Lewis basic site of the porphyrin structure.⁷³ The CP values for our decolorized biodiesel fuels were expected to be low, but the actual values that were obtained (-6.0 and -6.0, duplicate analysis for D-Iso-1; -5.8 and -5.6 C duplicate analysis for D-Iso-2) were even lower than what would be predicted based on the FAME profile. The pour points (PP) were also remarkably low taking into account the large amounts of saturated FAMES in the profile (e.g. 15% C16:0). For comparison, soybean biodiesel (SME) contains roughly 10% methyl palmitate (C16:0) and has CP and PP values of 1 C and 0 C. SME on the other hand also contains approximately 5% of even a higher melting point compound, methyl stearate (C18:0), where *Isochrysis* only has trace amounts. The CPs are easily influenced by small amounts of high melting point compounds and the difference between SME and our *Isochrysis* biodiesel can be partially explained by the methyl stearate. Efforts to explain the discrepancy between our biodiesel and refined predictive methods continue.

Cetane number

Prescribed minimum values of CN for commercial biodiesel are 47 and 51 according to the ASTM D6751 and EN 14214, respectively. Our initial green *Isochrysis* or non-decolorized biodiesel had a measured CN value of 36.5 (Table 2). The decolorized samples both had higher CN values than the non-decolorized samples, where one meet the standards for the ASTM standards (42.3 and 48.4). When comparing and calculating values of CN care must be taken, as these values are not absolute and often variable. For example, in a recent comprehensive evaluation of this value, the CN of methyl oleate was at best estimated to be within a range of 56-58 using data collected from 23 different CN

tests.⁷⁴ Regardless, pigment removal from our *Isochrysis* biodiesel improved the CN to a value very close to meeting US standards (avg. for samples = 45).

Kinematic viscosity

Biodiesel derived from algae with HiPUFAME content is expected to have low kinematic viscosity, although some with higher KV have been reported.⁷⁵ For our non-decolorized fuel we reported a viscosity of 2.46 mm²/s at 40 °C, which was lower than the predicted kinematic viscosity of 3.2 mm²/s, calculated from our FAME profile.⁷⁶ Attempts to check this value were not fruitful, as samples tested for accuracy of our original sample, consistently plugged viscometer tubes due to the presence of some insoluble material. However, our final decolorized biodiesel product was free of these problematic particulate and we were able to collect data from two samples. We measured kinematic viscosities of 3.38 and 3.76 mm²/s which were similar to the predicted value based on the FAME profile (3.2 mm²/s). Our decolorized samples kinematic viscosity are on the low end of the range for the ASTM D6751 prescribed standards and close to the minimum required value in EN 14214. While our sample did not meet the minimum viscosity of 3.5 mm²/s in the EN 14214, it is not clear as to why this is a prescribed requirement, as conventional petrodiesel fuels generally exhibit viscosity values below 3.5 mm²/s.

Oxidative stability

Non-decolorized *Isochrysis* biodiesel suffers from poor oxidative stability with values well below the ASTM minimum specification. The reason for this is the presence of the primarily high PuFAME in the fuel, where fatty acids with greater unsaturation results in lower oxidative stability (Table 9)⁶², although pigments have also been shown to have an adverse effect on biodiesel oxidative stability.⁷⁷

Table 9. FAME Composition of Non-Decolorized (Non-D),²³ and Decolorized *Isochrysis* Biodiesel (D-Iso) Samples.

FAMES	Non-D ^A	D-Iso-1	D-Iso-2 ^D	D-Iso-3
14:0	13.9	14.3	17.1	16.4
15:0	0.2	ND	0.4	trace
16:0	11.0	10.1	12.4	10.1
16:1 Δ9	5.9	7.0	6.6	7.6
16:2	0.6	ND ^F	trace	ND
16:3	0.7	ND	ND	ND
18:0	Trace	ND	1.1	Trace
18:1	11.4 ^B	10.8 ^B	11.0 ^B	12.1
18:2	7.4	9.9	6.5	8.1
18:3	6.8 ^C	10.3 ^C	6.9 ^C	8.5
18:4	20.7	21.0	18.3	19.8
18:5	1.6	ND	ND	ND
20:5	1.6	ND	ND	ND
22:5	1.1	ND	ND	ND
22:6	10.6	8.4	8.2	6.9
Σ	94.9	91.8^E	88.5^E	89.8^E

^AAverage values from three separate samples. ^BCombined 18:1 Δ9 + 18:1 Δ11. ^CCombined Δ6,9,12 and Δ9,12,15 isomers. ^DPrepared from an older hexane algal oil that was stored at ~20 °C for two years before being used for this study. ^EThe remaining material is roughly 50:50 other FAMES and non-FAME components (Total ~95% FAME). ^FND = Not detected.

The highest oxidative stability among all of the samples tested would therefore be predicted to be D-Iso-2, which had a higher proportion of saturated fatty acids and also lacked the presence of harmful pigments. D-Iso-2 in fact had a lower oxidative stability than D-Iso-1 (0.05 h vs. 0.35 h) and essentially the same value as the non-decolorized biodiesel (0.06 h). All of the oxidative stability for the samples

where however quite low, so the difference would likely not have a major effect on any practical applications of the fuel production. D-Iso-2 also had the lowest percentage of Identified FAMES (88.5%). Minor undetermined components in the sample might have a greater effect on the oxidative stability than predicted.

Lubricity and density

Lubricity is becoming an increasingly important and recognized property in the field of biodiesel with more stringent limitations on sulfur content due to environmental implications. The HFRR wear scars of the decolorized Isochrysis biodiesel samples were well below the maximum wear scars of 460 μm and 520 μm prescribed in the standards EN 590 and ASTM D975, respectively. The values collected (131 and 125 μm , duplicate analysis for D-Iso-1; 136 and 133 μm , duplicate analysis for D-Iso-2) show improvement from the non-decolorized biodiesel (260 μm), and values are now more in line with measured lubricities for other commercial biodiesel from other feedstocks (e.g. soy-derived biodiesel around 130 μm).⁷⁸

The value of fuel density relates to fuel performance (e.g. within the injection system). Biodiesel and petrodiesel have different densities which raises concerns about potential mismatching of engine parameters when using biodiesel in engines optimized for petrodiesel.⁷⁹ As a result, the European standard EN-590 232 establishes a density range for diesel fuels of 820–845 kg/m^3 at 15 °C. Biodiesel fuels usually have higher density values than petroleum. Care must therefore be taken in measuring accurate densities to calculate appropriate blend ratios that will meet this specification. Again, the availability of experimental density data for algal biodiesel fuels is limited.⁸⁰⁻⁸² While data is limited, density values can be predicted from FAME profiles using linear mixing rules and the known densities of neat FAMES.⁶² Our measured density for non-decolorized Isochrysis biodiesel at 15 °C was 934.92

kg/m³, above the maximum (900 kg/m³) prescribed value in EN 14214. After decolorization, the densities measured were 895.5 and 898.5 kg/m³ for D-Iso-1 and D-Iso-2 respectively, which now just fall within the EN 14214 range (max. = 900 kg/m³).⁷⁶ The FAME profiles for the decolorized and non-decolorized samples were essentially the same, which would suggest that the change in density observed between the decolorized and non-decolorized is related to the pigments present in the fuel (ref. Table 1). Additional experiments are needed to understand how such low levels of these compounds could cause these changes.

Glycerol and FFA and moisture content

Glycerol, FFA, and moisture content (345 ppm for D-Iso-1) have not been an issue for the fuel that we produce through our method according to ASTM D6751 and EN-14214. On the other hand, the acid values exceed the limitations according to these specifications. The reason for this specification is that acidity of diesel fuel can cause corrosion that could result in the formation of engine deposits.⁸³ In our processing we first convert all of the triglycerides to FFAs. The acid value therefore represents the percent yield for the esterification step, or 98.6% (Acid Value = 3.029 = 1.383% FFAs) and 97.7% (Acid Value = 5.139 = 2.347% FFAs) for D-Iso-1 and D-Iso-2, respectively. The ASTM D6751 and EN-14214 acid value limit of 0.50 corresponds to an exceedingly low FA content of approximately 0.25%, meaning we would need to achieve an esterification yield of 99.75%. Alternatively we might reduce the acid value of the final product by other means.⁸⁴ Future work on the project will include efforts in optimization of this parameter toward the production of a commercially viable *Isochrysis* biodiesel.

Comparison of Biodiesel Production with Isolation of Alkenones from Two Commercial *Isochrysis* Sources

Isochrysis is one of only a select number of algal species farmed commercially and is harvested as a major component of shellfish food. The availability of the algae used and the standard methods employed in this work, are in efforts to make this protocol presented widely accessible to other groups for further investigations. It is expected that the yields may differ as a result of different strains and cultivation methods used in the growth period³³. Yields may also be impacted by the nature of the product and any additional processing (e.g. drying or freezing) methods by the supplier. To test this, we purchased two different types of commercial *Isochrysis* products: a wet paste (80% water) from Reed Mariculture (San Jose, CA) and a dry (95% dry) milled powder from Necton S.A (Olhão, Portugal).



Figure 9. Comparison of algal biomass from commercial sources (Nekton left and Reed right)

The starting dry biomass material from Reed and Necton has stark differences in color (Figure 9), however after extraction, the corresponding hexane algal oils (i.e. *Iso*-paste-**hAO** and *Iso*-powder-**hAO**) were indistinguishable, both dark green/near black solids with melting points of approximately 50 °C. Yields of the algal oils were however different, 12% w/w of the *Iso*-paste-**hAO** and 7% w/w of

the *Iso*-powder-**hAO**. Another difference was the ratio of FFAs to neutral lipids within the two hexane extracts. After the algal oil was saponified and the neutral lipids were separated, we typically obtain 60% (w/w) FFAs and 40% (w/w) neutral lipids from the *Iso*-paste-**hAO**. The *Iso*-powder-**hAO** produced on average 46% (w/w) FFAs and 54% (w/w) neutral lipids. This leads us to believe that the starting algal powdered biomass either contains higher amounts of neutral lipids or Soxhlet extraction of the biomass with hexanes is somewhat selective for neutral lipids. In addition to the product yields from the two commercial biomasses being different, there were also differences within the fatty acid profiles of the resulting biodiesel. This is important because the fuel properties of the biodiesel are directly dependent on the nature and contents of individual FAMES.⁸⁵ As previously mentioned, to be commercialized, all biodiesel must conform to the standards described in the documents ASTM D6751 or EN 14214 in the U.S or Europe respectively. Overall, the FAME profile of biodiesel produced from the Necton biomass was similar to those previously tested, such that we can predict that certain fuel properties will be similar for both biodiesel fuels. For instance the polyunsaturated fatty acids (PuFAMES, more than two double bonds) account for approximately 40% of both FAME mixtures (35.2% and 39.9%, Table 10). This will empirically result in poor oxidative stability and favorable cold-flow values.⁸⁵ While there are many similarities, there are slight differences in the FAME profiles of the two biodiesel samples. Algal biodiesel produced from the powdered Necton contained higher amounts of 14:0 (19.4 mg/g vs. 16.4 mg/g), 18:3 (13.5 mg/g vs. 8.5 mg/g), and 22:6 (11.0 mg/g vs. 6.9 mg/g) FAMES, and lower amounts of 18:4 (10.4 mg/g vs. 19.8 mg/g). The extent to which these differences effect the ASTM properties of the fuel remains to be investigated. Both biodiesel samples from Reed and Necton were similarly dark green in color, which is explained by the presence of pigments, such as chlorophyll.⁸⁶ Chlorophyll, its derivatives and degradation products have been shown to have a negative effect on the stability of vegetable oils and their corresponding biodiesel.^{71,72} Again using the previously mentioned method of Issariyakul and Dalai,⁷² stirring our green biodiesel

Table 10. FAME composition of biodiesel produced from commercial Iso-Paste and Iso-Powder *Isochrysis sp.*

FAME	Iso-paste	Iso-powder
14:00	16.4	19.4
14:01	-----	0.3
15:00	Trace	0.3
16:00	10.1	8.8
16:1 Δ9	7.6	5.5
16:02	ND	0.3
16:03	ND	0.5
18:00	Trace	0.2
18:1b	12.1	14.3
18:02	8.1	7.1
18:03	8.5	13.5
18:04	19.8	10.4
18:05	ND	3
20:05	ND	-----
20:05	ND	2
22:06	6.9	11
Σ	89.8	96.2

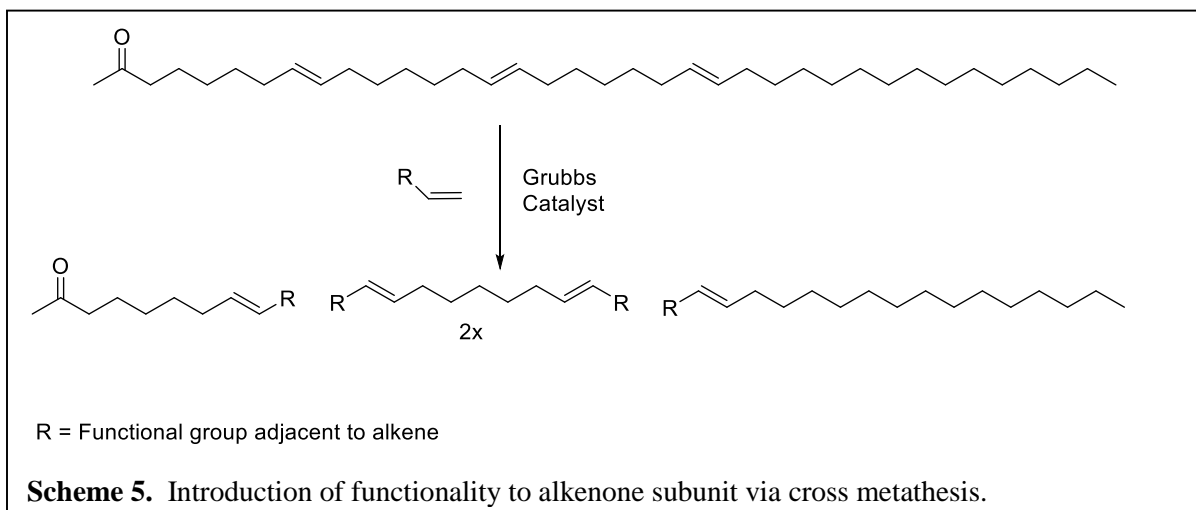


Figure 10. Comparison of non-decolorized (left) and decolorized (right) *Isochrysis* biodiesel fuels.

over 20% (w/w) MK10 at 60 °C for 1 h resulted in a dramatic reduction in pigment content by visual inspection (Figure 10). Mass recoveries for the decolorization process were on average 90%. Yields of the alkenones from *Iso-paste-hAO* and *Iso-powder-hAO* neutral lipids were comparable at 40% and 46% w/w respectively. Since neutral lipids represent a higher proportion of material contained in the Necton algal oil, the alkenone yield from the Necton exceeds the Reed yield by approximately 10% (25% w/w vs. 16% w/w). Though, we taking into consideration that yields of the Necton algal oil were lower than Reed algal oil (15% vs. 20% w/w), overall yields of alkenones from both dry *Isochrysis* biomasses are more similar ($0.2 \times 0.4 \times 0.4 = 3.2\%$ w/w from dried Reed and $0.15 \times 0.54 \times 0.46 = 3.7\%$ from Necton).

Chapter 4: Isolation of value added products from *Isochrysis sp.*

Our work has demonstrated that high-quality biodiesel can be produced from a common algae in large volumes, and that has passed a battery of ASTM standards. Nonetheless, challenges remain for the production of a commercial product. Critics of algal biofuel programs tend to focus on projected costs of the overall process, echoing one conclusion from Sheehan's report on the United States Department of Energy-sponsored Aquatic Species Program (ASP).¹⁴ For instance in a recent perspective on microalgal transportation fuels,⁹¹ van Beilen argues that "only if the algal biomass is a byproduct of the production of high-value compounds such as astaxanthin or β -carotene, commercially viable energy production from algal biomass might be feasible." Many others including Chisti⁹² and Wijffels⁹³ have stressed the importance of value added coproducts as a necessary component of algal biofuel production.

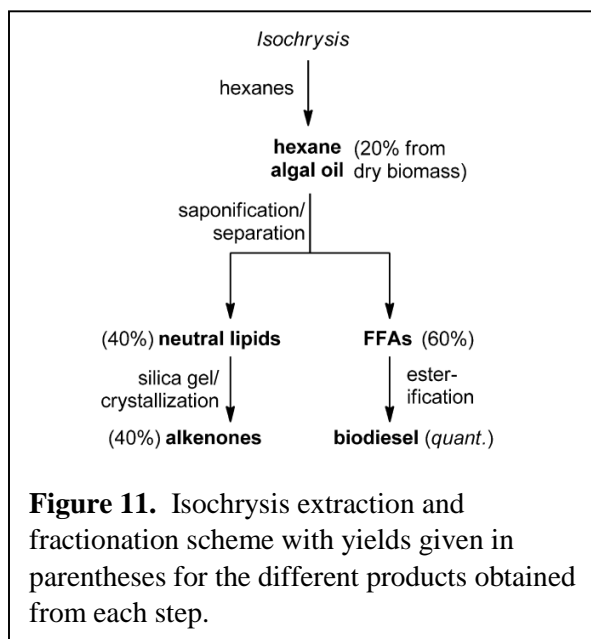


In fact, the United States Department of Energy (DOE) “National Algal Biofuels Technology Roadmap” (NABTR) identifies valuable coproducts as one of the key reasons for exploring algae as a source of biofuels.⁹⁴ Our processing of *Isochrysis* into biodiesel involves separation and isolation of alkenones. In addition to improving the fuel properties of the biodiesel, these alkenones could represent a secondary product stream. Alkenones contain a number of *trans*-double bonds. As shown in Scheme 5, reaction of these double bonds via cross-metathesis would produce smaller fragments. Depending on the choice of cross-metathesis partner, different size products could be formed which would represent different fuel ranges (e.g. C₁₀ – C₁₆ = kerosene/jet fuel).

Production of Jet Fuel Range Hydrocarbons as a Coproduct of Algal Biodiesel by Butenolysis of Long-Chain Alkenones

We decided to investigate jet fuel as a potential alkenone-derived cross-metathesis product. Alternative aviation fuels are an important target due to the fuel requirements for high performance jet engines⁹⁵. Before attempting any reactions, we isolated and purified the alkenones from the neutral lipid fraction containing other compounds including pigments such as chlorophylls and carotenes.⁹⁶ This was a challenging due to the low solubility of the alkenones in a wide variety of organic solvents (e.g., hexanes, diethyl ether, acetone, ethyl acetate). After optimization and investigation of the method, the dark colored pigment containing material, could be removed. This was done by applying the decolorization technique previously used on non-decolorized biodiesel to the neutral lipids. Where the neutral lipids were dissolved in minimal amount of hexanes, heated to 60 °C and to the solution MK10 was added as a 20% w/w ratio. The MK10 was then removed by filtration and the resulting material was then further purified by flushing it through silica using a minimal amount of dichloromethane (DCM) as eluent. The eluent, now containing mostly alkenones

with minimal pigments, was then decolorized once more. Upon removal of the solvent, the resulting orange-colored solid was further purified by recrystallization with hexanes affording analytically pure alkenones as a white solid. This procedure generally resulted in 40% isolated yield (w/w) from the neutral lipids or 3.2% of the Isochrysis dry biomass (Figure 11), which is close to the total alkenone content of 5% that we determined previously.

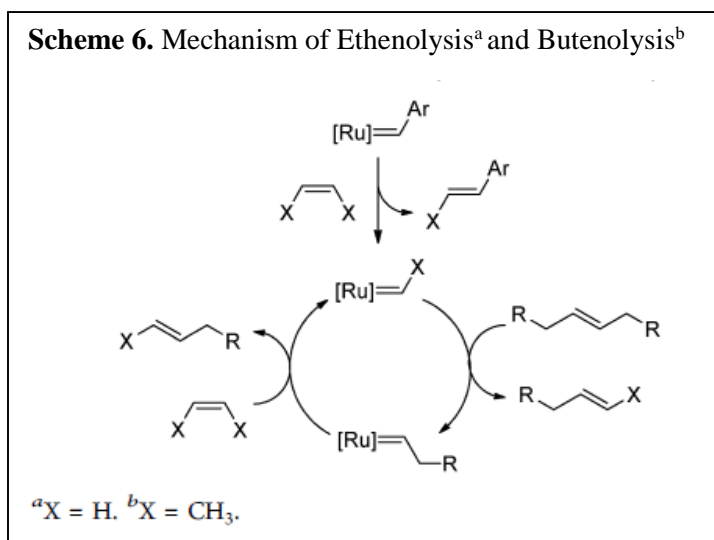


Analysis of the purified alkenones by gas chromatography and comparison to standards revealed the presence of C37:3 (42%), C37:2 (27%), C38:2 (23%), and C38:3 (5%) alkenones with the small remainder accounted by C39:3 (1%) and C39:2 (2%) (Using nomenclature defined in Chapter 2).

Cross-Metathesis of Alkenones with 2-Butene

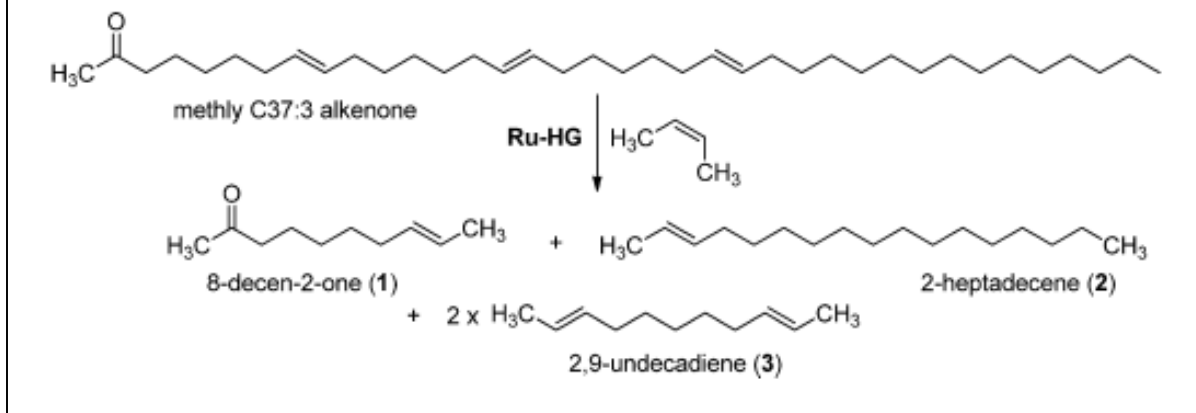
Olefin metathesis has long been embraced by the synthetic organic and polymer communities⁹⁷, often used to create larger molecules from small alkene-containing starting materials as in the case of cross-

metathesis. These reactions typically occur with the release of ethylene gas, which serves as an entropic driving force. The opposite process, which is, the addition of ethylene across a double bond (“ethenolysis”), would result in creating two smaller subunits. Ethenolysis of FAMES and other fatty acid derivatives using Grubbs’-type ruthenium initiators has been reported, as a method for producing valuable smaller hydrocarbon mixtures from renewable feedstocks.⁹⁸⁻¹⁰⁵ One challenge associated with ruthenium-catalyzed ethenolysis is that this reaction requires propagation of a ruthenium methyldiene species that is prone to decomposition ($X = H$, Scheme 6).¹⁰⁶



Additionally, the products containing terminal alkenes have a tendency to undergo the reverse self-metathesis and yields tend to be modest (~40–60%).¹⁰⁶ One strategy to improve this approach is to use 2-butene in place of ethylene ($X = Me$), thus avoiding formation of a ruthenium methyldiene and producing methyl capped alkene products that are less reactive toward selfmetathesis.¹⁰⁷ Recent work by Patel and co-workers reported the rapid and high-yielding cross-metathesis reaction of methyl oleate (methyl (9Z)- octadecenoate) with 2-butene in the presence of the second-generation Hoveyda–Grubbs catalyst (Ru-HG) to produce methyl 9- undecenoate and 2-undecene (Scheme 7).¹⁰⁷

Scheme 7. Alkenone Butenolysis Reaction



Certain fundamental structural differences between long chain alkenones and FAMES need to be considered when applying these reaction conditions to alkenones. The alkenones contain *trans* alkenes as opposed to the more metathesis reactive *cis*-reactive configured double bonds found in FAMES. Secondly, the limited solubility of the alkenones in organic solvents used in olefin metathesis, especially the cold temperatures required to condense 2-butene (*trans*-2-butene, bp = 0 °C). This made it uncertain whether the alkenones would even dissolve in solution and, if so would the *trans* double bonds be reactive enough to engage with the catalyst at low temperatures. Results from the cross-metathesis reactions of isolated alkenones with 2-butene using Grubbs' first- (Ru-I) and second-generation (Ru-II) catalysts **42** and Ru-HG **43** are summarized in Table 2.

All of the performed butenolysis reactions were done with an excess of 2-butene (15 equiv, calculated as 5 equivalents per alkene for the most abundant (37:3) alkenone in the starting mixture) to drive the equilibrium toward products using 2 mol % of the catalyst. After 18 h at 4 °C, the alkenones were consumed when using both catalysts Ru-II and Ru-HG (Entries 1– 3, Table 11), whereas Ru-I gave only 70% conversion under these same conditions (Entry 4). Interestingly Patel and coworkers reported very low conversion (>1%) for the butenolysis of methyl oleate with *cis*-2-butene (10 equiv) using both

Ru-I and Ru-II. This is likely due to the differences in reaction conditions, as the reaction with methyl oleate was conducted at a lower temperature (-5 °C), catalyst loading (0.1 ppt), and times (2 h).¹⁰⁷

Table 11. Results from Butenolysis Reactions of Alkenone Mixtures Isolated from Isochrysis

entry ^a	catalyst	solvent, 2-butene	time	% conversion ^b
1	Ru-HG	DCM, <i>cis</i> -butene	18 h	100
2	Ru-HG	DCM, <i>trans</i> -butene	18 h	100
3	Ru-II	DCM, <i>cis</i> -butene	18 h	100
4	Ru-I	DCM, <i>cis</i> -butene	18 h	70.0
5	Ru-HG	DCM, <i>cis</i> -butene	3 h	100
6	Ru-HG	DCM, <i>cis</i> -butene	1 h	100
7	Ru-HG	DCM, <i>trans</i> -butene	1 h	100
8	Ru-HG	DCM	10 min	62.9
9	Ru-HG	DCM	20 min	98.8
10	Ru-HG	DCM	30 min	99.5
11	Ru-I	DCM	3 h	9.5
12	Ru-I	DCM	6 h	16.7
13	Ru-HG	PhMe	10 min	52.5
14	Ru-HG	PhMe	20 min	84.4
15	Ru-HG	PhMe	30 min	98.3
16	Ru-HG	DCM/ <i>trans</i> -butene	15 min	37.4
17	Ru-HG	DCM/ <i>trans</i> -butene	30 min	95.5

^aAll reactions were performed by adding alkenones (100 mg) to condensed 2-butene (15 equiv) at -78 °C followed by solvent (1 mL) and catalyst. The flask was then sealed and placed in a refrigerator (4 °C, Entries 1–7) or ice bath (0 °C, Entries 8–17) for the indicated time before quenching with ethyl vinyl ether (50 equiv) and concentrating in vacuo. ^bSamples were completely dissolved in DCM before analysis by GC-FID. ^bPercent conversions for the butenolysis reactions were determined by comparing the integration ratios for combined alkenones to methyl stearate (inert internal standard) relative to a starting alkenone/methyl stearate reference mixture. For those reactions reported as 100% conversion, no alkenone signal was detectable by GC-FID.

Patel's work with methyl oleate using Ru-HG at -5 °C for 2 h gave nearly quantitative conversion was reported and upon closer examination was essentially complete within 30 min.¹⁰⁷ Butenolysis of alkenones using either *cis*- or *trans*-2-butene in the presence of Ru-HG appeared similarly rapid with 100% conversion observed after 1 h (Entries 6 and 7). ¹H NMR was not remarkably effective at monitoring the alkenone butenolysis reactions as the measured spectra were essentially identical.

GC-FID, however was useful for monitoring the reaction mixture as it showed 100% consumption of the alkenones (Figure 11).

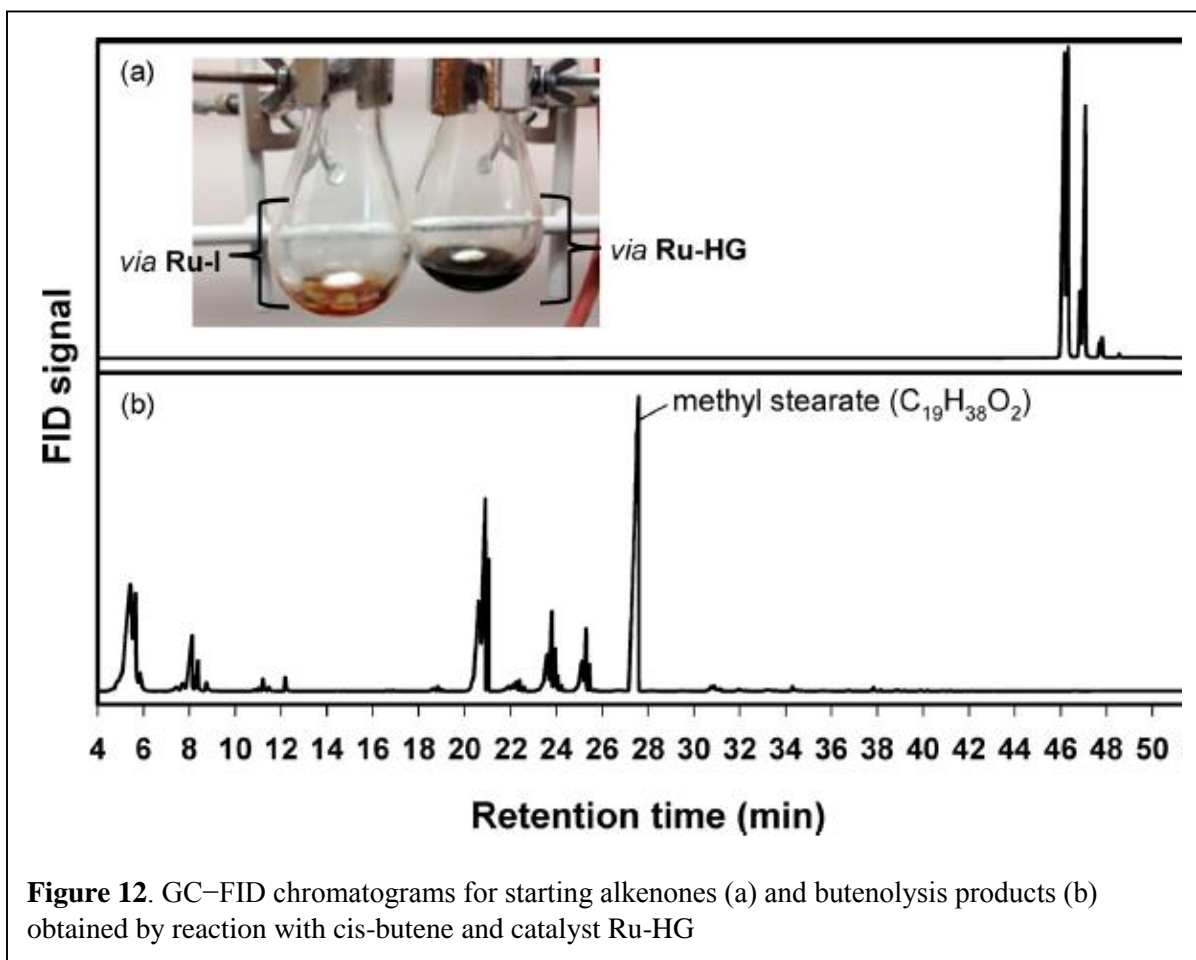
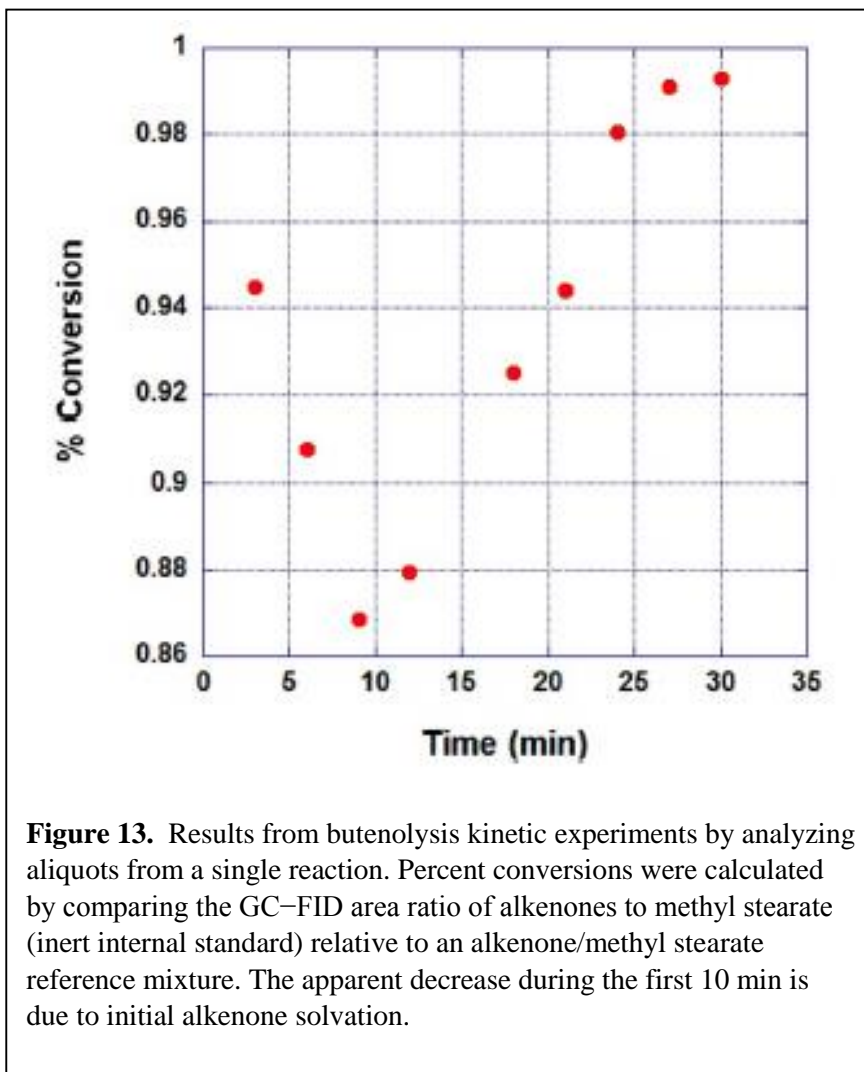


Figure 12. GC-FID chromatograms for starting alkenones (a) and butenolysis products (b) obtained by reaction with *cis*-butene and catalyst Ru-HG

What was equally diagnostic of reaction completion was the dramatic change in reaction appearance upon successful butenolysis. At the beginning of the reaction, the white alkenones seem to be completely insoluble and after conversion to butenolysis products using RU-II or Ru-HG the mixture becomes homogenous and takes on a dark brown to black color. In an attempt to understand the kinetics of the reaction, we made efforts to monitor the progress of the reaction using the standard method employed by Patel and coworkers for their buteneolysis of methyl oleate¹⁰⁷. Aliquots were

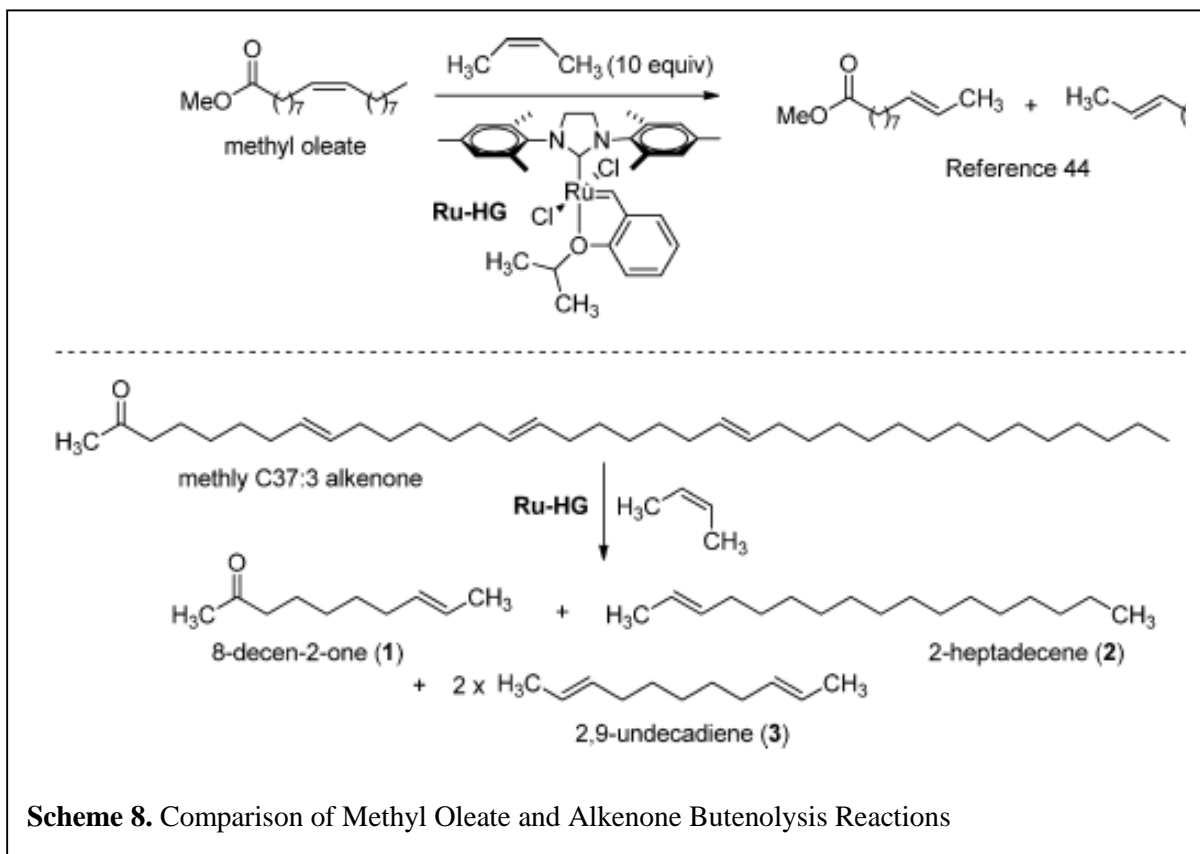
removed from the reaction mixture via syringe that were then quenched by addition of ethyl vinyl ether¹⁰⁸ and analyzed by GC-FID (Result in Figure 13).



Percent conversions were calculated by comparing the GC-FID area ratio of alkenones to methyl stearate as an inert internal standard relative to an alkenone/methyl stearate reference mixture. The kinetics were quite unexpected for the reaction first showing an apparent decrease during the first 10 mins and then a return to near completion 25 min later. We interpret these results to represent a

dynamic system of alkenone solvation and butenolysis. Initially, the alkenone concentration in the solvent sampled is low due to poor solubility. Over time the dissolved alkenone concentration increases resulting in a lower calculated percent conversion. After 10 min where the decrease is seen, the rate of butenolysis appears to exceed the rate of alkenone solvation and the calculated percent conversion increases. In efforts to acquire accurate rate data, it was found necessary to perform multiple individual butenolysis reactions quenched at different time increments. Entries 8-17 in Table 11 show the results from the individual reactions. After sampling and quenching, samples from each reaction mixture were completely dissolved in DCM prior to analysis by GC-FID to avoid any solubility issues. Several interesting observations were made during the course of this somewhat laborious process. As expected, catalyst Ru-HG outperformed catalyst Ru-I, with only 16.7% conversion recorded for Ru-I after 6 h (Entry 12). The reaction with Ru-HG was exceptionally fast and gave greater than 90% conversion after only 20 min. The reaction was essentially complete within 30 min (Entries 9 and 10). These results are very similar to those reported by Patel and co-workers for the butenolysis of methyl oleate.¹⁰⁷ This is quite remarkable with consideration of the structural differences noted earlier between the alkenones and this FAME. The reaction with *trans*-2-butene had significantly lower conversion at the 15 min mark (Entry 16) and this may result due to a more rapid initiation of *cis*-2-butene by the parent catalyst. After 30 min the reaction still gave >95% conversion (Entry 17). The solvent selected for these reactions was DCM, as it had demonstrated the greatest solubility, despite its use being undesirable for any “green” processing.¹⁰⁹ With this concern in mind we examined the reaction in toluene (PhMe), a more tolerated solvent, that showed some alkenone solubility and is often used in olefin metathesis reactions. Reactions performed in toluene gave lower conversions at 10 and 20 min when compared to those in DCM (Entries 8 and 9 vs 13 and 14), likely a reflection of diminished alkenone solubility. Regardless, the butenolysis in toluene was still very efficient giving comparable conversion (98%) after 30 min at 0 °C (Entry 15).

Scheme 8 shows the expected products from complete butenolysis of the major alkenone (methyl 37:3) out of the PULCA's isolated from *Isochrysis*. The actual product mixture is much more complex as our butenolysis reactions use a mixture of alkenones not just the pure 37:3, but the complete set of alkenones extracted from the biomass that ranged from 37 to 39 carbons with 2–3 double bonds



and methyl or ethyl ketones. Plus, there is also the potential for incomplete butenolysis products along with *cis*- and *trans*isomers. The actual product mixture is therefore quite complex. For this reason, we chose to use comprehensive two-dimensional gas chromatography (GC×GC) to analyze select butenolysis reactions.

Like one dimensional GC, GC×GC works by separating gaseous compounds based on their affinity with the solid stationary phase. However, GC×GC employs two serial joined columns, which each have different stationary phases and allows for greater separation of similar compounds. GC×GC has higher

chromatographic resolution increases the signal-to-noise ratio and compounds are separated based on two physical properties (e.g., vapor pressure and polarity depending on choice of column stationary phase), which results in grouping of chemical classes in a GC × GC chromatogram. Combining of both GC × GC with a flame ionization detector (FID) allows for the quantification of numerous unidentified compounds because most hydrocarbons have similar response factors.¹¹⁰

The specific alkenones present in the samples were able to be identified by comparison of their mass spectra with published elution order on GC columns¹¹¹, textbooks, and recent studies detailing alkenone structure analysis.^{112, 113} Relative amounts of individual alkenones were determined by GC-FID, which had results that correlated well with those previously reported for the same Isochrysis strain used in our study (Table 3).¹¹⁴

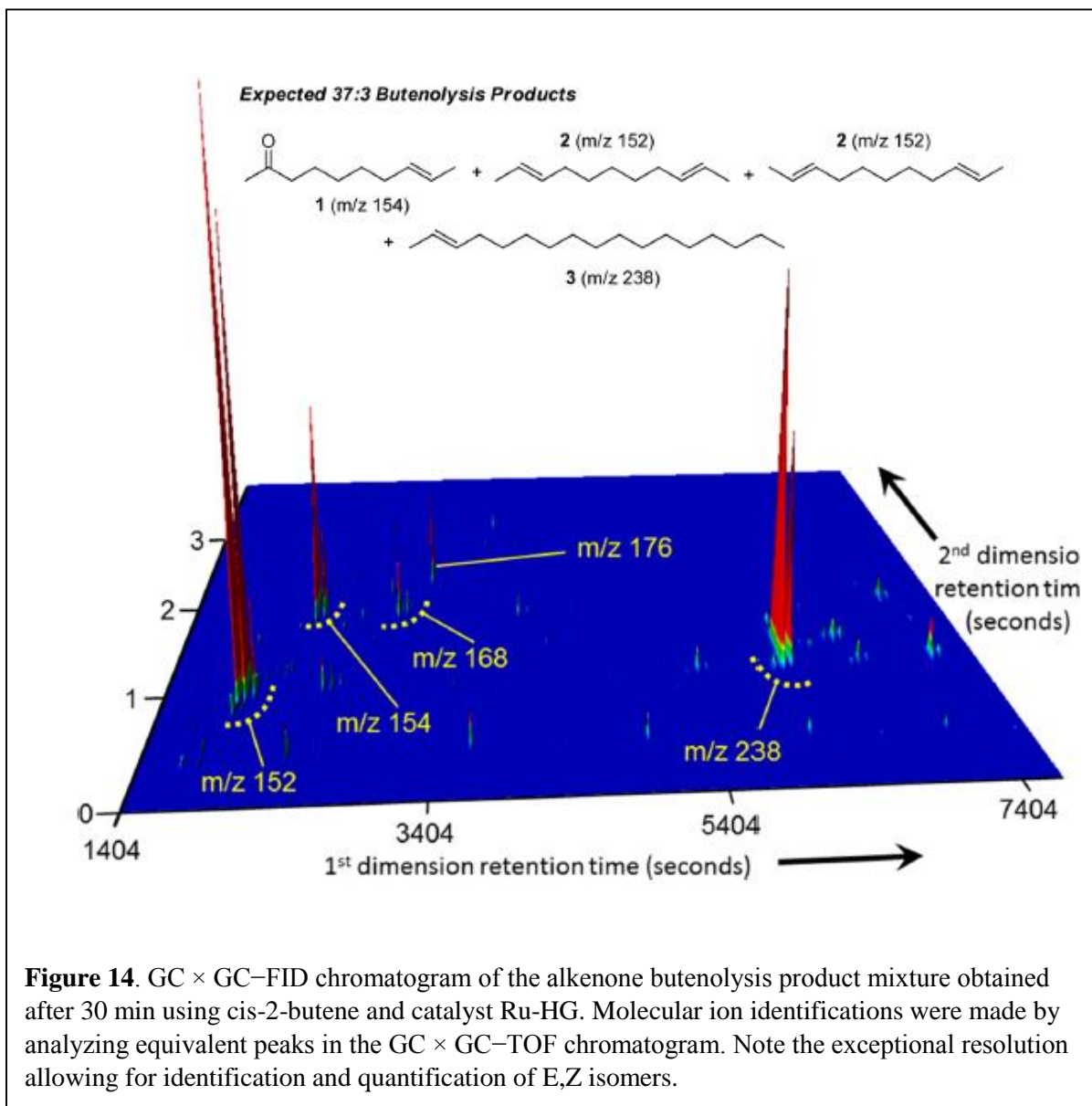
Table 12. Alkenone Composition and Expected Butenolysis Products

alkenones (double bond position) ^a	% composition ^b this study	% composition ^c ref 54	predicted butenolysis products (%) ^d
Me 37:3 (8E,15E,22E)	42	40	1 (12.4), 2 (28.2), 3 (42.7), 15-heptadecen-2-one (8.0), 9-undecen-3-one (1.4), 16-oct-3-one (6.6), 2-nonadecene (0.7)
Me 37:2 (15E,22E)	27	29	
Et 38:3 (9E,16E,23E)	5	6	
Et 38:2 (9E,16E,23E)	23	22	
Me 39:3 (8E,15E,22E)	1	ND	
Me 39:2 (15E,22E)	2	ND	

^aDouble bond positions are based on information in ref 51–53. ^bDetermined by GC-FID and calculated as percent of total alkenones. ^cA values for T-Iso and C-Iso from ref 54. ^dPercent of total predicted products. ND = not determined.

Based on the alkenone profile the products of the buteneolysis reaction can be predicted. For instance each of the C37 and C38 alkenones should produce 2-heptadecene (**2**) and two equivalents of 2,9-undecadiene (**3**) (Scheme 8). The buteneolysis product of C37 and C39 would give 3 along with 8-decen-2-one (**1**). With consideration to the relative alkenone percentages, this would give a distribution outlined in Table 12, where compounds 1, 2, and 3 represent 83% of the products. A typical GCxGC chromatogram of the buteneolysis products obtained by reaction of our alkenone

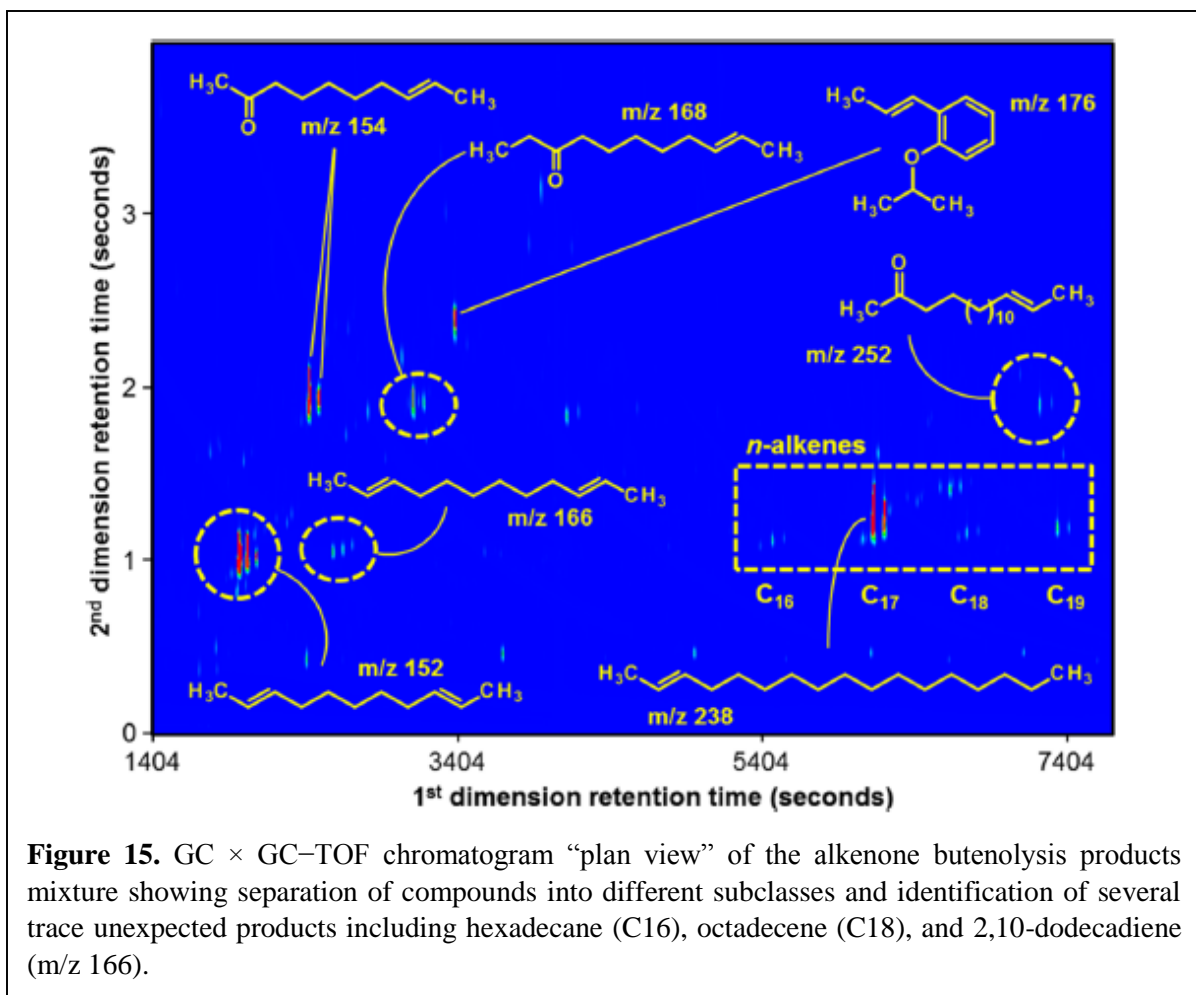
mixture with *cis*-2-butene using catalyst Ru-HG, can be seen in Figure 5. The butenolysis was complete in times under 30 mins in DCM at 0 °C (refer to Entry 3, Table 11).¹¹⁵



Each of the major products predicted of 1, 2, and three are clearly identifiable in the GCxGC spectrum. For both 1 and 3, two peaks are clearly visible with integration ratios from the GC × GC–FID of 3.9:1 that were able to be assigned as the *trans*- and *cis*-isomers, respectively. Patel and co-workers also

reported a 4:1 trans:cis ratio for 2-undecene obtained by butenolysis of methyl oleate.¹⁰⁷ Three peaks in our alkenone butenolysis product mixture were identified with $m/z = 152$ in a ratio of 17.9:7.5:1 that have been assigned to the three possible isomers for 2 (*E*, *E*-, *E*, *Z*- and *Z*, *Z*-). Other signals include cis- and trans-9-undecen-3-one ($m/z = 168$) obtained from the 38:3 ethyl alkenone contained in our sample and catalyst-derived 1-isopropoxy-2-(propenyl) - benzene ($m/z = 176$). The ratio of the butenolysis products **1:2:3** by GCxGC FID analysis was found to be 1:2.0:2.5 respectively. This is slightly different than what would be predicted from the alkenone profile (1:2.3:3.4). Upon closer inspection of the GC × GC–TOF chromatogram data showed the presence of multiple unexpected products compared to those shown in Table 12 that could be responsible for this discrepancy. In the “*n*-alkene” region of the chromatogram, in addition to expected products C17 and C19, there were also unexpected minor products with shorter chain hydrocarbons (C16 and C18). For each of these there were two peaks with area ratios of approximately 1:4, consistent with our previous *cis*- and *trans* isomer assignments¹⁰⁷.

2-octadecene (C18) could have arisen from our sample containing very small amounts of a 38-methyl or 39-ethyl alkenone. Extending the argument further, hexadecene formation could have been formed from a methyl C36 alkenone that we did not detect in our sample nor has a C36 alkenone been reported for *Isochrysis* elsewhere. However, this could also be explained by double bond isomerization which occurred during the cross-metathesis reaction. However, it is interesting that only C16–C19 alkenes were detected for our butenolysis conducted at both short (e.g., 30 min) and longer (18 h) reaction times rather than the larger range of alkenes that could be envisioned from an isomerization process. Yet another possible reason is that *Isochrysis* biosynthesizes trace amounts of alkenones with differing double bond positions. This would also a possible explain the peak with $m/z = 166$ present in the diene region of the chromatogram that we have identified as 2,10- dodecadiene.



Synthesis of an alkenone-derived polyester monomer via cross metathesis

With continuing efforts towards investigating reactions that convert alkenones into a value added product, we decided to use cross metathesis to introduce ester or carboxylic acid functionality (Scheme 10). One product from these reactions would be a diester (or diacid) that could presumably be polymerized to make new materials (e.g. polyester) (Scheme 9.) To test this, isolated alkenones were treated with the Hoveyda-Grubbs catalyst (**Ru-Z**) in the presence of an excess of methyl acrylate (15 equiv) in DCM at room temperature.

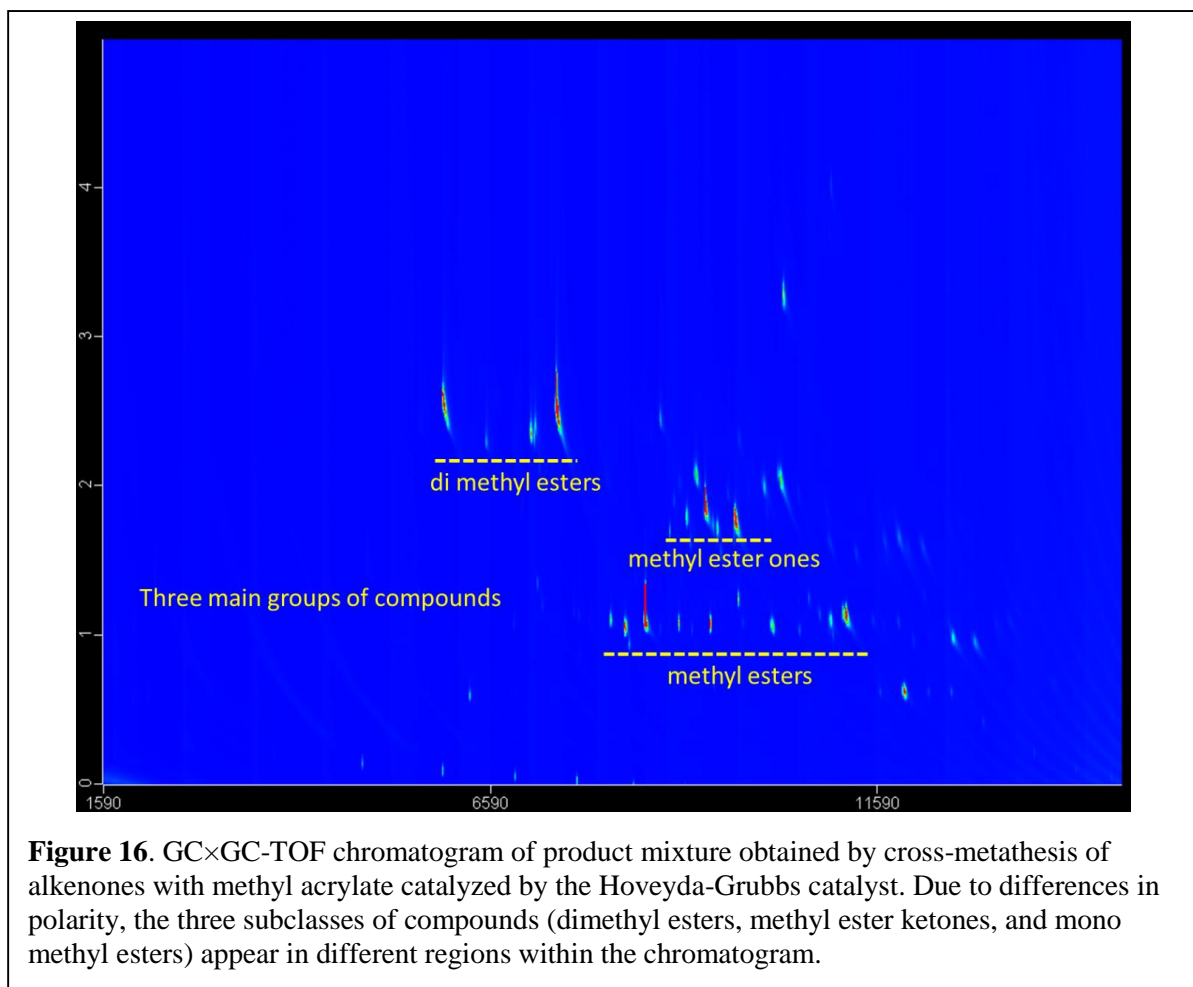
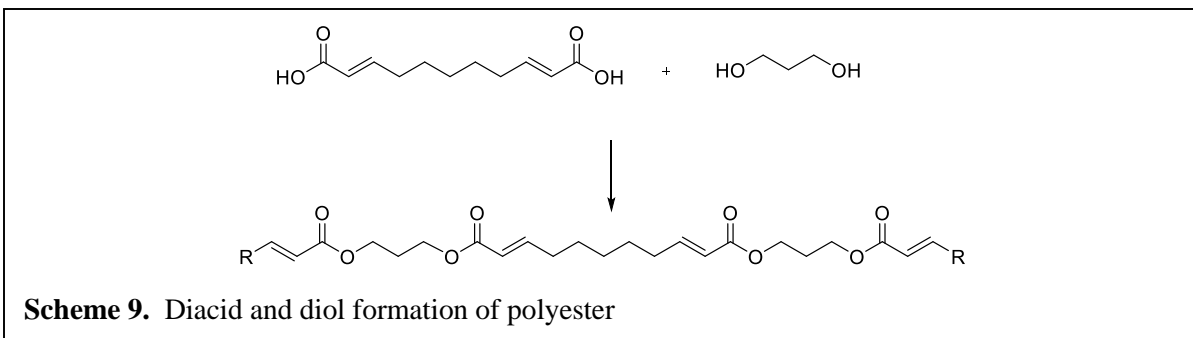


Figure 16 is the GCxGC-TOF chromatogram from this reaction, showing complete consumption of the alkenones and formation of the three expected subclasses of cross-metathesis products (diesters, ketoesters, and mono-esters). While the reaction appeared to have proceeded cleanly, the ratio of

products we obtained was different than what would be expected based on our alkenone profile. Specifically, from each of the alkenones identified, we can predict their corresponding cross-metathesis products and determine the overall product distribution based on their relative contributions (Scheme 10). From this analysis, we would predict that the major component would be the diester dimethyl (2*E*,9*E*)-undeca-2,9-dienedioate at 38%. However the major product proved to be methyl (E)-heptadec-2-enoate (42%, Figure 17). Other values were however close to what was predicted. Recall that the butenolysis reaction also gave a slightly different ratio of products that what was predicted (1:2.0:2.5 vs. 1:2.3:3.4) that we explained by the possibility of alkene isomerization occurring during the reaction. In an attempt to suppress isomerization during the methyl acrylate metathesis reaction, we set out to investigate the use of additives that had been reported to do so.

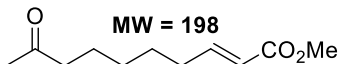
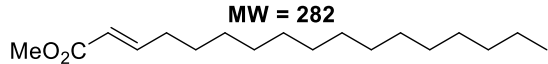
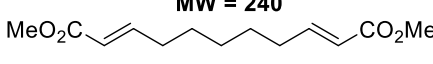
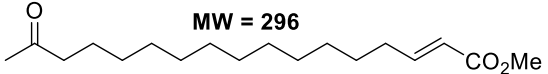
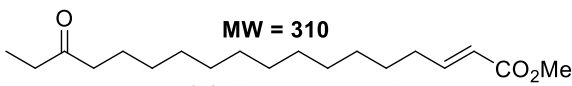
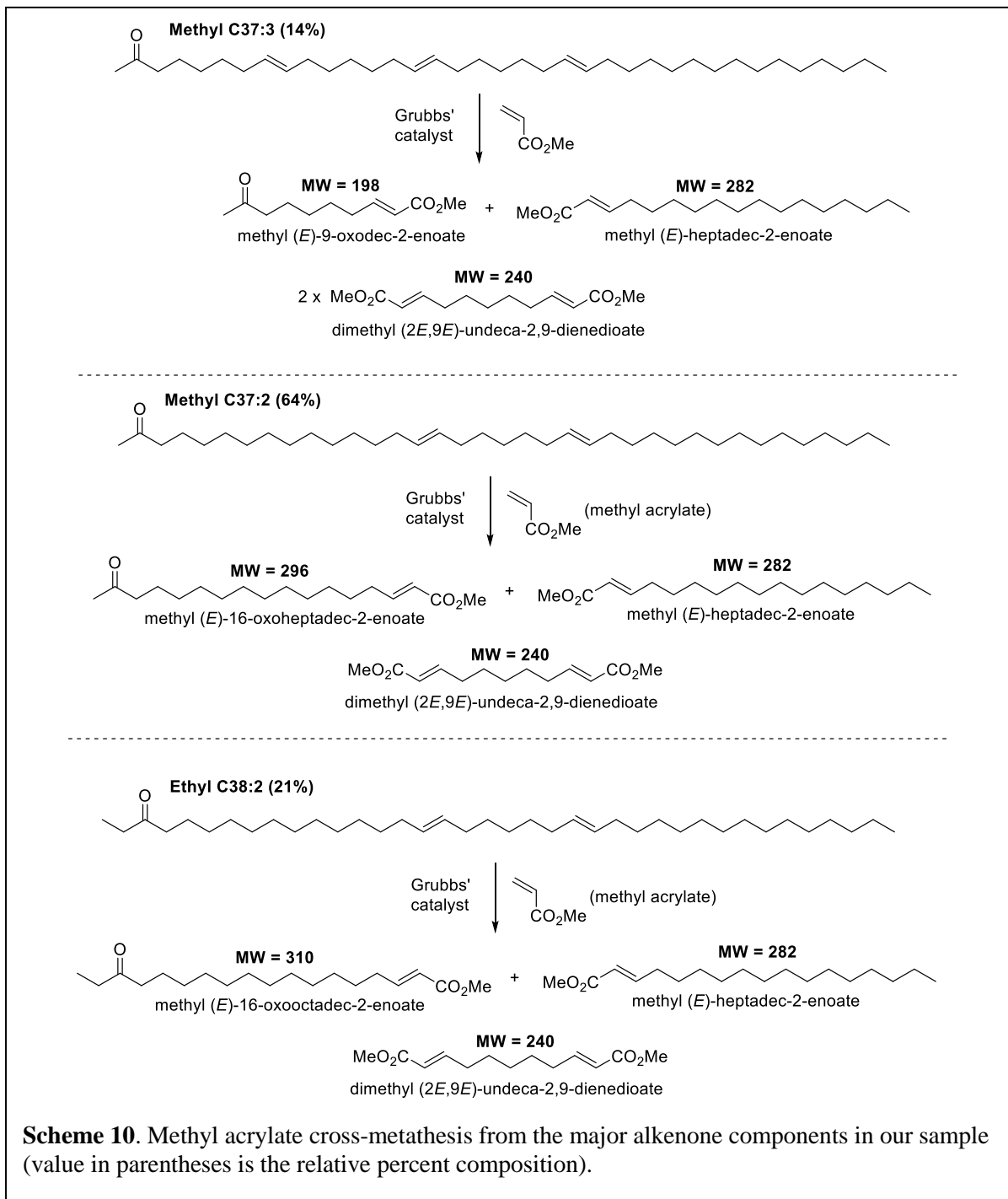
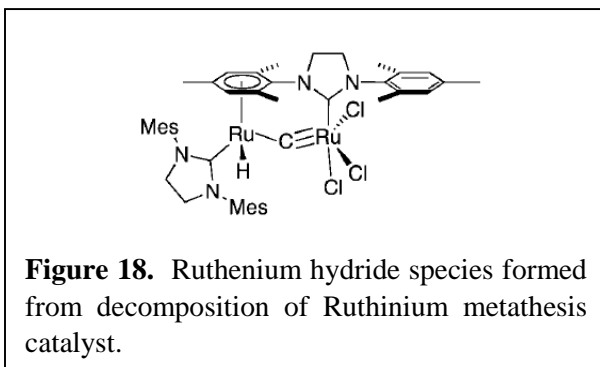
	Predicted	Obtained
 MW = 198 methyl (E)-9-oxodec-2-enoate	4.5	5.5
 MW = 282 methyl (E)-heptadec-2-enoate	31.7	41.9
 MW = 240 dimethyl (2 <i>E</i> ,9 <i>E</i>)-undeca-2,9-dienedioate	36.7	27.5
 MW = 296 methyl (E)-16-oxoheptadec-2-enoate	20.1	18.3
 MW = 310 methyl (E)-16-oxooctadec-2-enoate	6.5	6.8

Figure 17. Comparison of predicted vs. actual amounts of methyl acrylate alkenone cross-metathesis products.



While the exact mechanism(s) responsible for this isomerization are unknown (metal-based hydride, δ -allyl, or other pathways)^{116, 117} recent reports indicate that the ruthenium hydride species (Figure

18), formed from the decomposition of the ruthenium metathesis catalysts can catalyze the migration of olefins under metathesis conditions.¹¹⁸



Work by Soon Hyeok Hong and coworkers, showed that moderate pK_a acids, such as acetic acid or 1,4-benzoquinone, work well in preventing olefin migration during olefin metathesis reactions. They demonstrated that both acetic acid and 1,4-benzoquinone were effective in preventing the isomerization during the ring-closing metathesis of diallyl Ether. Soon et al. also investigated radical scavengers as additives, such as BHT, TEMPO, phenol, and 4-methoxyphenol, but in general these were not as effective in preventing isomerization.¹¹⁹ Recently it has been reported that quinones are reduced to the corresponding hydroquinones upon reacting with ruthenium hydrides and abstracting the proton.¹²⁰ For the purpose of our work with alkenones we decided to use phenol and 1,4-benzoquinone as isomerization inhibitors of olefin metathesis. In this study we performed CM reactions between alkenones with methyl acrylate using Grubbs' second-generation catalyst (**137**) or the Hoveyda catalyst (**138**) with or without phenol (Ph) or benzoquinone (Bz). These reactions were also performed using acrylic acid instead of methyl acrylate as the cross-metathesis partner. Data from these reactions obtained by GCxGC-TOF are presented in the Tables 13-15.

	137 no add		137 Ph		137 BZ	
Name	peak area	% total area	peak area	% total area	peak area	% total area
methyl (E)-9-oxadec-2-enoate	446699506	6.79	462495334	5.49	354349099	8.26
dimethyl (2E,9E)-undeca-2,9-dienedioate	1368095447	20.79	1906440342	22.63	687041439	16.01
methyl (E)-heptadec-2-enoate	3015503000	45.83	3859547294	45.82	2212443949	51.56
methyl (E)-16-oxoheptadec-2-enoate	1270451072	19.31	1599570420	18.99	760631498	17.72
methyl (E)-16-oxooctadec-2-enoate	478742201	7.28	595881052	7.07	276874574	6.45
total area	6579491226		8423934442		4291340559	

	138 no add		138 Ph		138 BZ	
Name	peak area	% total area	peak area	% total area	peak area	% total area
methyl (E)-9-oxadec-2-enoate	476629325	5.45	396840081	4.60	402003579	4.61
dimethyl (2E,9E)-undeca-2,9-dienedioate	2403934684	27.49	2343267901	27.16	2374700918	27.23
methyl (E)-heptadec-2-enoate	3666398346	41.93	3755814671	43.54	3718915461	42.64
methyl (E)-16-oxoheptadec-2-enoate	1602979228	18.33	1558761369	18.07	1626437823	18.65
methyl (E)-16-oxooctadec-2-enoate	593947661	6.79	571901112	6.63	600279998	6.88
total area	8743889244		8626585134		8722337779	

	139 no add		139 Ph		139 BZ	
Name	peak area	% total area	peak area	% total area	peak area	% total area
methyl (E)-9-oxadec-2-enoate	515438812	6.33	487636534	6.58	264772357	6.94
dimethyl (2E,9E)-undeca-2,9-dienedioate	2216710201	27.22	1933768155	26.09	497693993	13.04
methyl (E)-heptadec-2-enoate	3518474397	43.21	3287068480	44.35	2033973227	53.30
methyl (E)-16-oxoheptadec-2-enoate	1382895239	16.98	1246380382	16.82	752971036	19.73
methyl (E)-16-oxooctadec-2-enoate	509574115	6.26	455978607	6.15	275679448	7.22
total area	8143092764		7410832158		3825090061	

Table 13-15. Comparison of monomer products from influences of metathesis additives.

As can be seen, the ratio of products from each of these reactions was essentially identical. An examination of the GC×GC-TOF chromatograms, however, revealed that those reactions containing benzoquinone gave many additional high molecular weight compounds products (Figure 19).

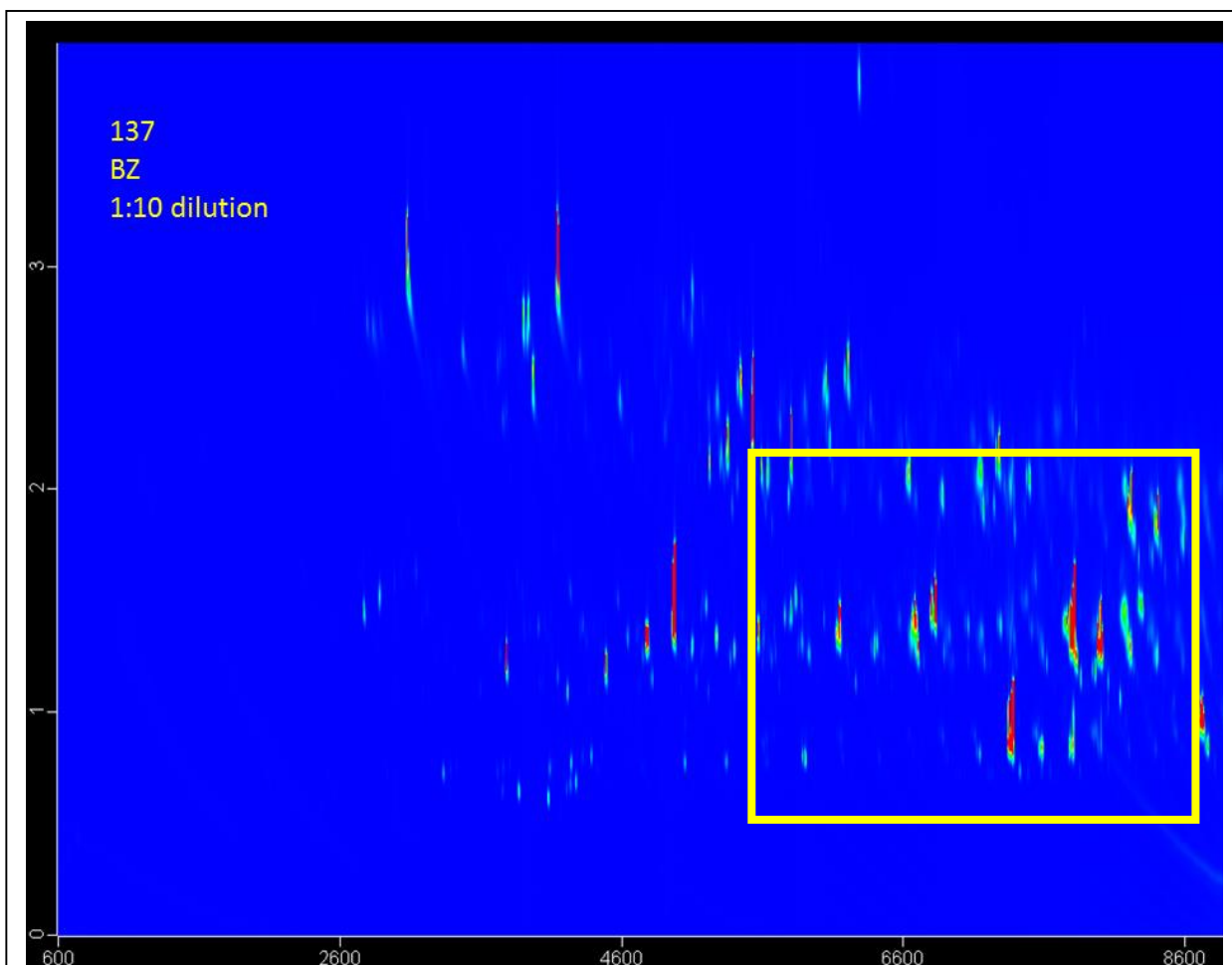


Figure 19. GC×GC-TOF chromatogram of the alkenone/methyl acrylate cross-metathesis reaction using Grubbs' second-generation catalyst conducted in the presence of benzoquinone. The boxed-in area shows higher molecular weight compounds that were not observed in the reaction without the additive (see Figure 16)

Some of the products obtained can be explained by incomplete metathesis (e.g. $m/z = 378$) while others such as the $C_{30} - C_{32}$ n -alkenes are not as clear. Future work will be aimed at better understanding the formation of these products and the impact of benzoquinone as an additive (Figure 20).

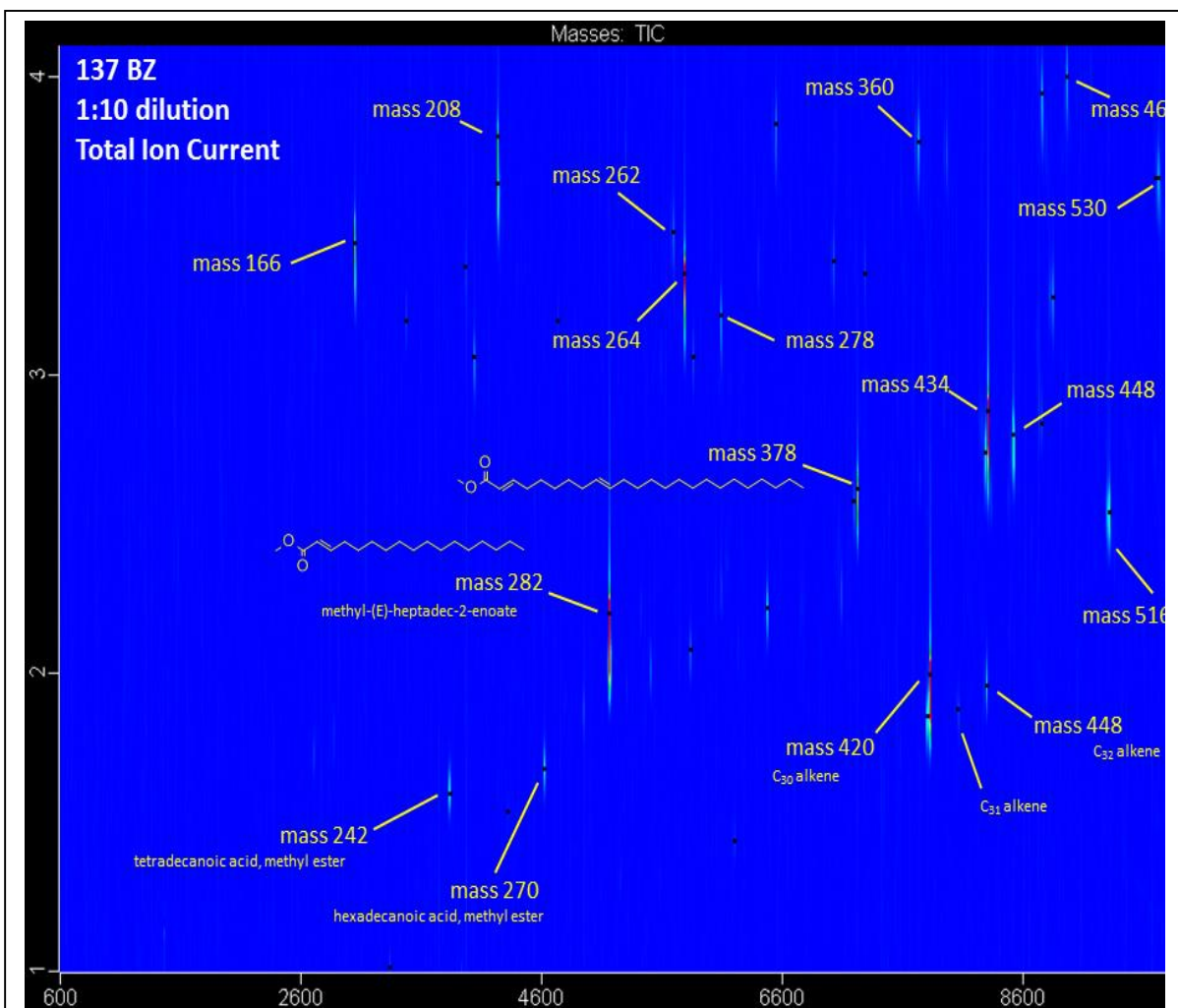


Figure 20. GCxGC-TOF chromatogram of the alkenone/methyl acrylate cross-metathesis reaction using Grubbs' second-generation catalyst conducted in the presence of benzoquinone showing identification of incomplete metathesis products and *n*-alkenes.

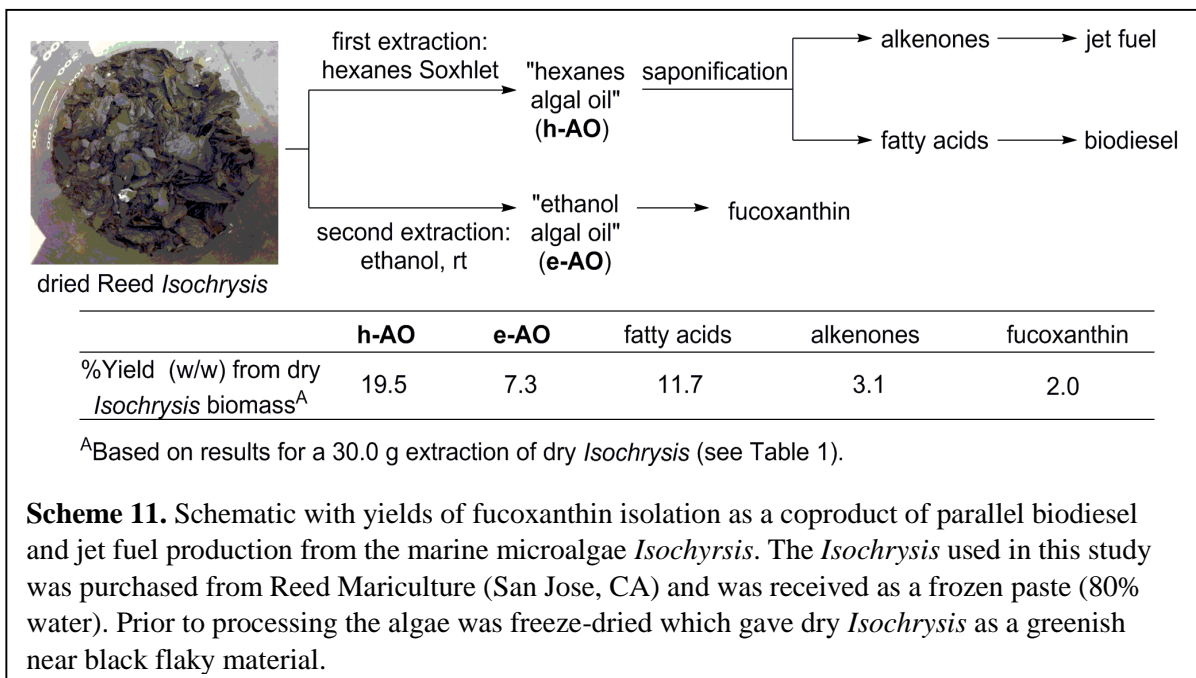
Fucoxanthin Isolation from Waste Algal Biomass as an Added Coproduct to *Isochrysis* Biofuels

Based on our previous work with algal biodiesel synthesis (Chapter 3), we have developed a method for the isolation of a valuable carotenoid fucoxanthin in parallel with the production of two liquid fuel streams from the marine microalgae *Isochrysis* based on selective extractions. The fucoxanthin is

extracted after the dry algal biomass is first extracted with hexanes in a Soxhlet apparatus to extract lipids containing both triglycerides and long-chain alkenones (C36-C39). The residual waste biomass is then extracted with ethanol to afford a fucoxanthin-rich algal oil (~20% w/w) representing near total amounts of fucoxanthin contained within the initial biomass. This technique gives near quantitative isolation of a valuable coproduct to potentially and has potential to offset algal biofuel production costs.

Many critics state that algal biodiesel is not feasible⁹¹ in competition with petroleum fuels. For instance van Beilen who echoes the sentiments of many opponents of algal biofuels and argues that “only if the algal biomass is a byproduct of...the production of high-value compounds such as astaxanthin or β -carotene, commercially viable energy production from algal biomass might be feasible.” Our investigation of fucoxanthin and its extraction conditions from waste biomass are in efforts to answer these concerns. There has been an increased emphasis on opening dialog about the potential for the isolation/production of value added coproducts to augment and offset the cost of algal biofuel production (the so-called “biorefinery” concept),¹²¹⁻¹²³ to the best of our knowledge this is the first report with experimental data from a successful process for the parallel production of multiple liquid fuels and co-isolation of a high-value metabolite from an algae feedstock. This processing of biomass has the potential to be quite fruitful as we are able to produce a biodiesel of high quality and in addition we are the recovery of a neutral lipid fraction from the original h-AO as a potential secondary product stream in line with recommendations from the U.S DOE NABTR”.¹²⁴ Our main focus in this body of work has been on the alkenones which comprise approximately 40% (w/w) of the neutral lipids. We argue that alkenones represent a potentially underdeveloped renewable

carbon feedstock especially in light of the recent demonstration of their conversion to jet fuel range hydrocarbons by cross-metathesis with 2-butene (ref. Scheme 11).¹²⁵



While investigating the isolation and purification of alkenones via silica gel chromatography, we obtained a few fractions that appeared as bright red solutions. There have become an increasing number of reports describing the isolation and quantification of the carotenoid fucoxanthin from *Isochrysis*.^{126,127} Fucoxanthin is a structurally complex oxidized form of β -carotene (a xanthophyll) that has received significant interest for its range biological activities including anti-inflammatory,¹²⁸ anti-angiogenic,¹²⁹ anti-diabetic,¹³⁰ anti-obesity,¹²⁸ and anti-carcinogenic effects.¹³¹ The red colored fractions showed a UV-Vis spectrum with characteristic peaks at 428, 446, and 475 nm that were consistent with the spectrum obtained for a fucoxanthin standard and reported elsewhere (Figure 21).¹³²

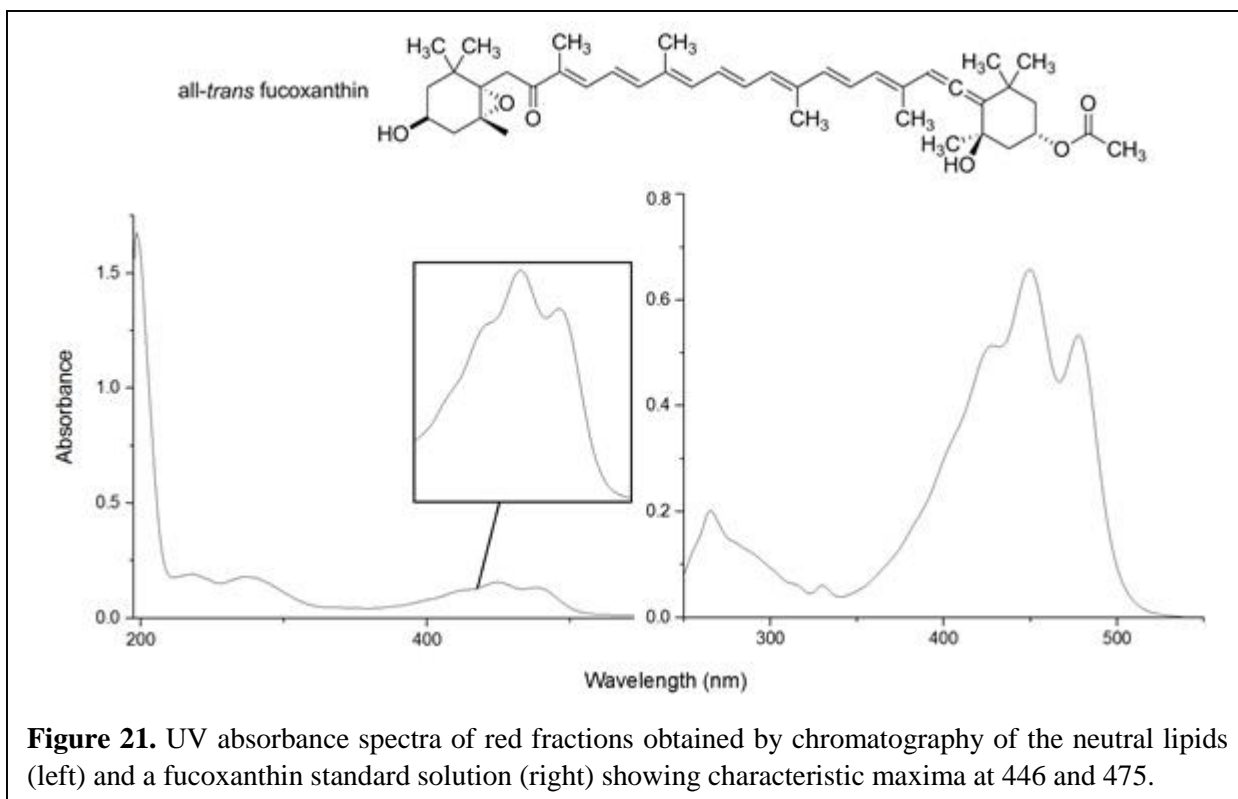


Figure 21. UV absorbance spectra of red fractions obtained by chromatography of the neutral lipids (left) and a fucoxanthin standard solution (right) showing characteristic maxima at 446 and 475.

Remarkably, hexanes, the solvent that was used for chromatography has been shown a poor solvent for fucoxanthin extraction from algal biomass. The ideal solvent for such extractions, is alcoholic solvents, like ethanol and methanol proving far superior to hexanes in recent studies.^{126, 133} A study by Kim et al extracted biomass with hexanes produced 1.04 mg of fucoxanthin from 1 g of dry *Isochrysis* biomass (1.04 mg/g DW) whereas gave 19.76 mg/g DW under identical conditions (1 h, room temperature).¹²⁶ These results are highly suggestive that after our hexanes extraction that we ultimately use to make biodiesel and alkenone-derived fuels, the majority of fucoxanthin remains in what was previously waste biomass and is still likely recoverable. We wanted to investigate and compare if we would have similar results to the literature with hexanes. A hexanes extraction of 30 g of dry *Isochrysis* biomass was performed as previously described which produced 5.85 g h-AO, consistent with our prior reports (Table 16).^{123,63} Post hexanes-extracted biomass was collected from the cellulose thimble and was place in an Erlenmeyer flask and then submerged in ethanol. Due to

the photosensitivity of the fucoxanthin and other carotenes,¹³⁴ the ethanol extraction along with all subsequent steps was performed in the dark to minimize exposure to light. The yield of e-AO after 24 h at room temperature was 7.3% (w/w starting dry *Isochrysis*) and fucoxanthin content was 19% (w/w e-AO) compared to only 3% (max.) fucoxanthin content for the h-AO by HPLC analysis (Table 16 and Figure 22).

Table 16. Yields and corresponding fucoxanthin content for algal oils obtained by sequential hexanes/ethanol extraction of dry *Isochrysis* biomass

<i>Isochrysis</i> DW (g)	30.0	50.6
h-AO (g)	5.86	8.09
e-AO (g)	2.18	2.22 (24 h) ^B 0.97 (1 h) ^B
e-AO Fucoxanthin Content (% w/w) ^A	18.9	21.5 (24 h) ^B 20.0 (1 h) ^B
h-AO Fucoxanthin Content (% w/w) ^A	3.2*	2.9

Footnotes for Table 16: ^ADetermined using HPLC by comparison to a calibration curve obtained from serial dilution of a standard fucoxanthin solution ($R^2 = 0.9987$). ^BThe post-hexanes extracted biomass was split (2 x 22.5 g) followed by extraction with ethanol at room temperature for 24 h or 1 h as indicated. *Values are calculated from the sum of non-resolved peaks in the HPLC chromatogram.

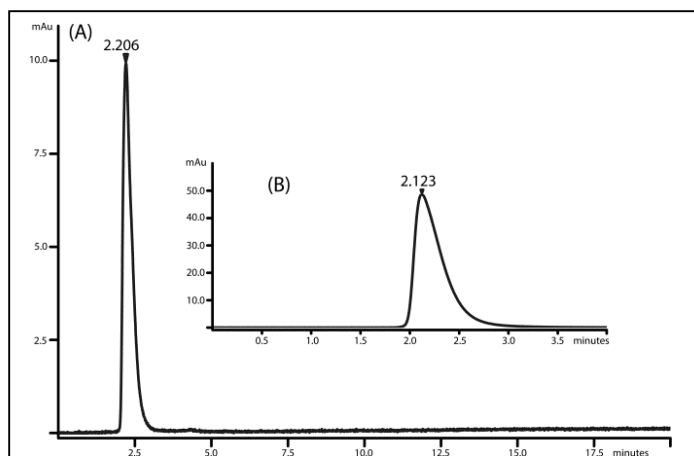


Figure 22. HPLC chromatogram of e-AO (A) and fucoxanthin standard (B, Inset). Conditions: column, Waters C₁₈ 5 μm, 250 mm x 4.6 mm i.d.; detection at 447 nm; flow rate 1.0 mL/min; 90:10 methanol:H₂O elution.

By comparing the UV-Vis spectra for our h-AO and e-AO showed selectivity in our sequential extraction process, with both the h-AO and e-AO exhibiting peaks corresponding to pheophorbide a and pheophytin A (410 and 665 nm).¹²³ The selectivity of ethanol for fucoxanthin and other carotenes extraction was elucidated by the e-AO spectrum, which contained the characteristic carotene peak in the 450-500 nm region (Figure 23).¹³²

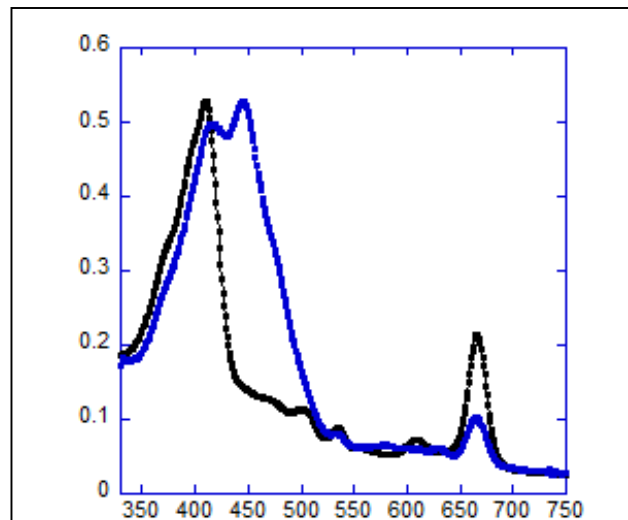
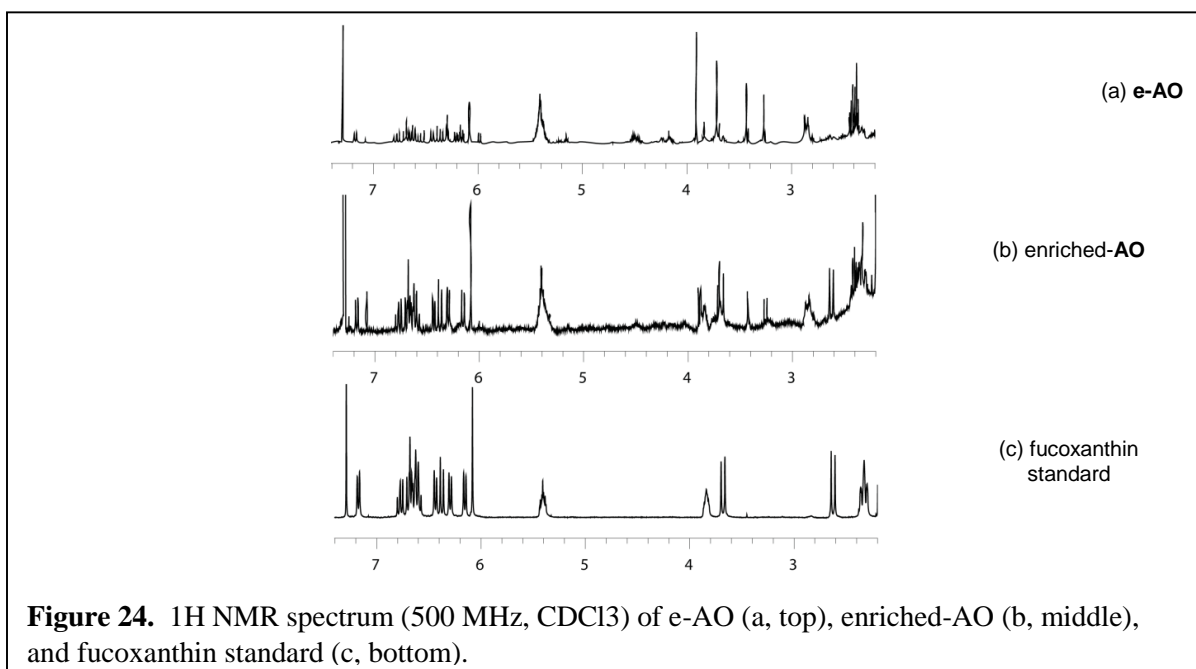


Figure 23. UV absorbance spectra of *Isochrysis* hexane extract (h-AO, black) and subsequent ethanol extract (e-AO, blue) in acetone (both samples were prepared at a concentration of 10 mg/100 mL). The maxima in the Soret band (410 nm) and Qy band (665 nm) in both the h-AO and e-AO are characteristic of chlorophyll a degradation products pheophorbide a and pheophytin a.²¹ Only the e-AO exhibited a shoulder between 450-500 nm corresponding to fucoxanthin.³¹ degradation products pheophorbide a and pheophytin a.²¹ Only the e-AO exhibited a shoulder between 450-500 nm corresponding to fucoxanthin.³¹

In efforts to further confirm the differences in extraction conditions, a fucoxanthin-enriched ethanol algal oil could be obtained by chromatography on silica to produce an ethanol oil (0.54 g from 1.89 g e-AO) that was now 44% fucoxanthin according to HPLC analysis. Here, the ¹H NMR spectra for both the e-AO and this enriched-AO showed peaks consistent with the presence of fucoxanthin standard (Figure 24).



Work by Kim and coworkers showed a strong correlation between the duration of ethanol extraction and the amount of fucoxanthin obtained.¹²⁶ Especially, with regards to maximum yields, that were reported after only 5 mins at room temperature (20.28 mg/g DW after 5 minutes vs. 17.38 mg/g after 24 h). This difference is explained in the report by the sensitivity of fucoxanthin toward decomposition. With efforts in testing the degradation of fucoxanthin with different extraction times, we first extracted lipids from the dry *Isochrysis* biomass (50.6 g) with in a Soxhlet apparatus. The post-extracted biomass was then split (2 x 22.5 g), with one half extracted in ethanol for 1 h and the other

extracted for 24 h (both at room temperature). In contention of the work by Kim et.al¹²⁶, the yield of fucoxanthin we obtained was substantially higher for the 24 h extraction (Table 16). This was not due to one e-AO being more enriched in fucoxanthin (21.5% w/w and 20.0% w/w for the 24 h and 1 h extractions respectively), but rather the amount of algal oil that was obtained from the different extraction times (2.22 g vs. 0.97 g). This could be due to the method by which the biomass is processed and how the material interacts with the solvent. Kim et al. described using dried biomass “powder” for their fucoxanthin extraction study compared to ours which was a flaky material we obtained after freeze drying Reed Isochrysis paste (ref. Scheme 1).¹²⁶ It is also worth noting that the scale Kim and coworker performed extractions on was substantially smaller scale (100 mg vs. 20 – 30 g dry biomass) which might also contribute to the discrepancy between our extraction time data and theirs. The amount of total fucoxanthin present in the biomass is 21.73 mg/g DW, if we combine the fucoxanthin contained in the h-AO and data obtained from the 30 g biomass extraction. This value is in the range of the maximum value reported by Kim et al. by extraction with ethanol for (5 min at room temperature 20.28 mg/g DW)¹²⁶ as well as the total fucoxanthin content in Isochrysis biomass reported by Crupi and coworkers (19.82 ± 3.72).¹²⁷ On average, our e-AO contained 75% of the total fucoxanthin contained in the biomass, which is similar to that obtained by Kim et al. using a complimentary two-phase lipid/fucoxanthin separation procedure.¹²⁶ Our method seems less labor intensive than two-phase separation procedure employed by Kim et. al, as it does not disrupt or alter the biomass-to-biofuels process nor do we introduce water that would presumably need to be removed at a later stage. Rather it is the biodiesel waste-stream to which value is being added, not unlike other reports describing the use of residual algal biomass as feed³⁴ or its gasification to fuel.¹³⁵ Microalgae are established sources of commercially produced high-value chemicals such as carotenoids and polyunsaturated fatty acids (e.g. docosahexaenoic acid (DHA)). To accurately assess these compounds value, it is necessary to consider how the value might be impacted if incorporated

into a fuel-production strategy. We recently estimated that to replace 10% of the petroleum fuel needs in the U.S would require producing approximately 1 L biofuel/person/day.¹²⁵ If we are able to convert algal biomass to fuel with a 15% total yield (12% from fatty acids + 3% from alkenones), this would require approximately 6.5 kg Isochrysis/person/day. Applying our fucoxanthin content value of 20 mg/g DW to this would correspond to 160 g fucoxanthin/person/day. For fucoxanthin to be able to offset the cost of fuel production by \$1/L, the profit associated with fucoxanthin sales would then have to be \$6/kg (calculated from \$1/0.16 kg). If we assume that the net profit that could be made to be 10-20% of production cost, the retail value would be required to be \$30-\$60/kg. Fucoxanthin is primarily as sold as a weight-loss supplement using extracts from several edible brown seaweeds.¹³⁵ Products of this type, use compound content in approximately 5 mg/dose at a cost of \$0.25/dose or \$500/g fucoxanthin, which far exceeds the \$1 fuel offset benchmark. However, the recommended doses of Fucoxanthin is only 15 mg/person/day, so supply of fucoxanthin as a biofuel coproduct would greatly outstrip the demand of its current market. With increased supply there is the potential for an increase in its commercial applications thus maintaining its value and a not-insignificant offsetting of the fuel cost.

Necton biomass was also used in addition to initial work with Reed. In contrast to the to the wet (80% water) black paste from Reed, the Necton product is a light brown dry milled powder (Figure 9). When previously comparing yields of lipid extracts of these two commercial sources of *Isochrysis* to be very similar. While the resulting biodiesel and algal oil had similar appearances, it was not clear whether the stark differences in appearance of the biomass would result in different fucoxanthin contents. To investigate this, Necton *Isochrysis* was processed into **h-AO** and **e-AO** as previously described. Once again, the resulting **e-AO** was highly enriched in fucoxanthin compared to the corresponding **h-AO** by HPLC analysis (21.3 % w/w fucoxanthin for **e-AO** vs. 1.4% w/w for **h-AO**, Table 17). Surprisingly, both Necton and Reed **e-AO** had very similar fucoxanthin amounts (21.3% w/w for Necton vs. 20.2 % (avg.)

w/w for Reed) and appearance, despite the noted different physical properties of the starting algal biomass. Again, the Yields of **e-AO** were also similar (7.9% from Necton vs. 8.3% (avg.) from Reed), meaning that total fucoxanthin amounts in the starting biomass were very close (21.7 mg/g DW Reed *Isochrysis* vs. 19.6 mg/g DW Necton *Isochrysis*). One area of uncertainty that requires caution in this comparison, is that the moisture contents of the different starting dry *Isochrysis* biomasses were not rigorously determined. As, Necton advertises their product as containing 5% water and was used without further drying. It is also assumed that the freeze dried Reed paste has approximately the same water content, such that we conclude fucoxanthin amounts in both commercial products is similar (Table 17).

Table 17. Comparison of fucoxanthin recoveries from Reed and Necton *Isochrysis*.

<i>Isochrysis</i>	Reed ^A	Necton
h-AO (% DW)	17.3	15.0
e-AO (% DW)	8.0	8.3
e-AO Fucoxanthin Content (% w/w) ^B	20.2	21.3
h-AO Fucoxanthin Content (% w/w) ^B	3.05	1.04
Total Fucoxanthin Content (mg/g DW)	21.7	19.6

^AAverage values from Table 17. ^BDetermined by HPLC.

Other polar solvents such as acetonitrile and acetone were also explored for their efficiency in extracting fucoxanthin from post-hexanes extracted *Isochrysis* biomass. Ethanol gave the highest overall yields, while acetonitrile produced the most fucoxanthin-rich **e-AO**.

In summary, there is currently great interest in the coproduction of value added chemicals to improve the economic viability of algal biofuels. By exploiting differences in solvent extraction efficiencies, a

tandem biomass extraction protocol has been developed that allows for the parallel production of two separate lipid-based fuels and isolation of a high-value carotenoid fucoxanthin from two commercial sources of marine microalgae *Isochrysis*. Quantification of the amount of fucoxanthin in the ethanol algal oil revealed that this sequential extraction is quite selective, with total values near the maximum found in other reports describing fucoxanthin from *Isochrysis*. Efforts are ongoing to optimize and analyze this procedure as a general strategy for the coproduction of fuel and high value natural products from *Isochrysis* and other algae feedstocks.

Investigation of Heterogeneous Catalysis for *Isochrysis* biofuel production

There have been a number of reports describing the production of biofuels from an algae feedstock by heterogeneous catalytic upgrading.¹³⁶⁻¹³⁸ Most of studies have focused on algal triglycerides¹³⁹, which can be converted to for instance hydrogenated biodiesel (HBD).¹⁴⁰ Our group was drawn to heterogeneous catalysis as a potentially more industrially relevant method for converting alkenones to fuel than our previous butenolysis reaction. That cross-metathesis reaction employs a homogenous metathesis initiator which is not easily recovered/regenerated and is fairly expensive. Also, we thought that a heterogeneous catalyzed reaction might be able to be performed on the total lipid extract containing both alkenones and triglycerides leading directly to various fuel products. For these reasons we decided to investigate the hydrocracking of alkenones isolated from *Isochrysis sp.* as a compliment to the hydrocarbon products formed by our butenolysis reaction.

Catalysis Systems

Kazuhisa Murata and coworkers recently reported the hydrocracking of algal *Botryococcus braunii* oil (Bot-oil) with a Pt-Re/SiO₂-Al₂O₃ (SA) catalyst. The hydrocarbon product distribution from the cracking of Bot-oil at 330 °C/797 psi H₂ with a 1 wt% Pt-3 wt% Re SA catalyst was found by GCMS analysis to be 4.63% C₁-C₄, 17.2% C₅-C₉, 50.2% C₁₀-C₁₅, 16.7% C₁₆-C₂₀, and 10.9% C₂₁₊.¹⁴¹ Based on the product selectivity attained (50.2% aviation fuel hydrocarbons, C₁₀-C₁₅) by Murata et al. and the feed chosen, this catalyst system was chosen for cracking of the alkenones. Bot-oil is unique in that it is composed of non-oxygenated triterpenic hydrocarbons (C₃₀ - C₃₄, e.g. squalene),¹⁴²⁻¹⁴⁴ and therefore similar to the alkenones with their long (C₃₆-C₃₉) unsaturated carbon chains (Figure 25). It might be expected therefore that this catalytic system would similarly produce primarily aviation range hydrocarbons from alkenones.

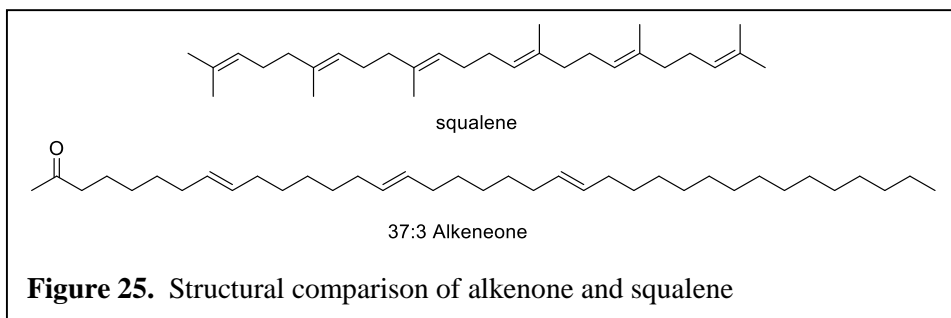
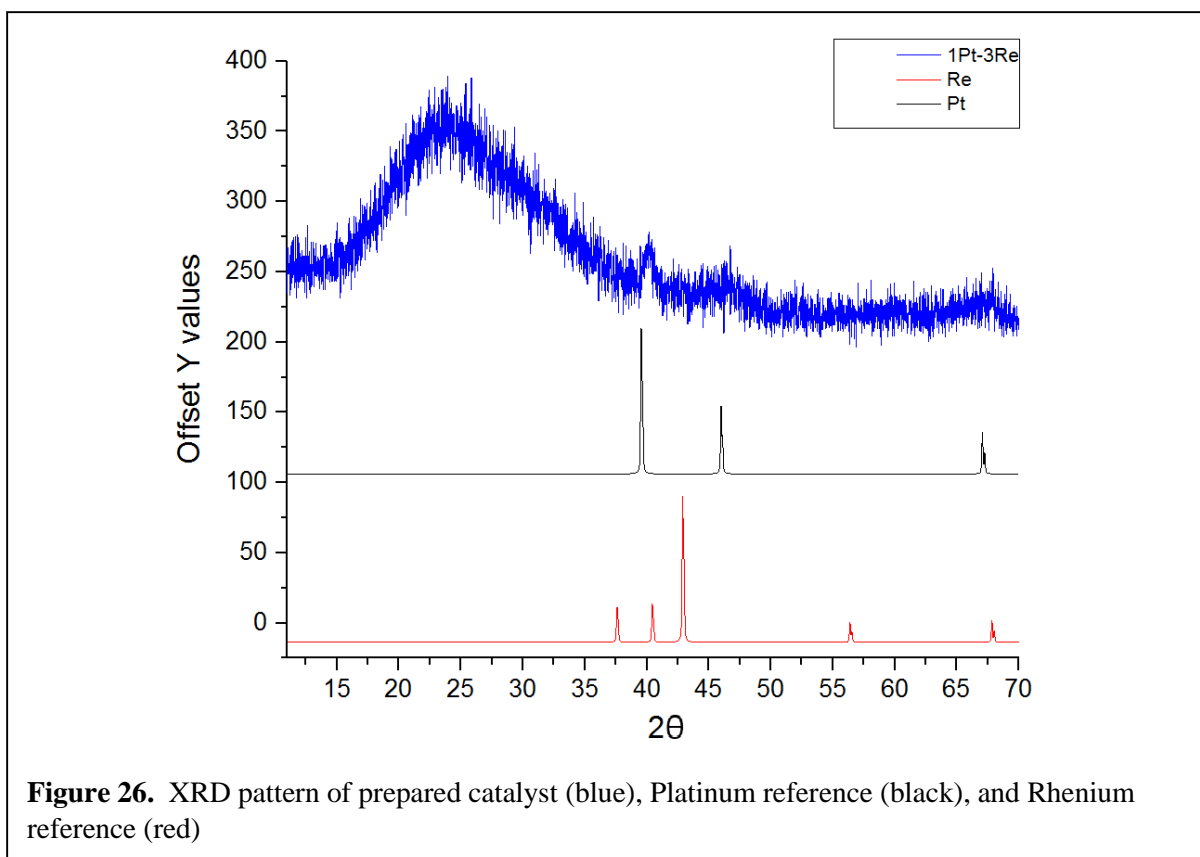


Figure 25. Structural comparison of alkenone and squalene

Catalyst Preparation and Characterization

Fresh 1Pt-3Re/SiO₂-Al₂O₃ was prepared by incipient wetting SA support (45% SiO₂: 55% Al₂O₃) with aqueous tetra-amine platinum (II) chloride and ammonium perrhenate sequentially. The catalyst was then dried at 100 C and calcined for 5 hr at 500 C. . Powder X-ray diffraction (XRD) patterns of the fresh catalysts were collected on a PanAnalytical X'Pert Pro MRD diffractometer using a

monochromatic Cu K α with a wave length of (λ) of 0.15418. Catalyst samples (15 mg) were ground to a fine powdered and mounted on glass slides by saturating the sample with methanol followed tapping with a scoopula to develop an evenly dispersed layer which is allowed to air dry. The samples were then scanned over a Bragg angle of (2θ) range of 35-65 with a step size of 0.015 $^\circ$ and a dwell time of 25 s. By application of the Scherrer equation to the width at half maximum signal for peaks corresponding to metals present in the support, the average particle size was determined to be 41.4 nm. The XRD pattern for 1Pt-3Re/SiO $_2$ -Al $_2$ O $_3$ and its reference metals and can be seen in (Figure 26).

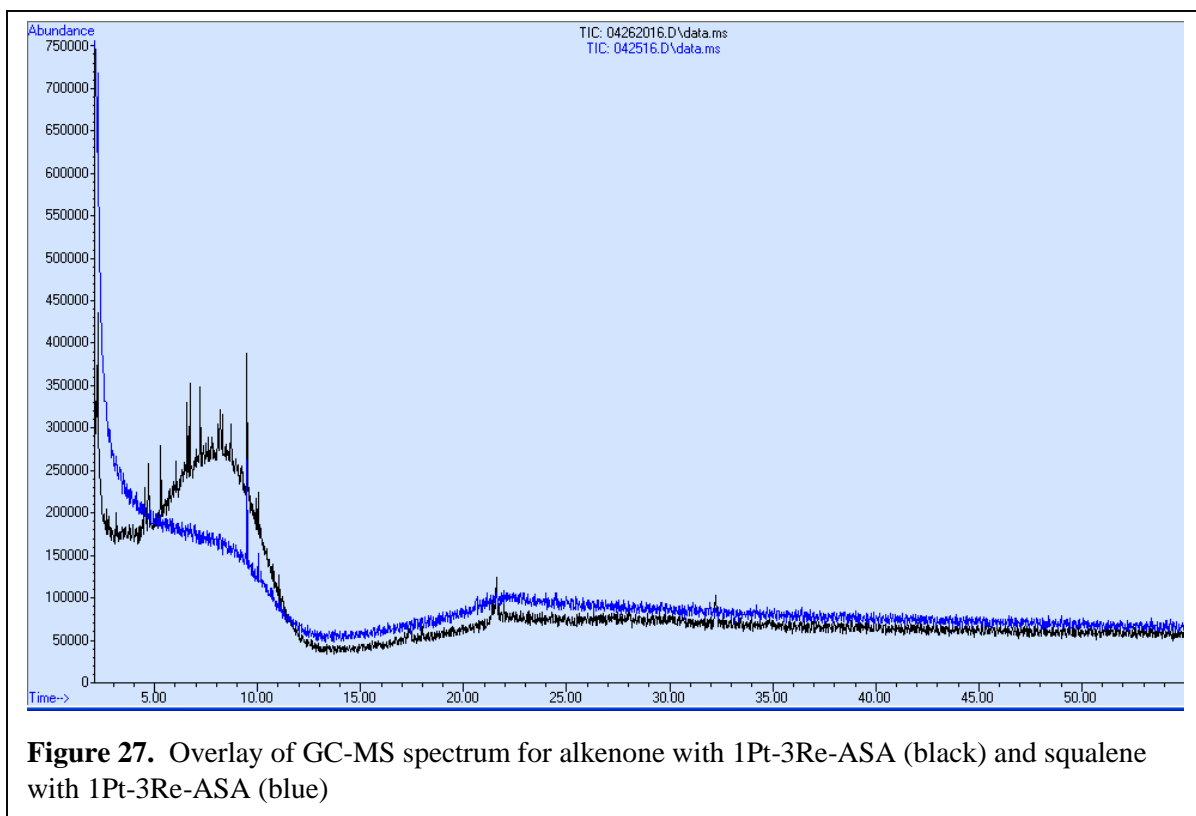


The 1Pt-3Re/SiO $_2$ -Al $_2$ O $_3$ catalysts were subjected to temperature programmed reduction (TPR) to form the final catalyst. Approximately 0.100 g of the precursor was placed into a quartz U-tube above approximately 0.1 g of quartz wool. The precursor was then purged in 60 mL/min He (Airgas,

99.9999%) for 30 min at room temperature. The precursor was then reduced in 100 mL/min H₂ (Airgas, 99.9999%) while heating from room temperature to 473.15 K at a rate of 5 K/min at which point the temperature was held for 5 h. The catalyst was then cooled to room temperature, purged with 60 mL/min He for 30 min followed by passivation in 60 mL/min 1 mol% He/O₂ (Airgas, 99.9999%) for 2 hr. Brunauer–Emmett–Teller (BET) surface area for the pure support and the impregnated catalyst were determined by N₂ physisorption using a Micromeritics Autochem 2950HP equipped with a thermal conductivity detector (TCD) and liquid-N₂ at a temperature of -196 °C. The pure support surface area was found to be 400 m²/g which decreased to 296.6 m²/g after impregnation, calcination and reduction.

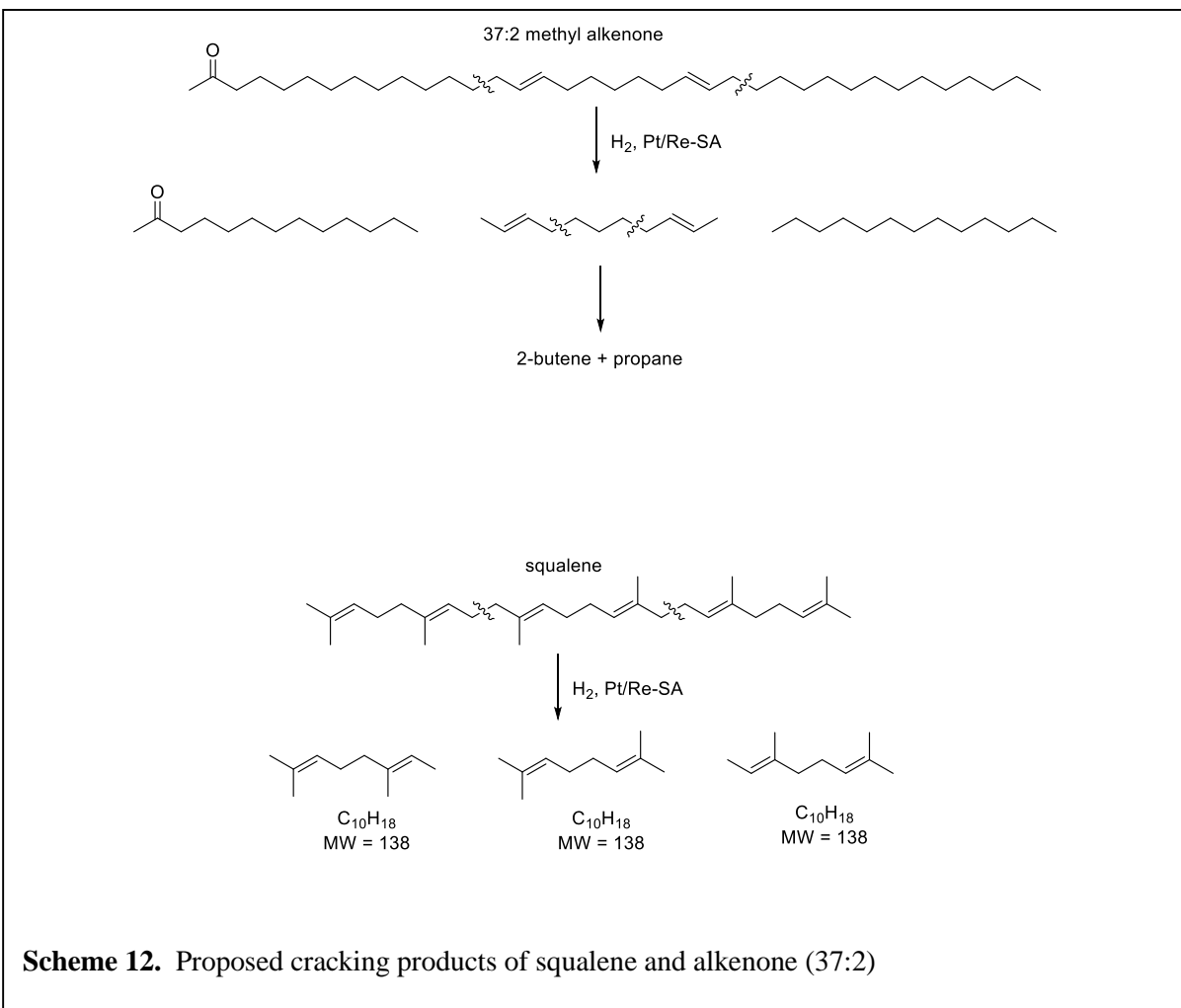
Product Analysis

With the characterized catalysts in hand, we could then begin investigating their use in cracking the alkenones. First, however, we wanted to compare results obtained with our catalyst to those reported by Murata for the hydrotreatment of squalene. In a high temperature/high pressure Parr batch reactor, our Pt-Re/SA catalyst was reduced to the active catalyst form under 290 psi H₂ at 200 C for 5 hours. After cooling the autoclave to room temperature, 200 mg squalene was then introduced under an argon atmosphere. The reactor was then pressurized with H₂ (797 psi) and heated to 310 C and is held at that temperature for 12 hours. Once the reactor had once again cooled to room temperature, the hydrogen pressure was carefully released, and the reactor autoclave containing catalyst and reaction mixture was rinsed with DCM. This DCM solution was separated from the catalyst by filtration and was then analyzed by GC-MS.



Results from GC-MS analysis showed overall very trace amounts of product, suggesting that the majority of components were either converted to gaseous products or coke (Figure 27). One major peak in the GC-MS chromatogram was at $m/z = 138$, which we have identified as compound 2,7-dimethylocta-2,6-diene that would result from cracking at the allylic positions of squalene. Formation of 2,7-dimethylocta-2,6-diene would also suggest that 2-methyl-2-butene was produced from squalene by a similar mechanism. This might also explain the low mass recovery (0.1%) due to the low boiling point of 2-methyl-2-butene (b.p = 39 C). Based on the results obtained from squalene, we can predict that cracking of the alkenones might also occur at the allylic positions. From our major alkenone component (methyl C37:2), this would then give the products outlined in Scheme 12. To test this, alkenones (200 mg) were subjected to identical cracking conditions used for squalene. Mass recovery from the alkenone cracking was 2.8%. The GC-MS chromatogram showed many more peaks

than the mixture obtained from squalene (including what appears to be an unresolved complex mixture between 4.5 - 11 min), perhaps suggesting many different cracking events. This could be due to presence of the oxygen atom in the alkenones, as this is the major structural difference between the alkenones and squalene. Further investigation into the products will include analysis by GCxGC, amounts of coke formed on the catalyst and cracking of various algal biofuel products (algal oil and biodiesel).



Experimental

Microalgae and Sample Preparation

The marine microalgae *Isochrysis* sp. “T-iso” used in the one step processing was obtained from Reed Mariculture (strain CCMP1324) (Santa Cruz, CA). The algae were grown in greenhouse ponds under natural sunlight in a modified F/2 media. Average water temperatures were 18–20 °C. Approximately 2 kg of wet biomass was poured into large crystallizing dishes and freeze-dried. These efforts led to ~290 g of dry *Isochrysis* sp. biomass, which was a greenish, dark-brown waxy amorphous solid.

Extraction and Quantification of Lipids

The dry *Isochrysis* sp. biomass obtained from Reed Mariculture was extracted in 50–150 g batches with n-hexane in a large Soxhlet extraction apparatus. The Soxhlet was allowed to cycle for 48 h (approximately 60 cycles) until the color of the solvent was a faint yellow. Hexane was removed with a rotary evaporator, and the remaining material was transferred to a pre-weighed vial with dichloromethane and evaporated to dryness with a gentle stream of N₂. The weight of the hexane-extractable material (typically ~10 g from a 50 g dry biomass extraction event) was recorded and will be referred to as “algal oil”.

1-Step Acid-Based Esterification of Algal Oil and Production of “Crude Biodiesel”

Following the method of Johnson and Wen, a mixture of methanol (3.4 mL), concentrated sulfuric acid (0.6 mL), and chloroform (4.0 mL) was added to of the algal oil (1 g) in a 40 mL glass vial containing a

small magnetic stir bar. The mixture was then heated to 90 °C for 40 min while stirring. After cooling, the reaction mixture was transferred to a separatory funnel and washed with deionized water (10 mL). Once the phases had separated, the bottom layer was drained into a preweighed vial and dried under a stream of N₂ and the resulting crude biodiesel was weighed [~0.9 g, 90% (w/w) of algal oil].

Saponification of Algal Oil and Separation of Neutral and Polar Lipids

To a solution of the algal oil (5–10 g) in MeOH (50 mL), CHCl₃ (25 mL) and H₂O (20 mL) was added KOH (4.0 g), and the mixture was heated with stirring to 60 °C for 3 h with a reflux condenser. The reaction was cooled to room temperature, and solvents were removed by rotary evaporation.

Isolation of Alkenones from Soap

The remaining aqueous mixture containing the algal soaps was then extracted with hexanes (3 × 25 mL). Concentration of the combined organic extracts gave the neutral lipids (typically, 40% w/w of the algal oil) as a green-yellow solid, which contains the nonpolar alkenones. Alkenones present in the collected neutral lipids can be isolated by various solvent systems with flash column chromatography on silica gel. Initial isolation of alkenones were performed using 20:1 hexanes/ethyl acetate but, required numerous recrystallizations to yield pure alkenones by ¹HNMR and GC-FID.

Acidification of Soaps to Free Fatty Acids

The aqueous phase containing the algal soaps was then acidified with a 1:1 ration of DI H₂O:HCl (6 M) until the aqueous layer has a pH \approx 2. After the soaps are converted to the resulting free fatty acids (FFAs) they were then extracted with hexanes (3 \times 25 mL). Removal of the solvent from these combined organic extracts gave the FFAs as a dark green near-black oily residue (typically, 60% w/w of the algal oil)

Acid-Catalyzed Esterification of Free Fatty Acids and Production of Biodiesel

To the FFAs obtained above (2.0 g) was added methanol (8.0 mL), concentrated H₂SO₄ (1.0 mL), and CHCl₃ (8.0 mL), and the mixture was heated to 90 °C while stirring for 1 h. After cooling, the reaction product was transferred to a separatory funnel and mixed with 10 mL of distilled water. Once the phases separated, the bottom layer was drained into a preweighed round-bottom flask and dried in *vacuo*, and the resulting biodiesel was weighed (1.84 g, 92% w/w of FFAs). Samples were stored at 4 °C before being combined into batches as needed for analysis. During this time, some settling of insoluble material occurred that was generally not included in the analysis. Nonetheless, some fine precipitates remained suspended in the biodiesel

Decolorization of Algal Biodiesel

To the dark green colored biodiesel obtained above (15 g) at 60 C was added montmorillonite K 10 (MK10) powder (3.0 g, 20% w/w of the biodiesel) and the mixture was stirred for 1 h. The solution was then filtered through Celite with hexanes and the hexanes were removed on a rotary evaporator

to produce an orange/red biodiesel (13 g, on average 90% w/w mass recovery). Samples were stored at 4 °C during which time some settling of insoluble material (<10% w/w) occurred. Decanting gave a clear homogeneous biodiesel that was analyzed separately.

Isolation and Purification of Alkenones from the Neutral Lipids

Neutral lipids (10 g) were dissolved in a minimal amount of dichloromethane and flushed through silica gel (230–400 mesh, 100 g) with pressure using dichloromethane (approximately 150 mL) as eluent. Solvent was then removed on a rotary evaporator and the resulting orange-colored solid was recrystallized in hexanes to give pure alkenones (typically 4 g) as a white solid.

Alkenone Butenolysis, General Procedure

2-Butene (0.2 mL, 15 equiv) was condensed in a reaction flask at –78 °C under a nitrogen atmosphere. Alkenones (100 mg), methyl stearate (methyl octadecanoate) (56 mg), dichloromethane or toluene (1.0 mL), and catalyst (2 mol %, 2–3 mg) were then added and the resulting heterogeneous mixture was placed in a refrigerator (4 °C) or ice bath (0 °C) for the allotted time. Reactions conducted were quenched with ethyl vinyl ether (0.9 mL, 50 equiv) and stirred for 15 min before concentrating on a rotary evaporator and analyzing by ¹H NMR and gas chromatography.

Analysis by One-Dimensional Gas Chromatography with Flame Ionization Detection (GC–FID) and Gas Chromatography– Mass Spectrometry (GC–MS)

The purified alkenones and butenolysis reactions were analyzed on a Hewlett-Packard 5890 Series II GC–FID. Samples (1 μL) were injected cool-on-column and separated on a 100% dimethyl polysiloxane capillary column (Restek Rtx-IMS, 30 m length, 0.25 mm I.D., 0.25 μm film thickness) with H_2 as the carrier gas at a constant flow of 5 mL min^{-1} . The GC oven was programmed from 70 $^\circ\text{C}$ (7 min hold) and ramped at 6 $^\circ\text{C min}^{-1}$ to 320 $^\circ\text{C}$ (15 min hold). Percent conversions for the butenolysis reactions were determined by comparison of integration ratios for combined alkenones ($rt = 44\text{--}48$ min) to methyl stearate (retention time = 27.5 min) relative to a starting alkenone/methyl stearate standard mixture. Select samples were also analyzed by GC–MS on an Agilent 6890 GC with a 5973 MSD. Splitless 1 μL sample injections, were separated on a DB-XXL capillary column (60 m \times 0.25 mm \times 0.25 μm film thickness) using helium as the carrier gas (10.5 psi constant pressure), and the following GC temperature program: 4 min at 40 $^\circ\text{C}$ and ramped to 320 at 5 $^\circ\text{C}/\text{min}$ (held 15 min).

Analysis by Comprehensive Two-Dimensional Gas Chromatography with Flame Ionization Detection (GC \times GC–FID) and Time-of-Flight Mass Spectrometer (GC \times GC–TOF).

Select butenolysis reaction mixtures were analyzed by GC \times GC–FID and GC \times GC–TOF MS according to previous described methodologies (Chapter 4).

Fucoxanthin extraction of the post-hexanes extracted Isochrysis biomass.

After the final Soxhlet cycle with hexanes, the apparatus was allowed to cool to room temperature. The residual biomass remaining in the cellulose thimble was dry at this point and could be easily removed from the extraction thimble and added to a 500 mL Erlenmeyer flask. To the waste biomass was then added ethanol, acetonitrile, or acetone (volume = 5 x mass of algal biomass, e.g. 200 mL for 50 g algae) in a static vessel for various time increments. Care was taken at this stage to ensure that the samples and subsequent materials were exposed minimally to light. The biomass was then removed by filtration into a tared round bottom flask and the ethanol removed with a rotary evaporator. The masses of the ethanol extracts were recorded and will be referred to as “ethanol algal oil” (e-AO).

Isolation and purification of fucoxanthin by normal phase chromatography on silica.

Fucoxanthin from the **h-AO** neutral lipids and ethanol algal oil (**e-AO**) was purified by flash chromatography on silica using an automated Combiflash Rf system (Teledyne Isco): Approximately 2.0 g of either the **h-AO** neutral lipids or **e-AO** was loaded with DCM (~2-3 mL) onto a 24 g pre-packed silica gel cartridge (230-400 mesh). The chromatography was programmed as follows: 15-minute run time, gradient from 100% hexanes to 100% ethyl acetate. For preparation of the fucoxanthin-enriched algal oil (**enriched-AO**), fractions that were bright red in color and mostly pure by TLC (1:1 hexanes ethyl acetate, R_f fucoxanthin = 0.36) were combined into a tared round bottom flask and concentrated on a rotary evaporator in the dark. The weight of **enriched-AO** was recorded and the fucoxanthin content analyzed by ¹H NMR and HPLC.

Analysis and quantification of fucoxanthin by HPLC.

Fucoxanthin contents in the hexane- and ethanol algal oils were quantified using a Varian ProStar HPLC system. The system consisted of a binary pump, 410 autosampler, and photodiode array detector. A reverse-phased C₁₈ column (Waters length 250 mm x i.d 4.6 mm x particle size 5µm) was eluted with a mobile phase (100% methanol) at a flow rate of 1 mL/min. Detection wavelength was set at 446 nm. Fucoxanthin content was determined based on the comparison to a calibration curve, constructed by analyzing fucoxanthin (purchased from Sigma-Aldrich) samples at concentrations of 0.016 – 1.0 mg/mL with $R^2 = 0.9987$.

Hydrogenation and cracking of PULCA's in presence of Pt-Re ASA catalyst

For the batch reaction, the catalyst (0.02 g) was introduced into a 100 cm³ autoclave-type reactor and first pretreated by reduction with 2 MPa of H₂ at 473 K for 5 h. After the reduction, 0.200 g alkenones or squalane was introduced and the autoclave was pressurized with 5.5 MPa of a H₂. The reaction was carried out at the prescribed temperature for 12 h. The autoclave was then rinsed with CH₂Cl₂ solvent, the catalyst is filtered off by pipet column and the solution is then analyzed by GCMS.

Conclusions

A method has been developed for the efficient synthesis of a decolorized alkenone-free biodiesel along with the quantitative recovery of an alkenone-rich neutral lipid fraction from the industrially produced microalgae *Isochrysis sp.* using standard saponification, extraction, esterification and

decolorization techniques. The process provided sufficient quantities of biodiesel to allow for comprehensive fuel testing of this material. Further processing of biodiesel to remove pigments, such as chlorophylls and other derivatives can be efficiently separated from *Isochrysis* biodiesel using montmorillonite K10 clay. Pigments such as chlorophylls and other derivatives can be efficiently removed from *Isochrysis* biodiesel using montmorillonite K10 clay. The process was performed on sufficient scale to allow for comprehensive fuel testing of the resulting decolorized biodiesel. This was made possible in part due to the commercial availability of *Isochrysis* in multi-kilogram quantities from several suppliers. Results from the fuel tests provided important experimental data that can be used to validate and refine often used predictive models for algal biodiesel fuel properties. For instance, oxidative stability remains an issue for our *Isochrysis* (and presumably other algal) biodiesel, and appears highly sensitive to even minor amounts of PUFAMES. Through the decolorization process we were now able to obtain a CP, with the measured CP for our decolorized biodiesel lower than what would be predicted based on the FAME profile. A comparison of the fuel testing results for our decolorized sample to that previously obtained for a non-decolorized *Isochrysis* biodiesel also revealed certain impacts of pigments on fuel properties. Specifically, pigment removal resulted in a 24% increase in CN (from 36.5 to 45.4 (avg.)), 40% increase in kinematic viscosity (from 2.5 to 3.5 mm²/s), a 50% decrease in lubricity (from 260 to 131 μm), and 4% decrease in density (from 935 to 897 kg/m³). Work is therefore ongoing to fully characterize these mixtures, and the isolation of fine chemical products in parallel with continued studies toward the production of an ASTM-certified *Isochrysis* biodiesel.

References

(1) National Science Foundation: Climate introduction: Report.

http://www.nsf.gov/news/special_reports/climate/intro_background.jsp (accessed April 20th, 2016)

(2) (Environmental Protection Agency: Causes of Climate Change: Science

<http://www3.epa.gov/climatechange/science/causes.html> (accessed April 19th, 2016)

(3) "EPA's Budget and Spending | Planning Budget Results". US EPA. United States Environmental Protection Agency. 2014-03-04. Retrieved 2014-03-28.

(4) National Renewable Energy Laboratory: "EPA's Budget and Spending | Planning Budget Results". <http://www.nrel.gov/docs/fy06ost> (accessed April 18th, 2016)

(5) United States Department of Energy: Alternative Fuels Data Center: Blends

http://www.afdc.energy.gov/fuels/biodiesel_blends.html (accessed April 21th, 2016)

(6) T. J. Wallington,* J. E. Anderson, S. A. Mueller, E. Kolinski Morris, S. L. Winkler, and J. M. Ginder. "Corn Ethanol Production, Food Exports, and Indirect Land Use Change" Environ. Sci. Technol. 2012, 46, 6379–6384

(7) The World Bank: Development Prospects Group: JULY 2008 POLICY RESEARCH WORKING PAPER 4682: <https://openknowledge.worldbank.org/bitstream/handle/10986/6820/WP4682.txt> (accessed April 20th, 2016)

(8) OSU Biological and Ecological Engineering Department: Lecture Six Cellulose, Hemicellulose and Lignin http://stl.bee.oregonstate.edu/courses/BFP/Class_Slides_W2011/BFP_Lecture6.pdf (accessed April 19th, 2016)

- (9) Saritha M, Arora A, Lata. Biological Pretreatment of Lignocellulosic Substrates for Enhanced Delignification and Enzymatic Digestibility. *Indian Journal of Microbiology*. **2012**; 52(2):122-130.
- (10) Rosa Dominguez-Faus, Christian Folberth, Junguo Liu, "Climate Change Would Increase the Water Intensity of Irrigated Corn" *Environ. Sci. Technol.* **2013**, 47, 6030–6037.
- (11) Universtiy of Twente and Labratoty of Thermal Engenering: A new technology for fast pyrolysis of biomass: development of the PyRos reactor
<http://web.archive.org/web/20050601051827/http://www.thw.ctw.utwente.nl/research/Fuelconv/bramer.pdf> (accessed April 19th, 2016)
- (12) Adam J. Liska, Haishun Yang, Maribeth Milner, "Biofuels from crop residue can reduce soil carbon and increase CO2 emissions", *Nature Climate Change* 4, **2014** 398–401.
- (13) Biofuels: Third Generation Biofuels <http://biofuel.org.uk/third-generation-biofuels.html> (accessed April 19th, 2016).
- (14) Sheehan, J., Dunahay, T., Sheehan, J., Dunahay, T., Benemann, J., Roessler, P.A. A look back at the U.S. Department of Energy's Aquatic Species Program: Biodiesel from algae; National Renewable Energy Laboratory, report NREL/TP-580-24190; 1996.
- (15) U.S First Crude Oil Purchase Price. U.S. Energy Information Administration.
http://www.eia.gov/dnav/pet/hist/LeafHandler.ashx?n=PET&s=F000000_3&f=A (accessed April 1, 2016)
- (16) Energy: Secretary Chu Announces Nearly \$80 Million Investment for Advanced Biofuels Research and Fueling Infrastructure <http://energy.gov/articles/secretary-chu-announces-nearly-80-million-investment-advanced-biofuels-research-and-fueling> (accessed April 1, 2016)

- (17) Schenk, P. M.; Thomas-Hall, S. R.; Stephens, E.; Marx, U. C.; Mussgnug, J. H.; Posten, C.; Kruse, O.; Hankamer, B. *Bioenerg. Res.* 2008, 1, 20–43.
- (18) Griffiths, M. J.; Harrison, S. T. L. *J. App. Phycol.* 2009, 21, 493– 507
- (19) American Society for Testing and Materials (ASTM). ASTM Standard D6751, Standard Specification for Biodiesel Fuel Blend Stock (B100) for Middle Distillate Fuels; ASTM International: West Conshohocken, PA, 2003; DOI: 10.1520/D6751-11B, www.astm.org
- (20) For recent reviews that include Isochrysis, see: (a) Mata, T. M.; Martins, A. A.; Caetano, N. S. *Renewable Sustainable Energy Rev.* 2010, 14, 217–232. (b) Huerlimann, R.; de Nys, R.; Heimann, K. *Biotechnol. Bioeng.* 2010, 107, 245–257. (c) Singh, J.; Gu, S. *Renewable Sustainable Energy Rev.* 2010, 14, 2596–2610.
- (21) O’Neil GW, Carmichael CA, Goepfert TJ, Fulton JM, Knothe G, Lau CP-L. Beyond fatty acid methyl esters: expanding the renewable carbon profile with alkenones from *Isochrysis* sp. *Energy Fuels* 2012;26: 2434–41.
- (22) Rontani, J.-F.; Marchand, D.; Volkman, J. K. *Org. Geochem.* 2001, 32, 1329–1341.
- (23) Rontani, J.-F.; Prahl, F. G.; Volkman, J. K. *J. Phycol.* 2006, 42, 800–813.
- (24) Volkman, J. K.; Eglinton, G.; Corner, E. D. S. *Phytochemistry* 1980, 19, 2619–2622.
- (25) Marlowe, I. T.; Brassell, S. C.; Eglinton, G.; Green, J. C. *Org. Geochem.* 1984, 6, 135–141.26
- (26) Imahara, H.; Minami, E.; Saka, S. *Fuel* 2006, 85, 1666–1670.27
- (27) O’Neil, G. W.; Moser, D. J.; Volz, E. O. *Tetrahedron Lett.* 2009, 50, 7355–7357.
- (28) M Pagani, “Biomarker-Based Inferences of Past Climate: The Alkenone pCO₂ Proxy” Yale University, New Haven, CT, USA. 12.13, 2014, 363-366

- (29)** Freeman KH and Hayes JM (1992) Fractionation of carbon isotopes by phytoplankton and estimates of ancient CO₂ levels. *Global Biogeochemical Cycles* 6: 185–198
- (30)** Farquhar GD, O'Leary MHB, and Berry JA (1982) On the relationship between carbon isotope discrimination and the intercellular carbon dioxide concentration in leaves. *Australian Journal of Plant Physiology* 9: 121–137.
- (31)** Francois R, Altabet MA, Goericke R, McCorkle DC, Brunet C, and Poisson A (1993) Changes in the $\delta^{13}C$ of surface water particulate organic matter across the subtropical convergence in the SW Indian Ocean. *Global Biogeochemical Cycles* 7: 627–644.
- (32)** Hollander DJ and McKenzie JA (1991) CO₂ control on carbon isotope fractionation during aqueous photosynthesis: A paleo-pCO₂ barometer. *Geology* 19: 929–932
- (33)** Pond, D. W. & Harris, R. P. 1996. The lipid composition of the coccolithophore *Emiliana huxleyi* and its possible ecophysiological significance. *J. Mar. Biol. Assoc. UK* 76:579–94.
- (34)** Henderson, R. J. & Sargent, J. R. 1989. Lipid composition and biosynthesis in ageing cultures of the marine cryptomonad, *Chroomonas salina*. *Phytochemistry* 28:1355–61.
- (35)** Epstein, B. L., D'Hondt, S. & Hargraves, P. E. 2001. The possible metabolic role of C₃₇ alkenones in *Emiliana huxleyi*. *Org. Geochem.* 32:867–75.
- (36)** Prah, F. G., Wolfe, G. V. & Sparrow, M. A. 2003. Physiological impacts on alkenone paleothermometry. *Paleoceanography* 18: 1025–31.
- (37)** Marlowe, I.T., Green, J.C., Neal, A.C., Brassell, S.C., Eglinton, G. and Course, P.A. "Long-chain (n-C₃₇-C₃₉) alkenones in the Prymnesiophyceae. Distribution of alkenones and other lipids and their taxonomic significance." *British Phycological Journal* (**1984**), 19, 203-216

- (38) Antoni Rosell-Melé, Erin L. McClymont, Chapter Eleven Biomarkers as Paleoceanographic Proxies: “Proxies in Late Cenozoic Paleoceanography” *Developments in Marine Geology: Volume 1*, **2007**, Pages 441–490
- (39) Muradyan, E.; Klyachko-Gurvich, G.; Tsoglin, L.; Sergeyenko, T.; Pronina, N. Changes in lipid metabolism during adaptation of the *Dunaliella salina* photosynthetic apparatus to high CO₂ concentration. *Rus. J. Plant Physiol.* **2004**, *51*, 53–62.
1302, 17–45.
- (40) Converti, A.; Casazza, A.A.; Ortiz, E.Y.; Perego, P.; del Borghi, M. Effect of temperature and nitrogen concentration on the growth and lipid content of *Nannochloropsis oculata* and *Chlorella vulgaris* for biodiesel production. *Chem. Eng. Process.* **2009**, *48*, 1146–1151.
- (41) Shifrin, N.S.; Chisholm, S.W. Phytoplankton lipids: Interspecific differences and effects of nitrate, silicate and light-dark cycles. *J. Phycol.* **1981**, *17*, 374–384.
- (42) Wang, Z.T.; Ullrich, N.; Joo, S.; Waffenschmidt, S.; Goodenough, U. Algal lipid bodies: Stress induction, purification, and biochemical characterization in wild-type and starchless *Chlamydomonas reinhardtii*. *Eukaryot. Cell* **2009**, *8*, 1856–1868.
- (43) Demirbas, A. Use of algae as biofuel sources. *Energy Convers. Manag.* **2010**, *51*, 2738–2749.
- (44) Takagi, M.; Watanabe, K.; Yamaberi, K.; Yoshida, T. Limited feeding of potassium nitrate for intracellular lipid and triglyceride accumulation of *Nannochloris* sp. UTEX LB1999. *Appl. Microbiol. Biotechnol.* **2000**, *54*, 112–117.
- (45) Stephenson, A.L.; Dennis, J.S.; Howe, C.J.; Scott, S.A.; Smith, A.G. Influence of nitrogen-limitation regime on the production by *Chlorella vulgaris* of lipids for biodiesel feedstocks. *Biofuels* **2010**, *1*, 47–58.
- (46) Thompson, G.A., Jr. Lipids and membrane function in green algae. *Biochim. Biophys. Acta* **1996**,

- (47) Morris, I.; Glover, H.; Yentsch, C. Products of photosynthesis by marine phytoplankton: The effect of environmental factors on the relative rates of protein synthesis. *Mar. Biol.* **1974**, *27*, 1–9
- (48) Kilham, S.; Kreeger, D.; Goulden, C.; Lynn, S. Effects of nutrient limitation on biochemical constituents of *Ankistrodesmus falcatus*. *Freshw. Biol.* **1997**, *38*, 591–596.
- (49) Fogg, G. Photosynthesis and formation of fats in a diatom. *Ann. Bot.* **1956**, *20*, 265–285.
- (50) Holm-Hansen, O.; Nishida, K.; Moses, V.; Calvin, M. Effects of mineral salts on short-term incorporation of carbon dioxide in *Chlorella*. *J. Exp. Bot.* **1959**, *10*, 109–124.
- (51) Lynn, S.G.; Kilham, S.S.; Kreeger, D.A.; Interlandi, S.J. Effect of nutrient availability on the biochemical and elemental stoichiometry in the freshwater diatom *Stephanodiscus minutulus* (*Bacillariophyceae*). *J. Phycol.* **2000**, *36*, 510–522
- (52) Heraud, P.; Wood, B.R.; Tobin, M.J.; Beardall, J.; McNaughton, D. Mapping of nutrient-induced biochemical changes in living algal cells using synchrotron infrared microspectroscopy. *FEMS Microbiol. Lett.* **2005**, *249*, 219–225.
- (53) Li, Y.; Horsman, M.; Wang, B.; Wu, N.; Lan, C.Q. Effects of nitrogen sources on cell growth and lipid accumulation of green alga *Neochloris oleoabundans*. *Appl. Microbiol. Biotechnol.* **2008**, *81*, 629–636.
- (54) Ben-Amotz, A.; Avron, M. The biotechnology of cultivating the halotolerant alga *Dunaliella*. *Trends Biotechnol.* **1990**, *8*, 121–126.
- (55) Borowitzka, M.A.; Huisman, J.M.; Osborn, A. Culture of the astaxanthin-producing green alga *Haematococcus pluvialis*. Effects of nutrients on growth and cell type. *J. Appl. Phycol.* **1991**, *3*, 295–304.
- (56) Harker, M.; Tsavalos, A.J.; Young, A.J. Factors responsible for astaxanthin formation in the chlorophyte *Haematococcus pluvialis*. *Bioresour. Technol.* **1996**, *55*, 207–214.

- (57) Collier, J.L.; Grossman, A. Chlorosis induced by nutrient deprivation in *Synechococcus* sp. strain PCC 7942: Not all bleaching is the same. *J. Bacteriol.* **1992**, *174*, 4718–4726.
- (58) Hu, Q. Environmental Effects on Cell Composition. In *Handbook of Microalgal Culture: Biotechnology and Applied Phycology*; Richmond, A., Ed.; Blackwell: Oxford, UK, 2004; pp 83–93.
- (59) Borchardt, J.A.; Azad, H.S. Biological extraction of nutrients. *J. Water Pollut. Control Fed.* **1968**, *40*, 1739–1754.
- (60) American Society for Testing and Materials (ASTM). ASTM Standard D6751, Standard for Biodiesel Fuel Blend Stock
- (61) Fisher, B. C. et al. “Measurement of Gaseous and Particulate Emissions from Algae-Based Fatty Acid Methyl Esters” *SAE Tech. Pap.* 2010-01-1523, **2010**
- (62) Knothe, G. *Energy Fuels* 2008, *22*, 1358–1364.
- (63) O’Neil, G.W., Knothe, G., Williams, J.R., Burlow, N.P., Culler, A.R., Corliss, J.M., Carmichael, C.A., Reddy, C.M. Synthesis and analysis of an alkenone-free biodiesel from *Isochrysis* sp. *Energy Fuels* **28** (4), 2677-2683, DOI: 10.1021/ef500246h (2014).
- (64) Paulo A.Z. Suareza, Comparing the lubricity of biofuels obtained from pyrolysis and alcoholysis of soybean oil and their blends with petroleum diesel. *Fuel*, *88*, *6*, **2009**, 1143–1147
- (65) Stansell, G. R.; Gray, V. M.; Sym, S. D. *J. Appl. Phycol.* **2012**, *24*, 791–801.
- (66) Valenzuela-Espinoza E., Millán-Núñez R., Núñez-Cebrero F. Protein, carbohydrate, lipid and chlorophyll a content in *Isochrysis* aff. *galbana* (clone T-Iso) cultured with a low cost alternative to the f/2 medium. *Aquacult. Eng.* **25**, 207-216, DOI: 10.1016/S0144-8609(01)00084-X (2002).
- (67) Suganya T, Gandhi NN, Renganathan S. Production of algal biodiesel from marine macroalgae *Enteromorpha compressa* by two step process: optimization and kinetic study. *Bioresour Technol* 2013; *128*: 392–400.

- (68) Rao YR, Deshmukh SS. Catalytic production of bio-diesel from algal oil. *Asian J Chem* 2010; 22: 1146–50.
- (69) Johnson MB, Wen Z. Production of biodiesel fuel from the microalga *Schizochytrium limacinum* by direct transesterification of algal biomass. *Energy Fuels* 2009; 23: 5179–83.
- (70) Vanessa D. Silva, Oxidative Stability of Baru (*Dipteryx alata* Vogel) Oil Monitored by Fluorescence and Absorption Spectroscopy, *Journal of Spectroscopy*, 2015, 803705, 6 pg.
- (71) Kulkarni MG, Dalai AK, Bakshi NN. Utilization of green seed canola oil for biodiesel production. *J Chem Technol Biotechnol* 2006; 81:1886–93.
- (72) Issariyakul T, Dalai AK. Biodiesel production from greenseed canola oil. *Energy Fuels* 2010; 24:4652–8.
- (73) Mokaya R, Jones W, Davies ME, Whittle ME. Preparation of alumina-pillared acid-activated clays and their use as chlorophyll adsorbents. *J Mater Chem* 1993; 3:381–7.
- (74) Knothe G. A comprehensive evaluation of the cetane numbers of fatty acid methyl esters. *Fuel* 2014; 119:6–13.
- (75) Ono M, Sawada K, Shiraiwa Y, Kubota M. Changes in alkenone and alkenoate distributions during acclimatization to salinity change in *Isochrysis galbana*: implication for alkenone-based paleosalinity and paleothermometry. *Geochem J* 2012; 46: 235–47.
- (76) O’Neil, G.W., Knothe, G., Williams, J.R., Burlow, N.P., Culler, A.R., Corliss, J.M., Carmichael, C.A., Reddy, C.M. Synthesis and analysis of an alkenone-free biodiesel from *Isochrysis* sp. *Energy Fuels* 28(4), 2677-2683, DOI: 10.1021/ef500246h (2014).

- (77)** Knothe G. “Designer” biodiesel: optimizing fatty ester composition to improve fuel properties. *Energy Fuels* 2008; 22: 1358–64.
- (78)** Hughes JM, Mushrush GW, Hardy DR. Lubricity-enhancing properties of soy oil when used as a blending stock for middle distillate fuels. *Ind Eng Chem Res* 2002;41:1386–8.
- (79)** Dzida M, Prusakiewicz P. The effect of temperature and pressure on the physicochemical properties of petroleum diesel oil and biodiesel fuel. *Fuel* 2008;87:1941.
- (80)** Perrier B, Crampon C, Guézet O, Simon C, Maire F, Lépine O, et al. Production of a methyl ester from the microalgae *Nannochloropsis* grown in raceways on the French west coast. *Fuel* 2015;153:640–9.
- (81)** Mathimani T, Uma L, Prabakaran D. Homogeneous acid catalyzed transesterification of marine microalga *Chlorella* sp. BDUG 91771 lipid – an efficient biodiesel yield and its characterization. *Renew Energy* 2015;81:523–33.
- (82)** Nautiyal P, Subramanian KA, Dastidar MG. Production and characterization of biodiesel from algae. *Fuel Process Technol* 2014;120:79–88.
- (83)** Mahajan S, Konar SK, Boocock DGB. Determining the acid number of biodiesel. *J Am Oil Chem Soc* 20
- (84)** Cooke BS, Abrams C, Bertram B. Purification of biodiesel with adsorbent materials. World Intellectual Property Organization patent 2005037969 A2; April 28, 2005.06;83: 567–70.
- (85)** Knothe, G. Dependence of biodiesel fuel properties on the structure of fatty acid alkyl esters. *Fuel Process. Technol.* **86**, 1059-1070, DOI: 10.1016/j.fuproc.2004.11.002 (2005).
- (86)** O’Neil, G.W., Culler, A.R., Williams, J.R., Burlow, N.P., Gilbert, G.J., Carmichael, C.A., Nelson, R.K., Swarthout, R.F., Reddy, C.M. Production of jet fuel range hydrocarbons as a coproduct of algal

biodiesel by butenolysis of long-chain alkenones. *Energy Fuels*. **29**(2), 922-930, DOI:

10.1021/ef502617z (2015).

(87) For a recent review see: Naika, S. N.; Goud, V. V.; Rout, P. K.; Dalai, A. K. *Renew. Sust. Energy Rev.* 2010, 14, 578–597.

(88) Shanahan, C. “The global algae oil omega-3 market in 2014” *AlgaeIndustryMagazine.com*, May 18, 2014 <http://www.algaeindustrymagazine.com/the-global-algae-oil-omega-3-market-in-2014>, (accessed April, 1st, 2016).

(89) Foley, P. M.; Beach, E. S.; Zimmerman, J. B. *Green Chem.* 2011, 13, 1399–1405.

(90) Inderwildi, O. R.; King, D. A. *Energy Environ. Sci.* 2009, 2, 343– 346.

(91) van Beilen, J. B. *Biofuels, Bioprod. Biorefin.* 2010, 4, 41-52.

(92) Chisti, Y. *Biotechnol. Adv.* **2007**, 25, 294–306.

(93) Wijffles, R. H.; Barbosa, M. J. *Science* 2010, 329, 796-799.

(94) Ferrell, J.; Sarisky-Reed, V. *National Algal Biofuels Technology Roadmap* (Eds. D. Fishman, R. Majumdar, J. Morello, R. Pate, J. Yang), United States Department of Energy, 2010, http://www1.eere.energy.gov/bioenergy/pdfs/algal_biofuels_roadmap.pdf (accessed August 24, 2015).

(95) International Civil Aviation Organization: A United Nations Specialized Agency: Alternative Fuels: Question 4, current commercial availability of alternative fuels, http://www.icao.int/environmentalprotection/Documents/AltFuels/Alternative%20fuels%20webpage_Questions_Answers_May%202014.docx (accessed April, 11, 2016).

(96) the butenolysis reaction was also performed on the hexane algal oil directly with complete conversion of the alkenones. See supporting info of O’Neil, G.W., Culler, A.R., Williams, J.R., Burlow,

N.P., Gilbert, G.J., Carmichael, C.A., Nelson, R.K., Swarthout, R.F., Reddy, C.M. Production of jet fuel range hydrocarbons as a coproduct of algal biodiesel by butenolysis of long-chain alkenones. *Energy Fuels*. **29**(2), 922-930, DOI: 10.1021/ef502617z (2015).

(97) Alkene Metathesis in Organic Synthesis; A. Fürstner, Ed.; Springer: Berlin, 1998.

(98) Burdett, K. A.; Harris, L. D.; Margl, P.; Maughon, B. R.; Mokhtar-Zadeh, T.; Saucier, P. C.; Wasserman, E. P. *Organometallics* 2004, **23**, 2027–2047.

(99) Schrodi, Y.; Ung, T.; Vargas, A.; Mkrtumyan, G.; Lee, C. W.; Champagne, T. M.; Pederson, R. L.; Hong, S. H. *Clean* 2008, **36**, 669– 673.

(100) Anderson, D. R.; Ung, T.; Mkrtumyan, G.; Bertrand, G.; Grubbs, R. H.; Schrodi, Y. *Organometallics* 2008, **27**, 563–566.

(101) Thurier, C.; Fischmeister, C.; Bruneau, C.; Olivier - Bourbigou, H.; Dixneuf, P. H. *ChemSusChem* 2008, **1**, 118–122.

(102) Forman, G. S.; Bellabarba, R. M.; Tooze, R. P.; Slawin, A. M. Z.; Karch, R.; Winde, R. J. *Organomet. Chem.* 2006, **691**, 5513–5516.

(103) Thomas, R. M.; Keitz, B. K.; Champagne, T. M.; Grubbs, R. H. *J. Am. Chem. Soc.* 2011, **133**, 7490–7496.

(104) Marinescu, S. C.; Schrock, R. R.; Müller, P.; Hoveyda, A. H. *J. Am. Chem. Soc.* 2009, **131**, 10840–10841.

(105) Warwel, S.; Brüse, F.; Demes, C.; Kunz, M.; Rusch gen Klaas, M. R. *Chemosphere* 2001, **43**, 39–48.

- (106)** Thomas, R. M.; Keitz, B. K.; Champagne, T. M.; Grubbs, R. H. *J. Am. Chem. Soc.* 2011, 133, 7490–7496.
- (107)** Patel, J.; Elaridi, J.; Jackson, W. R.; Robinson, A. J.; Serelis, A. K.; Such, C. *Chem. Commun.* 2005, 5546–5547.
- (108)** Tuba, R.; Grubbs, R. H. *Polym. Chem.* 2013, 4, 3959–3962.
- (109)** Hargreaves, C. R.; Manley, J. B.; ACS GCI Pharmaceutical Roundtable. Collaboration to Deliver a Solvent Selection Guide for the Pharmaceutical Industry; American Chemical Society: Washington, DC, 2008. <http://www.acs.org/content/dam/acsorg/greenchemistry/industriainnovation/roundtable/solvent-selection-guide.pdf> (accessed November, 21, 2014).
- (110)** Gros, J.; Nabi, D.; Wu, B.; Wick, L. Y.; Brussard, C. P. D.; Huisman, J.; van der Meer, J. R.; Reddy, C. M.; Arey, J. S. *Environ. Sci. Technol.* 2014, 48, 9400–9411.
- (111)** de Leeuw, J. W.; van der Meer, J. W.; Rijpstra, W. I. C.; Schenck, P. A. *Advanced Organic Geochemistry*; Douglas, A. G., Maxwell, J. R., Eds.; Pergamon Press: Oxford, 1979; pp 211–217.
- (112)** López, J. F.; Grimalt, J. O. *J. Am. Soc. Mass Spectrom.* 2004, 15, 1161–1172.
- (113)** Rontani, J.-F.; Prah, F. G.; Volkman, J. K. *J. Phycol.* 2006, 42, 800–813.
- (114)** Patterson, G. W.; Tsitsa-Tsardis, E.; Wikfors, G. H.; Gladu, P. K.; Chitwood, D. J.; Harrison, D. *Phytochem.* 1994, 35, 1233–1236.
- (115)** For those reactions that gave lower conversions (e.g., Entries 8, 12, 14, and 17; Table 2), incomplete butenolysis products (e.g., 8,15-heptadecadien-2-one and 2,9,16-octadecatriene) could also be observed. See Supporting Information for GC × GC and GC–FID data from these reactions.
- (116)** Ivin, K. J.; Mol, J. C. *Olefin Metathesis and Metathesis Polymerization*; Academic Press: San

- Diego, CA, 1997; p 4. (b) Pederson, R. L.; Fellows, I. M.; Ung, T. A.; Ishihara, H.; Hajela, S. *Adv. Synth. Catal.* 2002, 344, 728-735. (c) Lehman, S. E.; Schwendeman, J. E.; O'Donnell, P. M.; Wagener, K. B. *Inorg. Chim. Acta* 2003, 345, 190-198. (d) Schmidt, B. *Eur. J. Org. Chem.* 2004, 1865-1880
- (117)** Bourgeois, D.; Pancrazi, A.; Nolan, S. P.; Prunet, J. J. *Organomet. Chem.* 2002, 662, 247-252. (c) Sutton, A. E.; Seigal, B. A.; Finnegan, D. F.; Snapper, M. L. *J. Am. Chem. Soc.* 2002, 124, 13390-13391.
- (118)** Hong, S. H.; Day, M. W.; Grubbs, R. H. *J. Am. Chem. Soc.* 2004, 126, 7414-7415.
- (119)** Galvinoxyl is somewhat effective to prevent the isomerization, presumably due to the structural similarity with 1,4-benzoquinone (Table 2).
- (120)** Bačkvall, J.; Chowdhury, R. L.; Karlsson, U. *J. Chem. Soc., Chem. Commun.* 1991, 473-475. (b) Csjernyik, G.; Eäll, A. H.; Fadini, L.; Pugin, B.; Bačkvall, J. *J. Org. Chem.* 2002, 67, 1657-1662.
- (121)** Foley, P. M.; Beach, E. S.; Zimmerman, J. B. *Green Chem.* 2011, 13, 1399-1405.
- (122)** Yen, H-W.; Hu, I-C.; Chen, C-Y.; Ho, S-H.; Lee, D-J.; Chang, J-S. *Bioresour. Technol.* 2013, 135, 166-174.
- (123)** O'Neil, G. W.; Carmichael, C. A.; Goepfert, T. J.; Fulton, J. M.; Knothe, G.; Lau, C. P-L. Lindell, S. R.; Mohammady, N. G-E.; Van Mooy, B. A. S.; Reddy, C. M. *Energy Fuels*, **2012**, 26, 2434-2441.
- (124)** Reed Mariculture (San Jose, CA, <http://reedmariculture.com/>, accessed 8/21/15) has been growing *Isochrysis* commercially for approximately 20 years. Multi-kilogram quantities of *Isochrysis* can also be purchased from Necton S.A. (Olhão, Portugal, www.phytobloom.com, accessed
- (125)** Johnson, M. B.; Wen, Z.; *Energy Fuels* **2009**, 23, 5179-5183.
- (126)** Crupi, P.; Toci, A. T.; Mangini, S.; Wrubl, F.; Rodolfi, L.; Tredici, M. R.; Coletta, A.; Antonacci, D. *Rapid Commun. Mass Spectrom.* **2013**, 27, 1027-1035.
- (127)** Tan, C. P.; Hou, Y. H. *Inflammation* **2014**, 37, 443-450.
- (128)** Sugawara, S.; Matsubara, K.; Akagi, R.; Mori, M.; Hirata, T. *J. Agric. Food Chem.*, 2006, 54, 9805-9810.

- (129) Maeda, H.; Hosokawa, M.; Sashima, T.; Murakami-Funayama, T.; Miyashita K. *Molecular Med. Rep.* 2009, 2, 897-902.
- (130) Kumar, S. R. Hosokawa, M.; Miyashita, K. *Mar. Drugs* 2013, 11, 5130-5147.
- (131) Yamano, Y.; Tode, C.; Ito, M. *J. Chem. Soc., Perkin Trans 1* 1995, 1895 -1904.
- (132) Xia, S.; Wang, K.; Wan, L.; Li, A.; Hu, Q.; Zhang, C. *Mar. Drugs* 2013, 11, 2667-2681.
- (133) Mordi, R. C. *Biochem J.* 1993, 292(Pt 1), 310–312.
- (134) Ravishankar, G. A.; Sarada, R.; Vidyashankar, S.; VenuGopal, K. S.; Kumudha, A. “Cultivation of micro-algae for lipids and hydrocarbons, and utilization of spent biomass for livestock feed and for bio-active constituents,” in *Biofuel Co-Products as Livestock Feed: Opportunities and challenges* (Ed. Makkar, H. P. S.) FAO, 2012.
- (135) Miyashita, K., Nishikawa, S., Beppu, F., Tsukui, T., Abe, M., & Hosokawa, M. *J. Sci. Food Agric.* 2011, 91, 1166-1174.
- (136) Watanabe, M. M. *Handbook of Algae—Their Diversity and Utilization*; NTS: Tokyo, Japan, 2012; p 490.
- (137) Tran, N. H.; Bartlett, J. R.; Kannangara, G. S. K.; Milev, A. S.; Volk, H.; Hilson, M. A. Catalytic upgrading of biorefinery oil from micro-algae. *Fuel* 2010, 89, 265–274.
- (138) Zhang, Y. In *Hydrothermal Liquefaction to Convert Biomass Intocrude Oil*; Boaschek, H. P., Ezeji, T. C., Scheffran, J, Eds.; Blackwell: Oxford, U.K., 2010; pp 201–232.
- (139) Chisti, Y. Biodiesel from microalgae. *Biotechnol. Adv.* 2007, 25, 294–306.
- (140) Schenk, P. M.; Thomas-Hall, S. R.; Stephens, E.; Marx, U. C.; Mussgnug, J. H.; Posten, C.; Kruse, O.; Hankamer, O. Second generation biofuels: High efficiency microalgae for biodiesel production. *Bioenergy Res.* 2008, 1, 20–43.

- (141)** Murata, K. Liu, Y. Makoto M. Hydrocracking of Algae Oil into Aviation Fuel-Range Hydrocarbons Using a Pt-Re Catalyst. *Energy Fuels* **2014**, 28, 6999–7006
- (142)** Banerjee, A.; Sharma, R.; Chisti, Y.; Banerjee, U. C. *Botryococcus braunii*: A renewable source of hydrocarbons and other chemicals. *Crit. Rev. Biotechnol.* 2002, 22, 245–279.
- (143)** Metzger, P.; Largeau, C. *Botryococcus braunii*: A rich source for hydrocarbons and related ether lipids. *Appl. Microbiol. Biotechnol.* 2005, 66, 486–496.
- (144)** Nagano, S.; Yamamoto, S.; Nagakubo, M.; Atsumi, K.; Watanabe, M. M. Physical properties of hydrocarbon oils produced by *Botryococcus braunii*: Density, kinematic viscosity, surface tension, and distillation properties. *Procedia Environ. Sci.* 2012, 15, 73–79.